THE
PHYSICAL REVIEW
A journal of experimental and theoretical physics established by E. L. Nichols in 1893

SECOND SERIES, VOL. 66, NOS. 3 AND 4 AUGUST 1 AND 15, 1944

Reduction of the Natural Insensitive Time in G-M Counters

J. A. SIMPSON, JR.*
Department of Physics, New York University, University Heights, New York
(Received February 18, 1944)

The limitation on the Geiger-Müller counter insensitive time which is imposed by the presence of the positive ion space charge has been reduced by collecting the positive ions on the counter center wire instead of at the outer cylinder. The electronic circuit which carries out this process is described in detail. A reduction by another order of magnitude in the insensitive time or an insensitive time of about 2×10^{-4} sec. is obtained with no indication that the limit of the new method has been reached. The general properties of an inverse counter are discussed. The mechanism of this mode of counter operation is explained with considerable evidence indicating the presence of three distinct ion collection regions for the negative center wire. A stable circuit useful as a research tool has been devised for use with a large variety of counters.

I. INTRODUCTION

CAREFUL studies have been made[1,2] of the positive ion sheath which show that there is a natural insensitive or dead time associated with each type of G-M counter. This insensitive time exists because the positive ion space charge reduces the electric field in the center-wire region below the critical value for supporting a new avalanche until the space charge has moved outward about two-thirds of the distance toward the cathode. If a high mobility ion sheath could be formed, this transit time would be reduced considerably. Such a sheath is encountered in a permanent gas mixture of two light gases, but to date no method has been successful in preventing secondary electrons and photons from forming in such a counter. If an attempt is made to use polyatomic gases which have a very small mass and size, then the dissociation process from counting results in continual changes with time of the counter characteristics, and the counter has a very short lifetime.

This insensitive time of G-M counters places a severe limitation on their use in obtaining accurate data at high counting rates. Since, in general, the events which are recorded by such counters are purely random, at high counting rates there will be a large number of intervals between two successive events which are less than the insensitive time interval of any counter. This loss of counts at high rates is expressed in an equation derived by Ruark and Brammer[3] in which the insensitive time is σ; the true counting rate is N_t and the observed rate is N_a; the equation is

$$N_a=N_t/(1+N_t\sigma).$$

In order to obtain some idea of these losses for different values of σ, the family of curves for N_a, $(N_t/N_a)-1$ with σ as a parameter appears in Fig. 1. Some values for σ the order of 10^{-4} second

* Now at the University of Chicago, Chicago, Illinois.
[1] C. G. Montgomery and D. D. Montgomery, Phys. Rev. **57**, 1030 (1940).
[2] H. G. Stever, Phys. Rev. **61**, 38 (1942).
[3] A. E. Ruark and F. E. Brammer, Phys. Rev. **52**, 322 (1937).

have been chosen which agree with experimental values obtained for so-called "fast" counters. The very best conditions that can be obtained in recording data from a counter with insensitive time σ are attained when the amplifier responds to the very tiny pulses which may occur immediately after the elapse of the time interval σ following each ionizing event, unless the counter is operated just below the Geiger threshold. In the latter case, the sheath does not fully develop, and the pulses are not independent of the kind of ionizing event.

A solution to the problem is usually not found by changing the geometry of the sources of the ionizing events during the experiment, especially if the high counting rate is changing rapidly with time. If the source is placed at such a distance that it produces a counting rate low enough to avoid serious losses, then when the source decays rapidly, the counting rate will become so reduced that exceedingly long times are required to maintain the accuracy of the individual measurements.

II. A NEW COUNTER MECHANISM

Another mode of operation of a G-M counter is evidently necessary if progress is to be made in reducing σ. It has been effectively shown by Ramsey[4] that the total collection time for electrons on the center wire of an organic vapor-noble gas counter is less than 10^{-6} second, and most of the electrons are collected in about this time in a "slow" counter. Therefore, after the center wire begins to drop in potential, use is not made of the subsequent cycle so far as recording the event is concerned. Consider an alternative procedure. Instead of allowing the positive ion sheath which forms around the center wire to move outward, suppose these ions were almost immediately collected on the center wire. This may be accomplished by reversing the potentials on the center wire and cylinder long enough to insure collection. Since the ions are formed only in the immediate vicinity of the wire and will therefore be in a high field which accelerates them toward the center wire, this collection time will be very short, probably less than 10^{-5} second. As soon as all ions are collected, the counter should be immediately returned to its normal operating potential to be ready for the next event. In this case the outer cylinder serves only as a field-forming conductor.

It is important to consider the properties and action of a counter when it is inverted. As in the case of the positive center wire, the negative center-wire counter has a definite potential at which it breaks into corona. For the impure gases which exist in G-M counters, the breakdown potential at very low pressures when the center wire is positive is greater than when the center wire is negative. The pressure-potential curves, however, cross at higher pressures, and for pressures used in most counters the breakdown potential of the negative center-wire system will, in general, be greater.[5]

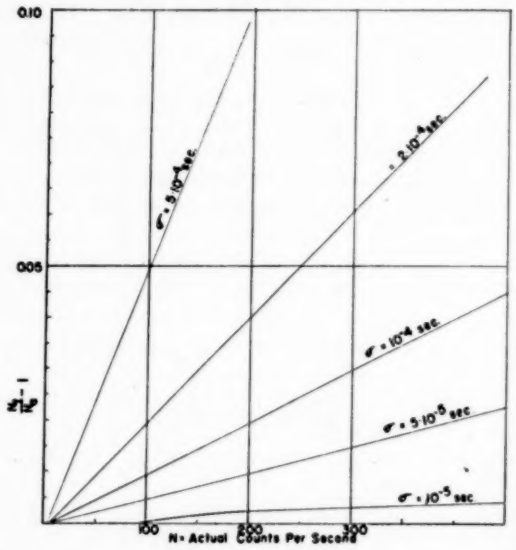

FIG. 1. This is a graph to determine the true counting rate N_t from the observed counting rate N_a for a given insensitive time σ.

Below the breakdown potential in a negative center-wire system there is a small region in which the system behaves like a G-M counter in some respects. An ionizing event in the volume results generally in a single pulse, and the pulse is independent of the number of primary ions produced. This may be called the inverse Geiger region. Counters operated in this fashion have been tried principally by Ramsey and Cowie.[6] However, it

[4] W. Ramsey, Phys. Rev. **57**, 1022–1029 (1940).

[5] M. J. Druyvesteyn and F. M. Penning, Rev. Mod. Phys. **12**, 122 (1940). These authors present a complete brief discussion on breakdown and corona with a concentric electrode system.

[6] D. B. Cowie, Phys. Rev. **48**, 883 (1935).

is evident that most ionizing events take place in the outer volume of the counter, and therefore the time before a positive ion reaches the center-wire region is a variable; the positive ion has a very low mobility compared to electronic mobility. As a result, negative wire counters cannot be used in a coincidence circuit. The background of such a counter is high, and it appears to have no appreciable plateau. If the potential is raised slightly, but not enough to cause breakdown, the counter may break into periodic groups of high frequency oscillations. The envelope of the groups is well defined. An explanation of this will be discussed below.

By making the center wire negative, the production of photoelectrons becomes negligible. Photoelectrons are produced at the cathode of the electrode system which in this case is the center wire. Therefore, this photo-effect is reduced by a factor approximately equal to the ratio of the wire radius to the cylinder radius. It should be noted that tungsten, which is widely used for center wires, has a work function of about 4.5 ev.

The behavior of positive ions near the negative center wire for potentials below the inverse Geiger region is probably quite complex and does not lend itself to an exact solution. It is desirable to know under what conditions the positive ions may acquire enough energy to produce secondary electrons by field emission at the wire. If the ions are polyatomic, they may be polarized near the wire and change the effective mean-free-path in that region. At the conclusion of this discussion something will be said concerning these processes in the light of experiments to be presented.

The avalanche process at the negative wire has many characteristics which differ from the well-known positive center-wire avalanche. If a positive ion approaches the center wire and causes the ejection of an electron by field emission, this electron will travel toward the outer cylinder. The field is decreasing as $1/r$. By the time electron avalanche production would be able to increase to very large values, as in an increasing field, the avalanche head has already entered a low intensity field region. Townsend's coefficient α, which is a measure of the number of ion pairs formed by an electron in one centimeter of its path, depends upon the field intensity and the pressure. Since α is decreasing almost exponentially as the avalanche head moves into a region of low E/p, the production will break off fairly sharply. The field is further distorted and reduced by the positive space charge left behind the avalanche. The current flow of electrons, therefore, increases rapidly to a value which is constant for most of the distance out to the cylinder. If many electrons initiate a large number of avalanches, the positive space charge may be sufficient momentarily to choke off further avalanche production until a large portion of the positive ions have been collected; the process then repeats. This would produce an oscillatory discharge in the counter of the nature previously described.

The negative ions play an important part if a great number exist when the counter potentials are reversed, for then the negative ions must travel out toward the cylinder. However, if only a few such ions are formed, they need cause no difficulty because they will not distort the field distribution; they will not lose their electrons in a region where a new avalanche could possibly start. The field in front of the outer cylinder is very low.

These general considerations indicate that the new mode of counter operation proposed can be successful if the proper inverted region is selected. Later, this will be shown to be possible.

III. THE EXPERIMENTAL CIRCUIT

The requirements for the design of an electronic circuit to produce the random reversals at a very high average rate with precision are:

1. The input to any amplifying device which operates on the first three or four volts' drop of the steep pulse front must be insensitive to the process of reversing the field.

2. The circuit must have extremely low RC times throughout; it must respond to frequency components around two megacycles and still possess fairly high gain.

3. The reversal process must be carried out so that not more than a few microseconds elapse before the field is inverted and ions are being collected.

4. No residual voltage "tails" more than three or four volts can be tolerated after collection time

is over or, at high counting rates, the effective operating potential will be changed.

5. Accurate control of the time and extent of the reversal of field must be possible over a wide range to accommodate all types of counters.

6. All supply potentials must be constant under extreme fluctuations of counting rates.

7. The circuit should be constructed from standard equipment available to all laboratories if it is to be of use as a research tool.

A circuit fulfilling these requirements has been developed and operated successfully; before describing it in detail, it would be best to outline the general method with the aid of a simplified block diagram, Fig. 2, representing the circuit elements. Normally no current flows in R_b; therefore the counter is operating at a potential V_2. When the electrons are collected from an ionizing event, a positive pulse begins to form across R. This is detected, and a sharp pulse passes through to the first trigger pair which produces a rectangular wave of time length t_1; this is fed back to the input circuit to act as a shutter preventing the first portion of the circuit from functioning for a time t_1. The second trigger pair is actuated by the incoming pulse also, and it produces a rectangular wave of width t_2. This rectangular pulse is converted to a rectangular pulse approximately $-(V_1+V_2)$ volts high appearing at a. If $t_1>t_2$, then all disturbances on the center wire are over before the shutter opens again.

The schematic diagram of the circuit actually used appears in Fig. 3. All values of the circuit constants are listed. A beam power tetrode of type 807 (or type 829 with its elements in parallel) is used for the high voltage pulse-forming tube with the grid bias of about -150 volts adjusted to place the grid potential beyond cut-off; thus the average plate current required is very low. With the center wire connected directly to the plate of the tube, the full counter operating potential V_2 is applied between ground and plate supply potential. The cathode and heater are $-V_1$ volts below ground potential with V_1+V_2 volts applied across the type 807 tube. The series of pulses to be described appears in Fig. 4A. The positive pulse front a which is several volts high in one or two microseconds appears across the resistor R since the impedance in the plate circuit of the 807 is negligible in comparison with R. Pentode A is biased just beyond cut-off, so it will produce a sharp negative pulse b across its plate impedance when the small positive pulse (1–3 volts) is applied directly to the grid of A. Pentode B amplifies and inverts this pulse c by operating well up on its normal characteristic curve. From here, the positive pulse is applied to the tube C which serves two purposes. It produces a negative pulse d for the trigger pair D and E; it also is used as the shutter for the amplifier by receiving a rectangular wave e from the trigger pair on the biased suppressor grid. The shutter time t_1 is controlled by R_{13}. The trigger pair operates in the conventional manner with tube D normally conducting and with E normally non-conducting. The steep front of the negative rectangular pulse is differentiated f by the circuit $R_{18}C_9$. This triggers the tubes F and G which are arranged exactly as D and E so as to produce a rectangular pulse g whose time width t_2 is determined by R_{18}. The pulse is now amplified by H and inverted h so it can drive the grid of the type 807 so far positive that small variations in the height of h will not affect the characteristics of the negative pulse i of approximate height V_1+V_2 volts. But the outer cylinder of the Geiger counter is near ground potential; therefore the center wire drops to approximately V_1 volts below ground potential. Since the plate circuit has a much lower impedance than R, the differentiated rectangular wave will appear at the input of the amplifier tube A, but a time $t_1>t_2$ must elapse

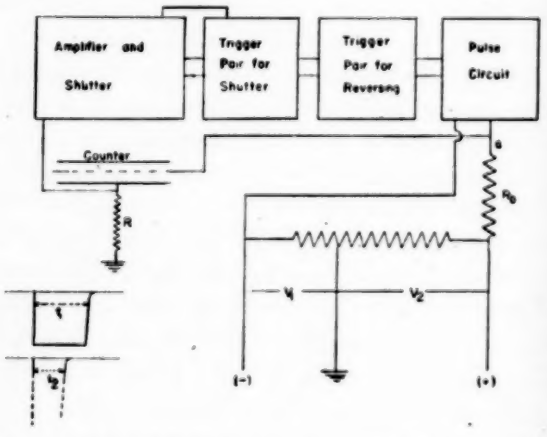

FIG. 2. This block diagram illustrates the manner in which the circuit elements are arranged to produce positive ion collection on the Geiger-Müller counter center wire in order to reduce the counter insensitive time.

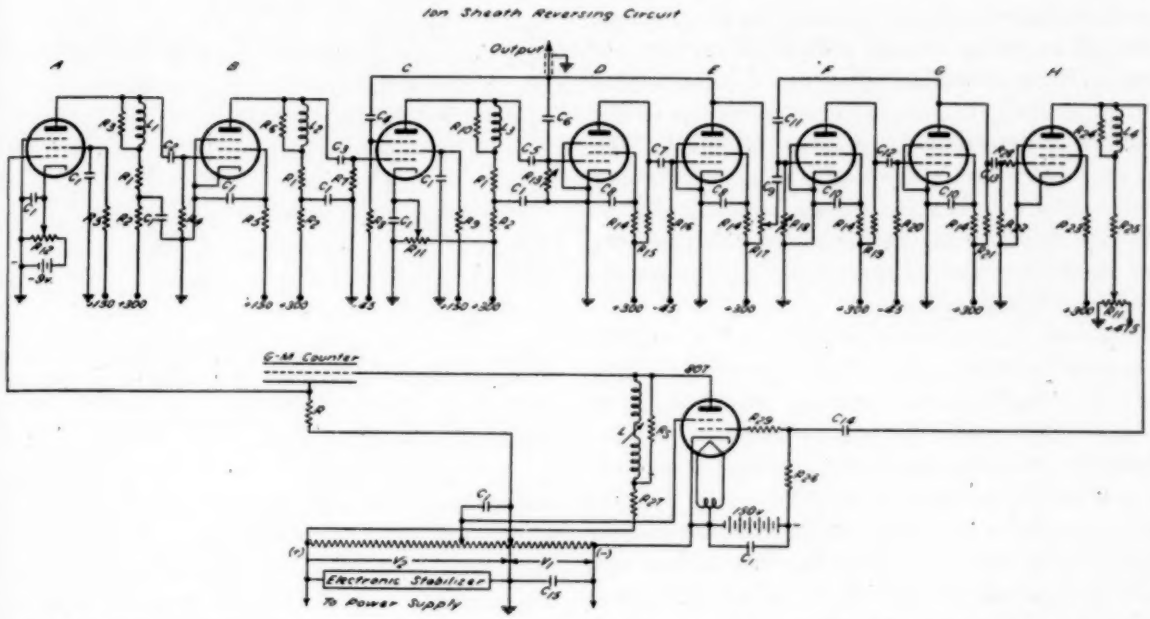

FIG. 3. Schematic diagram of electronic circuit to collect positive ions on the center wire after each ionizing event. The circuit constants are as follows:

$C_1 = 0.1\ \mu f$,	$C_{10} = 0.1\ \mu f$,	$L_4 = 80$ mh,	$R_9 = 2.5$ K,	$R_{18} = 1$ meg.,	$R_{27} = 4$ K,
$C_2 = 50\ \mu\mu f$,	$C_{11} = 100\ \mu\mu f$,	$R_1 = 3500\Omega$,	$R_{10} = 25$ K,	$R_{19} = 2$ K,	$R_{28} = 2500\Omega$,
$C_3 = 20\ \mu\mu f$,	$C_{12} = 0.02\ \mu f$,	$R_2 = 500\Omega$,	$R_{11} = 75$ K w.w.	$R_{20} = 50$ K,	$R_{29} = 500\Omega$,
$C_4 = 0.02\ \mu f$,	$C_{13} = 500\ \mu\mu f$,	$R_3 = 25$ K,	$R_{12} = 25$ K,	$R_{21} = 6$ K,	$R = 75{,}000$.
$C_5 = 20\ \mu\mu f$,	$C_{14} = 0.001\ \mu f$,	$R_4 = 25$ K,	$R_{13} = 2$ meg.,	$R_{22} = 0.1$ meg.,	
$C_6 = 100\ \mu\mu f$,	$C_{15} = 4\ \mu f$,	$R_5 = 2500\Omega$,	$R_{14} = 10$ K,	$R_{23} = 500\Omega$,	
$C_7 = 0.02\ \mu f$,	$L_1 = 1.2$ mh,	$R_6 = 25$ K,	$R_{15} = 4$ K,	$R_{24} = 0.1$ meg.,	
$C_8 = 10\ \mu f$,	$L_2 = 0.67$ mh	$R_7 = 0.1$ meg.,	$R_{16} = 50$ K,	$R_{25} = 15$ K,	A, B, C, D, E, F
$C_9 = 10\ \mu\mu f$,	$L_3 = 1.2$ mh,	$R_8 = 25$ K,	$R_{17} = 6$ K,	$R_{26} = 50$ K,	G, H are 6AC7.

before the amplifier passes any pulses through the shutter, and so this pulse is unrecorded.

A vertical section through the diagram (Fig. 5) of the potential changes on the counter electrodes as a function of time gives the potential between the electrodes at any instant. The shaded area is drawn between the two electrode potential curves. The first pulse *a* is purposely drawn incorrectly to point out the importance of avoiding "tails" on the pulses. With pulse *a* the counter does not get back onto its operating potential until the tail of the reversing pulse has disappeared. The tiny differentiated pulse appearing at the outer cylinder further tends to reduce the operating potential immediately after ion collection. Pulse *b* is the composite of the two pulses actually observed on the oscilloscope when the circuit is functioning correctly.

IV. CIRCUIT TESTS

The preliminary testing of circuit elements is of importance. The tubes *A*, *B*, and *C* were over-compensated with inductance to avoid severe losses of the higher frequency components of the pulses by tube and circuit capacities. Such amplifiers must be untuned because of the aperiodic nature of the pulses. The upper frequency limit of the amplifier is many times that of the pulses themselves. The very low frequencies were of no particular concern in this work. Decoupling in the plate circuits is provided wherever it might possibly avoid difficulties. Tests were made with microsecond pulses over a wide frequency range. The power supply for tubes *A* through *H* was a single unit run from a stabilized power line.

The shutter circuit composed of tubes *C*, *D*, and *E* must be carefully adjusted. The biases on the control grid and suppressor grid are so adjusted that the tube is normally just beyond cut-off. A pulse appearing on the control grid is amplified, but a negative rectangular wave applied to the suppressor grid will keep the tube non-conducting. This circuit element is checked

by applying sharp microsecond pulses at about 100–200 kc to the control grid while varying the time t_1. By so doing the frequency can be divided by the shutter by any integral factor up to the limit of t_1 determined by tubes D and E. The input to D must be carefully adjusted. Several methods of coupling the pulses from F and G to the type 807 have been tried with success, but the one illustrated was used in obtaining the results described in this paper.

Since the grid is V_1+150 volts below ground, it is essential that C_{14} be a high voltage condenser and that the separate filament transformer be insulated *if* widely varying potentials of V_1 are desired; otherwise, for normal operation no such precautions are necessary. The screen supply voltage may conveniently range from 300–600 v. On counters with low operating potentials a 6*C*6 tube or equivalent type has worked with some success.

It has already been pointed out that no tail (>3 or 4 v) must be present on the negative 1000 to 1500 v pulses produced by the type 807 tube. If only a plate resistor with the usual small compensating inductance were used, long tails starting about 150–200 v in height appear even with small values of R_b. This problem was effectively solved by means of an *LRC* circuit. Used with a variable inductance L_s (approximately 15 millihenries), the resistance R is

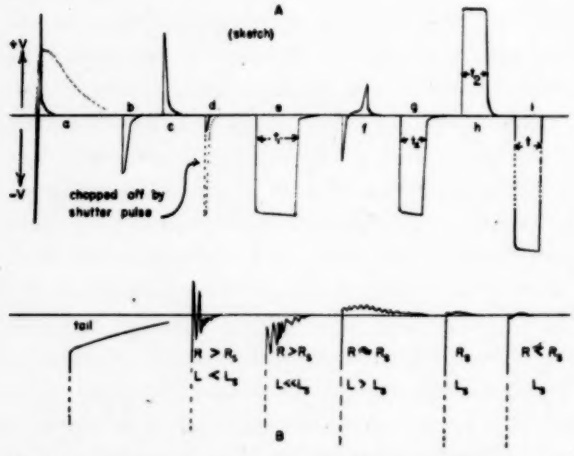

FIG. 4A (Above). The pulse shapes observed on an oscilloscope connected to different portions of the circuit. The pulses are not drawn to scale. The input pulse is the first positive front of *a*; the reversing pulse is *i*.

FIG. 4B (Below). The effect of varying the value of the inductance L_s and its shunt resistance R_s on the tail of the reversing pulse. The tail must be very small so that the counter can return to its operating potential rapidly.

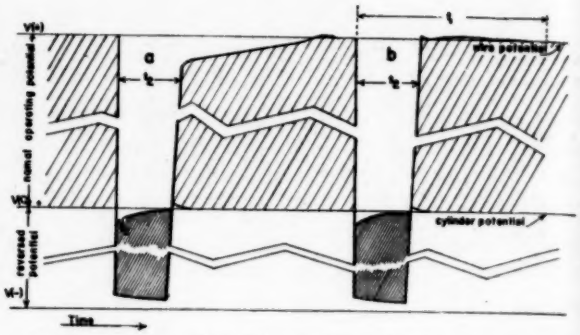

FIG. 5. A graphic illustration which indicates the potential difference between the center wire and outer cylinder of the counter at any instant of the counter reversal process. The shaded areas are drawn between the two electrode potential curves.

critical and has a value of about 550 ohms. Figure 4B shows the results (not drawn to scale) of varying both the shunting resistance and the inductance. The tail in pulse VI is less than 4 v high above the axis and disappears within the time t_2.

The separate power supply for the type 807 is stabilized electronically. Under a load of 100 to 150 milliamperes the voltage should not fluctuate.

By using periodic groups each of two pulses of width 10^{-6} second, spaced 10^{-6} second apart, the circuit is checked for selectivity. The second pulse is eliminated, and the circuit only reverses on the first pulse of each group as it should. The whole circuit has been tested at frequencies over 300 kc with a coupling condenser instead of a counter between tube 807 and the input of tube *A* which has the same value as the counter capacity.

All observations were made on a Dumont oscilloscope No. 241, a shielded probe, and high impedance attenuator. Care must be taken that the observation does not alter the circuit in any manner. Any oscilloscope whose amplifier characteristics are not flat in frequency response up to 2.5 megacycles should not be used.

The scaling and recording circuit is operated from the output at *E*. The first scale of 8 or 16 functions up to about 3 megacycles, and the remaining scalers to form a scale of 512 are conventional hard-tube circuits.

To find the time delay in making the center wire V_1 volts negative with respect to ground, the sharp input pulses were superposed with the reversing pulses on the oscilloscope screen. This delay is about 1.5×10^{-6} second for a 1000-v pulse.

V. RESULTS

The reduction of the insensitive time of a G-M counter by this circuit can be determined by any one of several methods for measuring resolving times. The most useful one for instantaneous observation is the single-sweep trigger circuit as used by Stever.[2] One event triggers off an oscilloscope to sweep across the screen; at high counting rates there is a fair probability that the next event will occur near the limit of the insensitive time. This is observed by pulses making their appearance on the screen after the insensitive time interval. Thus, by repetition of the pattern the interval between the trigger pulse and the next appearance of the pulses measures the insensitive time σ. By using this circuit connected to the first or second trigger pair in the reversing circuit, the circuit characteristics will not be changed. All pulses will be of the same height in contrast to the usual observations.[2] These observations have been made with a calibrating time scale (3 percent error) incorporated in the sweep.

Polyatomic-noble gas counters are most useful for the first experiments for two reasons. Whenever the reversing circuit is shut off, the counter will not be destroyed. Also this type of counter has the lowest range of insensitive times used at present, and therefore it is a suitable standard for comparison with results obtained by using the reversing circuit.

The factor of reduction of insensitive time is plotted in Fig. 6 as a function of the magnitude of the reversing potential for the first counters[7] used in the circuit. σ_{-off} is the insensitive time of the counter without the circuit; σ_{-on} is the insensitive time of the counter when the reversing circuit is used. Great care was taken that the smallest pulses would be recorded. For each counter V_2 is a constant. Preliminary experiments indicate that the new insensitive times lie around 2×10^{-5} second. This is nowhere near the limit to be expected in future trials. It should be noted that these values are obtained under very stable conditions; the apparatus may be turned off and warmed up again as desired without difficulty. Background counting rates remain a constant in using the circuit.

[7] Counter No. 2 has 10 percent amyl acetate; 90 percent argon. Counter No. 5 has 10 percent ethyl alcohol; 90 percent argon.

In obtaining the points for the curves in Fig. 6 the collection time was adjusted for its optimum value for each value of V_1 with the shutter pulse set at $t_1=1.5\times10^{-5}$ second. The time t_2 varied from 2.5×10^{-6} to about 6×10^{-6} for the ion collection.

Additional tests were made by using two γ-ray sources, one twice the intensity of the other. The intensities of these sources are first accurately determined. Then the lower intensity source (No. 1; 9.98 mg) is determined at, say, 10 counts per second; the second source (No. 2; 19.98 mg) is placed in the same position, and the counting rate is again determined. Finally, with both together the counting rate is obtained. After repeating this procedure at several distances from the counter the information can be used to obtain curves like those in Fig. 1.

By varying the potential and width of the reversal pulse three distinct regions in the inverse Geiger region are found in polyatomic-noble gas counters. This has been anticipated to some extent in the introductory remarks of this discussion. At low voltages (up to about 300 v with counters operating at around 1100 v) the ion sheath is collected within about 7×10^{-6} second without producing any detected secondary effect. The upper limit of this potential is defined within about 40 v, but its magnitude depends upon the counter properties, especially the mean free path at the center wire. The diameter of the center

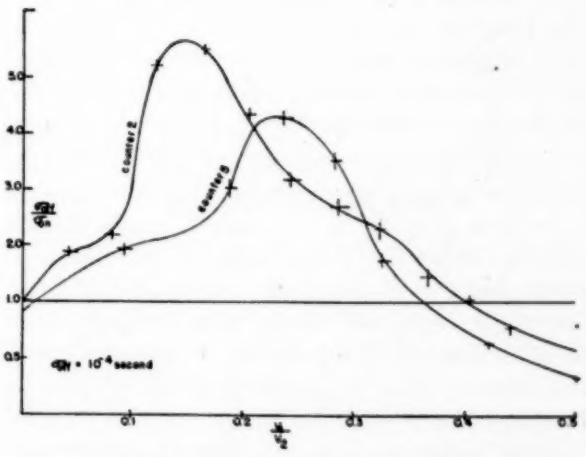

FIG. 6. Experimental evidence of the decrease in counter insensitive time produced by reversing counter electrode potentials for positive ion collection. σ_{off} is the insensitive time with the reversing circuit off; σ_{on} is the insensitive time using the circuit. V_2 is the counter operating potential; V_1 is approximately equal to the reversed potential.

wire will also determine the terminus of the first region. An experiment in which the diameter of the center wire is varied has been planned.

The second region begins when tiny sharp pulses (less than 0.3 v) appear at the outer cylinder about 2×10^{-4} second after the ionizing event *a*. Figure 7 illustrates the changing character of this "tail" as a function of V_1, which appears at the end of the differentiated negative pulse. In each successive drawing the potential V_1 has been increased. It is possible to hazard an interpretation of this phenomenon. In *a* and *b* the small pulses are due to positive ions arriving at the outer cylinder. The beginning of the second region is one in which the noble gas positive ions begin to have enough energy to produce secondary electrons at the center wire; these electrons will produce new local avalanches whenever the field is intense enough to support them. The space charge is being collected before transformation by electron transfer can occur; therefore a considerable portion of the sheath is composed of the noble gas ions. An example of this process appears in the literature. Penning[8] has observed that the number of electrons produced per positive ion impact varies from about 0.03 to 0.05 for ions having energies less than 50 v. This fraction increases nearly linearly with energy up to 0.42 for 1000-v ions.

How are the characteristic patterns of *a*, *b*, and *c* to be explained in view of the fact that the ion collection times can be varied somewhat without changing them? As the positive ion sheath is coming toward the center wire, the field between sheath and wire becomes more intense, but the region beyond the sheath drops to a relatively low value because of this space charge. Secondary electrons passing outward are, therefore, unable to start avalanches in this region. As the sheath is being collected, the field again rises to the point where local avalanches may be produced. The continued collection of the sheath brings new local avalanches closer and closer to the wire. If the counter were suddenly returned to normal conditions at this instant, small individual space charges would move out to the cylinder to be collected, thus producing small peaks in the ion collection pulse. But if the counter were not reversed at this instant, the new positive ions would arrive at the wire to continue the process until the counter potentials were changed. Again the ion collection pulse would be a series of peaks. Little or no spread of the discharge due to photons may be expected in the lower part of this region in which only a few of the positive gas ions have enough energy to produce secondary electrons. The resolution of pulses in *a* and *b* tends to confirm the assumption made in G-M counter theory that the ions move out without much spreading, i.e., the sheath can be treated as infinitely thin for purposes of calculation.

As the potential V_1 is increased, secondary electrons are produced all along the wire while positive ions are being more rapidly removed from the original sheath. A large space charge from the electron avalanches then forms not only around the wire, but also along its length; the role of photons in this process is questionable. The large space charge immediately chokes off further avalanche production, and the large burst of electrons which formed the avalanche shortly arrives at the outer cylinder. The collection of these electrons can be observed by the negative pulse appearing at α in *d*, *e*, and *f*. The magnitude of this pulse is a function of the potential V_1 and not of the counter overvoltage; therefore it cannot be interpreted as a collection of the original positive ions. This pulse is terminated within $4\text{–}5\times10^{-6}$ second from the time of reversal. It demonstrates that the original positive ion sheath is at least mostly collected within that time interval. When the time t_2 is extended, a repetition of the process takes place and a second negative peak is to be observed. When the

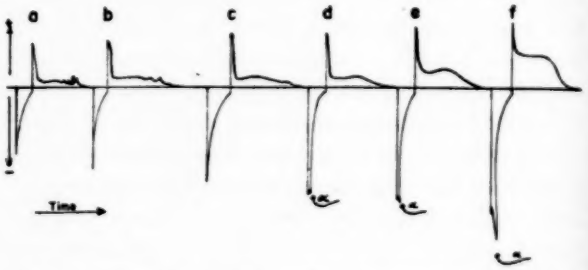

FIG. 7. Sketches of the pulses observed by using an oscilloscope connected to the outer cylinder. The potential V_1 is great enough to cause positive ions to produce secondary electrons at the center wire. V_1 is increasing from left to right.

[8] F. M. Penning, K. Akad. Wet. Amst. Proc. **33**, 841 (1930).

counter potentials are returned to normal operating potential, this extensive positive ion sheath moves outward producing the positive hump shown on the tail of the differentiated pulse. A counter operated in such a region obviously has its insensitive time increased rather than decreased.

The negative pulse α and the positive hump continue to increase with the potential of V_1 up to a value $|V_1| \cong |V_2|$ where the third region begins. This is the inverse Geiger region described in the introduction. Multiple and spurious pulses make their appearance. Above this potential lies the corona discharge region which is well known and is useless in these observations.

By triggering the reversing circuit artificially in any of these regions at a time when no ionizing event is present, it can be shown that the differentiated pulse lacks all the characteristic pulses described in the preceding paragraphs; the phenomena are due to counter action and not to the characteristics of the reversing pulse. In Fig. 6 the point where the curve crosses the unity axis indicates the vicinity of the boundary between the ion collection region and the region in which ions are beginning to produce secondary electrons.

Another way in which to collect the positive ions at high counting rates may be pointed out. Suppose the circuit reverses periodically, being inverted for a time t' and returning to normal for a much longer time t''. Further, t'' will be made smaller than the normal insensitive time t_d. A complete cycle of operation, therefore, requires a time $t'+t''<t_d$. Conservative values for these times can be chosen, such as

$$t' = 10^{-5} \text{ second},$$
$$t'' = 4\times10^{-5} \text{ second}.$$

To a first approximation the probability of two events in a random distribution occurring in a time interval less than τ with a counting rate $N/\text{sec.} = 1/\bar{t}$ is[9] $p = \tau/\bar{t}$. Assuming a counting rate of 500 per sec. the probability of two events occurring in a time interval 10^{-5} sec. is 5×10^{-3}, in a time interval 5×10^{-5} is 2.5×10^{-2}, and for 10^{-4} sec. (the dead time of a "fast" normal counter) is 5×10^{-2} sec. The advantage of such a procedure over using the counter alone is further emphasized since it is definitely known that $\frac{1}{2}$ of all the counts are purposely not being recorded.

Although the circuit in Fig. 3 was designed to study the properties and possibilities of reducing the insensitive time, it may be used as a research tool; there are several critical adjustments which have been described, but once adjusted, the circuit is stable. For use with a particular counter type a much simpler circuit may be devised. The gain requirement may be relaxed. A simple design would include two stages of amplification incorporating the shutter along with two LC circuits to produce rectangular waves of the desired widths and a pulse amplifier followed by a blocking oscillator using a pulse transformer. The large tail produced by such an oscillator may be corrected by the LRC circuit suggested earlier. The use of a high voltage trigger pair to obtain the reversing pulse has the disadvantages of requiring a large average plate current and producing pulses of an undesirable shape. The new techniques which will be available in the future for pulse production may result in a drastic simplification of the reversal circuit. Research is still to be carried out on the permanent gas counter; the advantage of using such a counter is that it should maintain its characteristics until the wire becomes badly pitted. Since the outer cylinder now only assumes the character of a field-forming electrode, serious consideration should be given to the fact that almost any surface layer which does not accumulate charges may be used to make the production of photoelectrons impossible.

ACKNOWLEDGMENTS

The writer wishes to express his sincere gratitude to Professor S. A. Korff for his encouragement and helpful suggestions and to both him and Professor R. D. Present for innumerable discussions which helped to clarify the problem. Thanks are due to Dr. V. C. Wilson for first suggesting the problem and for his continual interest in its development.

[9] J. Strong, *Procedures in Experimental Physics* (Prentice-Hall, Inc., New York, 1938).

The Energy Spectrum of Electrons in the Atmosphere Arising from the Disintegration of Mesotrons

HENRY E. STANTON
University of Chicago, Chicago, Illinois
(Received May 19, 1944)

The energy spectrum of electrons at the altitude of 14,618 feet originating from the decay of mesotrons is calculated by means of the cascade theory of showers. It is assumed that the mesotron decays into a neutrino and an electron, which are emitted with equal probability in all directions in the reference frame of the mesotron. The diffusion equations for the showers are derived with the boundary conditions that there are no incoming electrons or photons. By approximations similar to those used in the shower theory, it is possible to calculate the electron spectrum in the lower atmosphere, provided the mesotron spectrum is known. If we assume a mesotron spectrum in accordance with experiment, the theoretical calculations for the electron spectrum can be compared with new observations on the intensity of the soft component for energies higher than 5×10^7 ev. The calculations are in satisfactory agreement with experimental results found by D. Hall and later by W. Hazen.

1. INTRODUCTION

THE problem of the origin of the electrons in the lower atmosphere has been considered previously by several investigators in the field of cosmic rays. The earliest treatments attempted to show that the observed intensity of the cosmic rays was a consequence of the interaction of high energy primary electrons with the atmosphere, and the total intensities observed were secondary products of these high energy primaries. After the discovery of the mesotron and the hypothesis of its disintegration, Euler and Heisenberg[1] assumed that the soft component in the lower atmosphere was only partly the result of incident primary electrons, and that, in addition, there was an appreciable contribution by the electrons generated by the disintegration of the mesotrons.

Schein, Jesse, and Wollan,[2] on the basis of experiments carried out in the stratosphere, suggested that all the soft component might be attributed to secondary rays arising from the mesotrons—the majority being produced by decay processes. Later, Rossi and Greisen[3] calculated the intensity of the soft component based on this hypothesis and found that the theoretical number of electrons arising from the mesotron component was in close agreement with observations at sea level; but at the altitude of Mt. Evans, 14,618 feet, there was an appreciable discrepancy between theory and experiment. From their results, they concluded that such a simple mechanism was unable to account for the total soft component in the lower atmosphere. However, their method of calculation employed integral methods by which only the total number of electrons of all energies resulting from the mesotron intensity could be found; and the important problem of the energy distribution of the electrons could not be solved. The approach of Rossi and Greisen is also complicated by the fact that in calculating the total number of electrons, one has to include all the electron energies down to very low values where the shower theory is less easily treated and becomes more complex than at higher energies.[4] Since it is considerably more difficult to measure the number of electrons with very low energies in the soft component, an exact comparison between theory and experiment is difficult to achieve.

Considering the importance of the conclusions of Rossi and Greisen, it seemed necessary and desirable to try a more nearly accurate and direct method for calculating the soft component —particularly for the altitude of Mt. Evans where the deviations in their calculations from the experimental values were about the largest. D. Hall has measured the approximate energy spectrum of both mesotrons and electrons at this

[1] H. Euler and W. Heisenberg, Ergeb. d. exact. Naturwiss. **17**, 1 (1938).
[2] M. Schein, W. P. Jesse, and E. O. Wollan, Phys. Rev. **59**, 615 (1941).
[3] B. Rossi and K. Greisen, Phys. Rev. **61**, 204 (1942).
[4] B. Rossi and S. J. Klapman, Phys. Rev. **61**, 414 (1942).

location, and a more nearly complete theoretical solution of this problem can be compared with his results. This is possible if the energy spectrum of the mesotrons is known immediately above the point of observation. A power law spectrum can be assumed in accordance with the data on the zenith angle distribution and measurements of the penetration of mesotrons through lead thicknesses up to 91 cm,[5] and the calculations which follow show that the exponent of the power law spectrum can be varied between rather wide limits without appreciable change in the spectrum of higher energy electrons.

The mesotron spectrum was cut off at the value of the energy which is necessary to penetrate 18 cm of lead (3.8×10^8 ev) since the total number of mesotrons with energies greater than this limit has been measured in balloon experiments and is known throughout the atmosphere.[2] Also, below this energy, the power law rapidly fails to hold. The mesotrons with lower energies, in order to contribute to the soft component, must disintegrate within a few radiation units of the point of observation; and the electrons emitted in these processes will have an energy of 1.9×10^8 ev on the average, and will not multiply appreciably. Consequently, of these mesotrons, those which decay close to the point of observation contribute one electron each; and the total contribution of the low energy part of the mesotron spectrum can be calculated from the theory of the disintegration process.

The theory presented here is based on the cross sections for pair production and brehmsstrahlung calculated on the assumption of complete screening, and includes also the ionization loss of the shower electrons. This should, then, give the correct spectrum of electrons arising from the disintegration of the mesotrons for energies above 5×10^7 ev. However, a comparison with the experimental values must be considered to be only preliminary since the data available so far have limited accuracy. The mean life of the mesotron used in the calculations has been assumed to be the same throughout the entire atmosphere, and the value used is 2.15×10^{-6} sec. as given by Nereson and Rossi.[6]

With suitable changes in the mesotron spectrum, the calculations could be extended without modification to give the spectrum of electrons at other altitudes.

2. CALCULATIONS OF THE ELECTRON SPECTRUM

In calculating the soft component that arises from the mesotron component it is necessary to include at least three processes: (a) the decay of a mesotron giving rise to a high energy electron, (b) the cascade multiplication of electrons, and (c) electrons arising from close mesotron collisions. In addition to these processes, there are others (Compton effect and the angular scattering of the electrons in the shower) which may be considered as corrections although their inclusion in any other manner makes the mathematical analysis much more complicated. It can be shown, however, that for the lower atmosphere, these corrections are negligible for energies above about 5×10^7 ev.

(a) Decay

It is assumed that the elementary process of the decay of a mesotron consists of spontaneous disintegration into an electron and an unknown neutral particle (neutrino). It is further assumed that the rest mass of the neutral particle is negligibly small so that the electron will receive on the average one-half of the total mesotron energy. According to this hypothesis, in a reference frame in which the mesotron is at rest, the electron will be emitted with equal probability in any direction and with an energy equal to half the rest energy of the mesotron. If the mesotron is moving relative to a reference system fixed with the earth, it is necessary to use a Lorentz transformation to calculate the decay in this system. Under these conditions, the energy of the decay electron with respect to the earth's system will depend on its angle of emission in the system in which the mesotron is at rest, and hence on the corresponding angle of emission in the earth's system. If θ represents the angle in the earth's system between the trajectory of the decay electron of total energy E and the trajec-

[5] It can also be pointed out that the theoretical calculations of the mesotron spectrum, based on assumptions similar to those used by Euler and Heisenberg, lead to this type of spectrum as a close approximation.

[6] N. Nereson and B. Rossi, Phys. Rev. **64**, 199 (1943).

tory of the initiating mesotron of total energy E' and rest energy μ, then using the equations of the Lorentz transformation one obtains the following result:

$$\cos\theta=\frac{2EE'-\mu^2}{2E(E'^2-\mu^2)^{\frac{1}{2}}}. \quad (1)$$

In Fig. 1, the electron energy E is plotted for different values of θ in a polar diagram. The polar distance is proportional to the logarithm of the total energy E of the decay electron in the earth's system. The various curves correspond to different mesotron energies.

Since 10^8 ev is the critical energy of electrons in a shower in air, an electron with this energy cannot multiply appreciably in the atmosphere and will be brought to rest in a few hundred meters of normal air. As a result, these lower energy electrons will not contribute appreciably to the total intensity of the soft component. From the curves in Fig. 1, it is clear that decay electrons having energies greater than 3×10^8 ev always lie in a small solid angle (less than 11°) around the trajectory of the mesotron, and hence the approximation introduced by considering the decay process as one dimensional is satisfactory.

The probability that a mesotron will decay in a system in which it is at rest is equal to $d\tau/\tau_0$, where τ is the time in that system and τ_0 the mean life of the mesotron. Transformed to the earth's system, this probability becomes

$$P_1(E')dy=\frac{\mu}{\tau_0E'c}dy,$$

where $P_1(E')dy$ is the probability a mesotron with energy E' will decay in the length dy of its trajectory. If the depth from the "top" of the atmosphere is measured in radiation units t in a vertical direction, it follows that

$$P_1(E', t)dt=\frac{\mu}{\tau_0c}\frac{\rho(t)}{E'}dt, \quad (2)$$

where $\rho(t)=\alpha/t$ represents the barometric formula expressed in radiation units, and α has the value 7.0×10^5 cm to 7.5×10^5 cm. This implies that the barometric formula in the atmosphere is approximated by an isothermal relation.

Expression (2) gives the number of decay electrons generated by a mesotron of energy E' in a thickness dt at the depth t, without regard to its energy. Among these electrons there is a probability $P_2(E', E)dE$ that a decay electron will have the energy E to $E+dE$, and on the basis of the theory of decay assumed above, this probability is given by[7]

$$P_2(E', E)dE=\frac{1}{(E'^2-\mu^2)^{\frac{1}{2}}}dE. \quad (3)$$

The probability, then, that a mesotron will produce a decay electron of energy E in the thickness dt in air is

$$P(E', t)dEdt=P_1(E', t)P_2(E', E)dEdt. \quad (4)$$

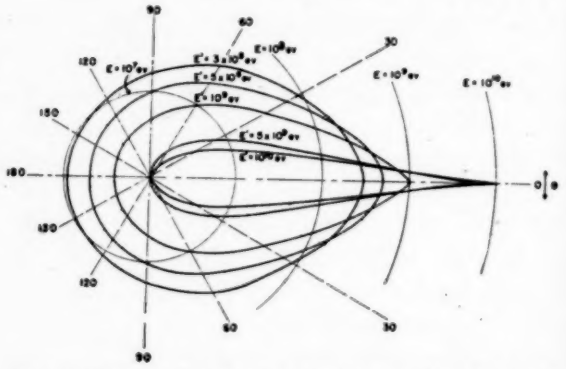

FIG. 1. Energy of a decay electron as a function of the angle of emission. The mesotron trajectory is directed along the line $\theta=0$. The mesotron energy E' is indicated on each curve. For a particular curve, the energy E of the decay electron in the earth's system depends on the angle θ between the trajectories of the mesotron and electron. The length of the radius vector for a given θ is constructed proportional to the logarithm of $E/10^6$ of the decay electron.

(b) Cascade Multiplication of Decay Electrons

The cross sections for brehmsstrahlung and pair production used in the process of cascade multiplication are taken from the calculations of Bethe and Heitler.[8] These cross sections depend in general on the energy of the initiating particle (electron or photon). If $\phi(E, W)dW$ is the probability that an electron with energy E will produce a photon with energy between W and $W+dW$, and $\psi(W, E)dE$ the corresponding probability for pair production, the following expressions apply for the cross sections in the limit for high energies:

brehmsstrahlung,

$$\phi(v)dv=[1+(1-v)^2-(1-v)(2/3-2b)]dv/v; \quad (5)$$

pair production,

$$\psi(u)du=[u^2+(1-u)^2+u(1-u)(2/3-2b)]du; \quad (6)$$

[7] See, for example, reference 3.

[8] H. A. Bethe and W. Heitler, Proc. Roy. Soc. **46**, 83 (1934).

where E is the electron energy, W the photon energy, and $v=W/E$, $u=E/W$, with $b=0.0135$.[9] These expressions are valid for complete screening, and since they do not depend explicitly on the energy of the initiating particle, they are more tractable mathematically.

The ionization loss of the shower electrons will be included in the calculations. According to the Bloch formula, the ionization loss of a particle increases very slowly for energies higher than the rest energy, and consequently it can be considered as a constant a, which has the value of 10^8 ev per radiation unit in air.

At low energies, the Compton effect becomes a relatively important factor, but nevertheless this process can be neglected in these calculations because the energy range considered includes only energies higher than 5×10^7 ev.

(c) Collision Electrons

Electrons arising from close collision with mesotrons will also give a contribution to the observed number of electrons and, therefore, should not be neglected although the majority of the electrons resulting from this source is in the lower energy range (below 10^8 ev). The number of collision or "knock-on" electrons in equilibrium with mesotrons has been calculated with good approximation by Tamm and Belenky.[10] Since the average energy of the mesotrons at Mt. Evans is much lower than at sea level, their calculations show that the contribution to the soft component from this process is negligible for the electron energies considered here.

The following calculations were carried out for electron energies greater than 5×10^7 ev for altitudes of 14,618 feet corresponding to a depth of 14.3 radiation units below the top of the atmosphere.

Diffusion Equations

In order to derive the fundamental equations for the problem described above, let $\pi(E,t)dE$ represent the number of electrons whose energy lies between E and $E+dE$ at an atmospheric depth t below a certain depth t_0 where, supposedly, most of the mesotrons are formed. Similarly $\gamma(W,t)dW$ and $f(E',t)dE'$ will be used for the corresponding spectra of photons and mesotrons, respectively. The principle of continuity applied to these differential spectra for the present problem leads to the following diffusion equation,[11]

$$\frac{\partial\pi(E,t)}{\partial t}=-\int_0^1\left[\pi(E,t)-\frac{1}{1-v}\pi\left(\frac{E}{1-v},t\right)\right]\times\phi(v)dv+2\int_0^1\gamma\left(\frac{E}{u},t\right)\psi(u)\frac{du}{u}+a\frac{\partial\pi(E,t)}{\partial E}+F(E,t), \quad (7)$$

$$\frac{\partial\gamma(W,t)}{\partial t}=\int_0^1\pi\left(\frac{W}{v},t\right)\phi(v)\frac{dv}{v}-D\gamma(W,t), \quad (8)$$

where

$$F(E,t)=\int_E^\infty P(E',t)f(E',t)dE', \quad (9)$$

$$D=\int_0^1\psi(u)du, \quad (10)$$

with t measured vertically, and all energies being total energies.

Equations (7) and (8) are the same as the diffusion equations of shower theory, except for the additional term $F(E,t)$ in (7) which depends on the spectrum of the mesotrons. The equations can be extended to include the Compton effect; however, its inclusion into the diffusion equations complicates considerably the process of solving the equations.

The usual method of solving the diffusion equations of the shower theory shows that (7) and (8) have unique solutions since the solutions not including the term $F(E,t)$ vanish if there are no incident particles present at zero thickness. Also, in case the rest energy of the mesotron can be neglected in comparison with the energy E', one can prove that half the total energy given out by the mesotrons which disintegrate spontaneously appears in shower particles (electrons and photons).[12]

[9] B. Rossi and K. Greisen, Rev. Mod. Phys. **13**, 240 (1941).

[10] I. Tamm and S. Belenky, J. Phys. Acad. Sci. U.S.S.R. **1**, 177 (1939).

[11] The derivation is analogous to that found in H. J. Bhabha and W. Heitler, Proc. Roy. Soc. **159**, 432 (1937); J. T. Carlson and J. R. Oppenheimer, Phys. Rev. **51**, 220 (1937); H. Snyder, Phys. Rev. **53**, 960 (1938); R. Serber, Phys. Rev. **54**, 317 (1938) and summarized in reference 9.

[12] This is only true under the condition that we neglect the term representing the ionization loss of the electrons in the shower equations.

Solutions

The shower equations (7) and (8) can be solved by using Mellin transforms. The homogeneous equations [omitting the term $F(E,t)$] have been studied extensively in the shower theory, and the results of these theoretical calculations can be used in part in this problem.

Equations (7) and (8) transformed by the Mellin integrals are

$$\frac{\partial M_\pi(s,t)}{\partial t}=-A(s)M_\pi(s,t)+B(s)M_\gamma(s,t)+M_F(s,t), \quad (11)$$

$$\frac{\partial M_\gamma(s,t)}{\partial t}=C(s)M_\pi(s,t)-DM_\gamma(s,t),$$

where the ionization loss a has been assumed zero and M_π, M_γ, and M_F are the Mellin transforms of $\pi(E,t)$, $\gamma(W,t)$, and $F(E,t)$, respectively, taken with respect to the energies E and W. At the thickness $t=0$, the transforms are denoted by $M_\pi(s,0)$ and $M_\gamma(s,0)$, and represent the boundary conditions. If $F(E,t)$ vanishes, (7), (8), and (11) represent the equations of showers produced by an incident spectrum of electrons or photons. However, if $F(E,t)$ does not vanish, the solutions of (11) are similarly obtainable by direct mathematical means. It is then possible to apply the inverse transformation to these solutions which gives the shower functions $\pi(E,t)$ and $\gamma(W,t)$ when the ionization loss is neglected. Having found these preliminary solutions, it is possible to construct the solutions for Eqs. (7) and (8) which include ionization loss.

With the same independent variable E for the electron and photon energies, the complete solutions, in matrix notation, are[13]

$$\begin{pmatrix}\pi(E,t')\\ \gamma(E,t')\end{pmatrix}=\frac{1}{2\pi i}\int_c ds\frac{E^{-(s+1)}}{\lambda_1(s)+\lambda_2(s)}\Bigg\{e^{\lambda_1(s)t'}\begin{pmatrix}[\lambda_1(s)+D]p_1(s,E/a) & B(s)p_1(s,E/a)\\ C(s)g_1(s,E/a) & -[\lambda_2(s)+D]g_1(s,E/a)\end{pmatrix}$$

$$\times\begin{pmatrix}M_\pi(s,0)+\int_0^{t'}M_F(s,t)e^{\lambda_1(s)t}dt\\ M_\gamma(s,0)\end{pmatrix}-e^{\lambda_2(s)t'}\begin{pmatrix}[\lambda_2(s)+D]p_2(s,E/a) & B(s)p_2(s,E/a)\\ C(s)g_2(s,E/a) & -[\lambda_1(s)+D]g_2(s,E/a)\end{pmatrix}$$

$$\times\begin{pmatrix}M_\pi(s,0)+\int_0^{t'}M_F(s,t)e^{\lambda_2(s)t}dt\\ M_\gamma(s,0)\end{pmatrix}\Bigg\} \quad (12)$$

where the functions $\lambda_1(s)$ and $\lambda_2(s)$ are the roots of the equation

$$[\lambda+A(s)][\lambda+D]-B(s)C(s)=0; \quad (13)$$

the functions $p_j(s,E/a)$ and $g_j(s,E/a)$ are given by

$$p_j(s,x)=\frac{1}{2\pi i}\int_{c'}\frac{\Gamma(-r)\Gamma(s+r+1)}{\Gamma(s+1)}\times K_j(s,r)x^{-r}dr, \quad (j=1,2)$$

$$g_j(s,x)=\frac{1}{2\pi i}\int_{c'}\frac{\Gamma(-r)\Gamma(s+r+1)}{\Gamma(s+1)}\times\frac{C(s+r)}{C(s)}K_j(s,r)x^{-r}dr; \quad (14)$$

and $K_j(s,r)$ is determined by the equation

$$\left[\lambda_j(s)+A(s+r)\frac{B(s+r)C(s+r)}{\lambda_j(s)+D}\right]\times K_j(s,r)=rK_j(s,r-1) \quad (15)$$

with the condition

$$K_j(s,0)=1.$$

The paths of integration are lines parallel to the imaginary axis, the path of integration c lying to the right of the origin and the path c' to the left, both lying in a region where the respective integrals converge.

The formal solution (12) becomes the solution

[13] The notation here is the same as that usually used in shower theory, see reference 9.

usually found for showers originating from single particles when $M_\gamma=0$. If the functions p_j and g_j, which are introduced because of the ionization loss of the electrons, are placed equal to unity, the solutions go over into those in which the ionization loss has been neglected.

The boundary conditions for the problem considered here are

$$M_\pi(s,0)=M_\gamma(s,0)=0, \tag{16}$$

which mean that the contribution to the soft component from primary electrons and photons incident at the top of the atmosphere is negligible at a depth of 14.3 radiation units or more. By introducing a known spectrum of mesotrons into (12), the line integrals can be evaluated approximately by the saddle point method. In all the following calculations, only the function $\pi(E,t)$ which refers to the electron spectrum will be considered.

For the differential spectrum of mesotrons, a power law of the following form is assumed,

$$f(E',t)dE'=N(t)E'^{-n}dE', \quad E'>E'' \tag{17}$$

with $2.5<n<3.0$ and $E''=3.8\times10^8$ ev.[14] The function $N(t)$ can be calculated from the measured spectrum. Such a law applies closely for depths corresponding to Mt. Evans and would apply as well or better for smaller depths. For greater depths, this simple law will no longer be true because a maximum in the mesotron spectrum appears at energies higher than 3.8×10^8 ev, this being especially pronounced close to sea level.

As pointed out above, the contribution of electrons arising from mesotrons with energies lower than 3.8×10^8 ev to the soft component will be small since they will not have sufficient energy to multiply appreciably in air, thus allowing the spectrum to be broken at this value.

Introducing the boundary conditions and mesotron spectrum mentioned above into Eqs. (12), one obtains for the differential spectrum of the electrons the following expression,

$$\pi(E,t)=\frac{\mu\alpha}{\tau_0 c}\frac{1}{EE''^n}\frac{1}{2\pi i}\int_0^t\frac{N(t')dt'}{(t'+t_0)}\times\int_c\frac{\lambda_1(s)+D}{(s+1)(n-s)[\lambda_1(s)-\lambda_2(s)]}\times p_1(s,E/a)(E''/E)^s e^{\lambda_1(s)(t-t')}ds, \tag{18}$$

where the path of integration is a line parallel to the imaginary axis. The intercept of this line with the axis of reals is such that $0<R(s)<n$. A similar expression can be obtained for the differential photon spectrum.

Since the mathematical procedure depends on the relative values of E and E'', two possible cases must be considered.

$$(a).\ E<E''$$

In this case, the integrand becomes positively infinite for $s=0$ and for $s=n$, and the method of the saddle point can be used. The saddle point for the integrand in (18) is determined by the equation

$$\lambda_1'(s)(t-t')+\log(E''/E)+\frac{2s-(n-1)}{(s+1)(n-s)}=0, \tag{19}$$

which gives the value of s. Using this method in evaluating the inner integral in (18), one finds finally that the differential electron spectrum is given by the expression,

$$\pi(E,t)=\frac{1}{\sqrt{2\pi}}\frac{\mu\alpha}{\tau_0 c}\frac{1}{EE''^n}\int_0^t\frac{N(t')}{(t'+t_0)}\times\frac{\lambda_1(s)+D}{(s+1)(n-s)[\lambda_1(s)-\lambda_2(s)]}\times\left(\lambda_1''(s)(t-t')+\frac{2(s+1)(n-s)+[2s-(n-1)]^2}{(s+1)^2(n-s)^2}\right)^{-\frac{1}{2}}\times p_1(s,E/a)(E''/E)^s e^{\lambda_1(s)(t-t')}dt'. \tag{20}$$

$$(b).\ E>E''$$

For these values of E, the method of residues can be used since there is a single pole in the

[14] Such a spectrum is in good agreement with the experimental data on the zenith angle distribution of mesotrons and also with balloon and aeroplane experiments on the mesotron intensity.

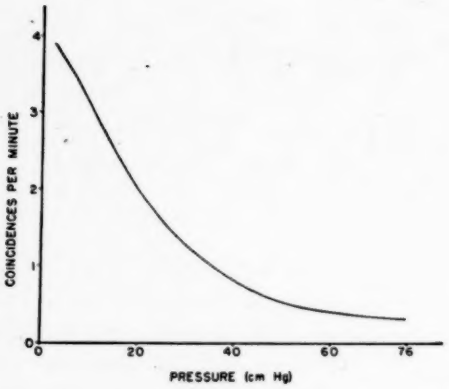

FIG. 2. The mesotron intensity as a function of atmospheric pressure, determined by Schein, Jesse, and Wollan. Ordinates represent the number of mesotrons per minute received in a vertical direction and able to penetrate 18 cm of lead. Abscissae represent atmospheric pressure.

positive half-plane at the point $s=n$, and the integrand vanishes for large real values of s. Consequently,

$$\pi(E,t)=\frac{\mu\alpha}{\tau_0 c}\frac{1}{E^{n+1}}\times\frac{\lambda_1(n)+D}{(n+1)[\lambda_1(n)-\lambda_2(n)]}p_1(n,E/a)\times\int_0^t\frac{N(t')e^{\lambda_1(n)(t-t')}}{t'+t_0}dt'. \quad (21)$$

The expressions (20) and (21) for the electron spectrum are considered as the final solutions of the problem treated here. Both integrals can be evaluated numerically and the corresponding spectrum of the electrons found. The actual comparison of the magnitudes of the two expressions using $E''=3.8\times10^8$ ev shows that (21) contributes only a very small part to the integral spectrum for values of E less than 10^8 ev.

Comparison with Experiments

In Fig. 2 the intensity of the mesotrons is shown for an absorber thickness of 18 cm of lead as a function of atmospheric pressure.[2] The minimum energy of the mesotrons recorded in these experiments was 3.8×10^8 ev. With these data, the integration of expression (17) will give the coefficient of the energy spectrum $N(t)$.

To calculate the electron spectrum for the altitude of Mt. Evans, the numerical quantities

TABLE I. Data used in the computations.

Mean life of the mesotron	$\tau_0=2.15\times10^{-6}$ sec.
Mass of the mesotron	$\mu=10^8$ ev
Barometric constant	$\alpha=7.2\times10^5$ cm
Depth	$t=14.3$ radiation units
Exponent (mesotron spectrum)	$n=2.5$, 2.6, and 3.0
Cut-off energy (mesotron spectrum)	$E''=3.8\times10^8$ ev

Vertical incidence

listed in Table I were used in the solutions (20) and (21). For vertical rays, the differential spectrum of electrons as calculated from (20) is shown in Fig. 3 for two different values of the exponent n in the mesotron spectrum, and for three different mesotron cut-off energies E''. In the two lower curves for the energies $E''=10^9$ ev and $E''=2\times10^9$ ev the value of n was taken as 2.6, and in the two upper curves, n was taken as 2.5 and 3.0 with a cut-off energy of $E''=3.8\times10^8$ ev.

The upper curves show clearly that the spectrum of the electrons arising from the decay of mesotrons does not depend very strongly on the value of the exponent n in the mesotron spectrum. Comparing the areas under the curves, one can see that the majority of the electrons in the lower atmosphere arise from mesotrons with energies lower than 10^9 ev. The electron spectrum rises sharply for lower energies, i.e., most of the decay electrons have energies below 10^8 ev, and hence one cannot expect any large number of

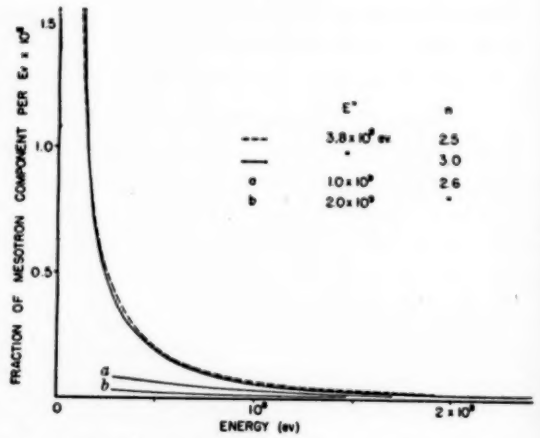

FIG. 3. The differential electron spectrum for an atmospheric depth of 14 radiation units. Ordinates are $\pi(E,t)$ and the abscissae are the electronic energy E. The curves show the changes in character resulting from variation in the exponent (n) of the power law for the mesotron spectrum and the cut-off energy (E'').

high energy electrons to be present in the lower atmosphere.

Since these calculations give only the number of electrons arising from the disintegration of mesotrons of energy greater than 3.8×10^8 ev, it is necessary to include further additional processes which contribute to the soft component in the lower atmosphere.

(a). First one must consider the electrons originating from the decay of mesotrons with energies below 3.8×10^8 ev. To calculate their number, the mesotron spectrum for energies below this limit must be known. Unpublished measurements of Hall give the approximate shape of the mesotron spectrum at Mt. Evans for energies below 10^9 ev.[15] A similar shape of the spectrum is indicated in the aeroplane experiments of Schein, Wollan, and Grotzinger[16] which were carried out at an altitude of about 7000 m. Using these data, the contribution of decay electrons arising from mesotrons of lower energies was calculated by means of Eq. (4) taking ionization loss into consideration.

(b). A further contribution to the soft component arises from collision electrons in equilibrium with mesotrons. The spectrum of these electrons was calculated by Tamm and Belenky.[8] Their data could be used for estimating the maximum contribution of knock-on electrons to the calculated number of electrons arising from the decay.

The integral spectrum of electrons resulting from all the different processes which were considered here are represented in Fig. 4. Curve *A* represents the integral spectrum calculated from Eqs. (21) and (22) for $n=2.5$ whereas curve *B* represents the same spectrum for $n=3.0$. However, the influence of the knock-on electrons in the integral spectrum of electrons down to an energy of about 5.0×10^7 is negligible as the average energy of the mesotrons at Mt. Evans is considerably lower than that at sea level and practically all knock-on electrons have energies below this value. Since experimental data are obtainable for energies only down to 7×10^7 ev, the knock-on electrons can be neglected. This is

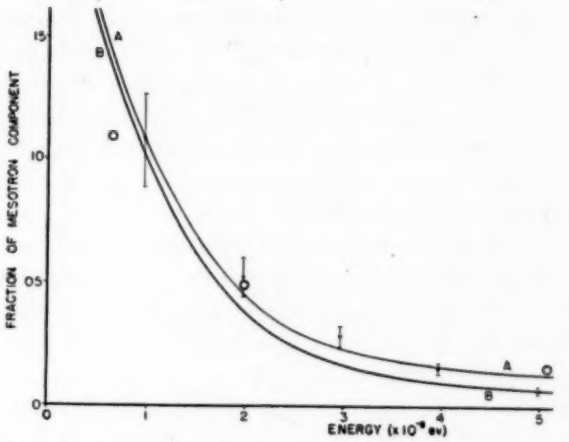

FIG. 4. The integral electron spectrum for an atmospheric depth of 14 radiation units and vertical incidence. Points indicated by O represent the results of Hall on Mt. Evans, and $\frac{1}{4}$ represent normalized results obtained by Hazen at an altitude of 10,000 ft.

in very good agreement with recent experiments on knock-on electrons by Hazen on Mt. Evans.[17]

If all the electrons in the lower atmosphere arise from the mesotron component, then the curves of Fig. 4 should represent the measured integral spectrum of electrons on Mt. Evans for vertical incidence. D. Hall carried out careful investigations of the penetration and shower production of electrons in different thicknesses of lead on Mt. Evans, and his data can be used for comparison with the present calculations. He determined the number of electrons which penetrated a given thickness of lead whereby the electron was identified by its property of producing a cascade shower in about 3 radiation units of lead. To obtain the integral spectrum from such experiments, it is necessary to calculate the minimum energy an electron must have to penetrate a given thickness of lead. This calculation was carried out for three different thicknesses (1.5 cm, 3.5 cm, 5.5 cm of lead) used in Hall's experiments.[18] By using this procedure, Hall's data for electrons are represented by the circles in Fig. 4. All of the ordinates

[15] The author is greatly indebted to Dr. Hall for communication of his data.

[16] M. Schein, E. O. Wollan, and G. Grotzinger, Phys. Rev. **58**, 1026 (1940).

[17] W. Hazen, Phys. Rev. **64**, 7 (1943).

[18] The minimum energy of an electron which is necessary so that at least one particle will emerge below the lead thickness was determined by shower theory including ionization loss. The values found were:

Lead thickness	Min. energy
1.5 cm	4×10^7 ev
3.5	2×10^8
5.5	5.5×10^8.

are fractions of the total intensity of the mesotrons of all energies at Mt. Evans, which has been adjusted to unity. If we use this normalization, the measurements of Hall give the value of 0.66 for the intensity of the mesotrons passing through 18 cm of lead or having an energy greater than 3.8×10^8 ev.

As shown in Fig. 4, the theoretical results are in approximate agreement with the experimental data for the higher electron energies. However, below 10^8 ev the calculations become more complicated and their reliability is also in question. Similarly the experimental evidence for electrons with low energies is uncertain because electron identification becomes more difficult because of the fact that their ability to produce cascade showers is greatly reduced.

Recently Hazen[19] has made cloud-chamber measurements of the soft component of cosmic rays at an altitude of 10,000 ft. By the method used, the number of electrons could be estimated by counting the showers produced in the eight lead plates placed in the chamber. Photons could be identified by showers but with the absence of an initiating ionizing particle, and mesotrons were counted by means of their characteristic sharp tracks and the absence of accompanying showers. This way, Hazen was able to determine the number of electrons with energies greater than 10^8 ev, and from a study of the subsequent showers, the energy of each individual electron could be determined.

The results of the experiment showed that the total soft component for energies greater than 2×10^8 ev was seven percent of the penetrating radiation. Of this soft component, 2.5/3.5 was electronic in nature. Consequently, the total number of electrons greater than 2×10^8 ev is about five percent of the total penetrating radiation. This value is in good agreement with the results of Hall's experiments and the value given by the calculations. Hazen was able to determine the energy spectrum of these electrons also, and a further experimental check of the theory is therefore possible although the comparison can only be considered as approximate. The results are shown in Fig. 4 together with those found by Hall.

There are two things which must be considered in Hazen's results. First, the solid angle open to electrons in the measurements of the soft component was presumably large and since zenith angle variations in intensity have not been calculated in the present paper, corrections for this effect have not been made. Second, the difference in altitude between the point where the calculations apply and the one used by Hazen, which amounts to two radiation units in atmospheric depth, is going to modify the mesotron spectrum slightly. In first approximation, however, the same exponent in the power law of the mesotron spectrum will apply to both locations. This means that the electrons generated by the mesotrons would have nearly the same energy distribution in both cases, their total numbers being in direct proportion to the total numbers of the mesotrons which produce them.

The writer wishes to express his gratitude and indebtedness to Dr. M. Schein for careful collaboration and guidance during the course of this investigation.

[19] W. Hazen, Phys. Rev. **65**, 67 (1944).

PHYSICAL REVIEW VOLUME 66, NUMBERS 3 AND 4 AUGUST 1 AND 15, 1944

Effect of Iron Tube on Its Magnetizing Field

S. T. LIN
National Research Institute of Physics, Academia Sinica, Kunming, China
(Received April 6, 1944)

It has been found that when an iron tube is magnetized along its length in a uniform field the intensities inside as well as outside the tube are reduced by some amounts which depend upon the intensity of magnetization. This is also true for the field outside an iron rod. From the distribution of the intensities of magnetization along the tube, which are experimentally determined, the amounts of reduction of the magnetic fields may be calculated by applying Würschmidt's theory of the demagnetizing factor. The theoretical values are in good agreement with those obtained through experiments.

1. INTRODUCTION

WALL[1] found that when a long steel tube is placed in a uniform magnetic field the intensity of the field H inside the tube is reduced. His results are as follows:

"(1) The reduction of the value of H inside the tube becomes greater as the thickness of the wall increases.

"(2) The reduction of H within the tube is a maximum when the tube is magnetized to a condition which about corresponds to the knee of the magnetization curve.

"(3) When the tube is magnetized to a condition of saturation, the value of H within the tube is practically unaffected by the material of the tube."[2]

From these facts Wall concluded that "one aspect of the classical theory of magnetization is incorrect,"[2] and that "the magnetization of a material is initiated at the surface and proceeds inwards by a kind of 'chain effect,' so that the flux density near the surface is a maximum and becomes progressively less as the distance from the surface increases."[2]

It was thought that the diminution of H inside a tube might be accounted for by the demagnetizing effect of the tube itself. Since, unless the tube is infinitely long, the applied magnetizing field would be affected by the free poles induced on its end surfaces, these free poles would have different effects at different points in space. Consequently, the magnetizing field, and hence the intensity of magnetization of the tube, would be non-uniform along its length. In general, the intensity is high and uniform in the central portion and becomes gradually lower and less uniform towards the two ends. The range of uniform region depends upon the intensity of magnetization, being of a minimum at about the knee of the magnetization curve and of a maximum at saturation.

The non-uniformity of magnetization appears to indicate that the free poles reside not only on the end surfaces, but are also distributed along the whole length of the tube. All these free poles give rise to their own field. The resultant field in the neighborhood of the tube is, in general, the vectorial sum of three parts, namely, the applied field, the field due to the free poles induced on the two end surfaces, and that due to the free poles distributed along the whole length of the tube. The last two are usually collectively called the demagnetizing field on account of their direction being opposite to that of the applied one. For a long tube the effect of the second part of the demagnetizing field on the central portion of the tube is larger than that of the first. Apparently the demagnetizing effect due to the distributed free poles other than those on the two end surfaces was not taken into consideration in Wall's experiment, although he mentioned that the demagnetizing effect was negligibly small. Thus it is quite reasonable to assume that the reduction of the applied field is simply another expression of the demagnetizing effect of the whole tube. If this is true, the applied field outside the tube should also be reduced. It will be seen later that the experimental results confirm this prediction.

[1] Wall, Nature **142**, 1039 (1938).
[2] Wall, Nature **143**, 331 (1939).

2. THEORY

According to Würschmidt's[3] theory, the demagnetizing field of a tube of finite dimension can be calculated in the following way. The distribution function of the intensity of magnetization of the tube magnetized along its axis in a uniform field is given by the relation,

$$I=I_0\{1-C_2(x/a)^2-C_4(x/a)^4-C_6(x/a)^6-\cdots\}, \quad (1)$$

where I is the intensity of magnetization at a position whose distance from the middle of the tube is x; I_0, the intensity of magnetization at the middle; a, the half-length of the tube, and C_2, C_4, C_6, etc., the constants to be determined from experiments. The free poles induced in the section dx at position x from the middle of the tube is

$$\pi b^2\frac{dI}{dx}dx=-\frac{2\pi b^2}{a^2}I_0\left(C_2x+\frac{2C_4x^3}{a^2}+\frac{3C_6x^5}{a^4}+\cdots\right)dx,$$

in which πb^2 is the cross-sectional area of the tube. The free poles induced on the two end surfaces are $\pm\pi b^2I_0(1-C_2-C_4-C_6-\cdots)$. Assuming the free poles to be concentrated along the axis of the tube, we find that the demagnetizing field in the central portion, near the inner (or outer) surface and in the direction of the axis, is:

$$H_d=-\frac{2\pi b^2}{a^2}I_0\left\{\int_{-a}^{a}\frac{C_2x^2dx}{(x^2+R^2)^{\frac{1}{2}}}+\int_{-a}^{a}\frac{2C_4x^4dx}{a^2(x^2+R^2)^{\frac{1}{2}}}+\int_{-a}^{a}\frac{3C_6x^6dx}{a^4(x^2+R^2)^{\frac{1}{2}}}+\cdots+(1-C_2-C_4-C_6-\cdots)\right\}, \quad (2)$$

where R is the inner (or outer) radius of the tube.

[3] J. Würschmidt, *Theorie des Entmagnetisierungsfaktors und der Scherung von Magnetisierungskurven* (Vieweg, Braunschweig, 1925).

Consider the general term of Eq. (2):

$$D_{2n}=\int\frac{x^{2n}dx}{(x^2+R^2)^{\frac{1}{2}}} \quad (n=1, 2, 3, \text{etc.})$$

$$=-\frac{x^{2n-1}}{(x^2+R^2)^{\frac{1}{2}}}+(2n-1)\int\frac{x^{2n-2}dx}{(x^2+R^2)^{\frac{1}{2}}}$$

$$=-\frac{x^{2n-1}}{(x^2+R^2)^{\frac{1}{2}}}+(2n-1)(D_{2n}+R^2D_{2n-2}),$$

$$\left(D_{2n-2}=\int\frac{x^{2n-2}dx}{(x^2+R^2)^{\frac{1}{2}}}\right).$$

Collecting all the terms for different n's in succession, introducing the limits of integration, and neglecting the terms containing R, which is small compared with a, we have

$$\int_{-a}^{a}\frac{x^2dx}{(x^2+R^2)^{\frac{1}{2}}}=-2+\log\frac{2}{\beta} \quad \left(\beta=\frac{R}{a}\right), \quad (3)$$

$$\int_{-a}^{a}\frac{x^4dx}{(x^2+R^2)^{\frac{1}{2}}}=a^2, \quad (4)$$

$$\int_{-a}^{a}\frac{x^6dx}{(x^2+R^2)^{\frac{1}{2}}}=\frac{1}{2}a^4. \quad (5)$$

From Eqs. (2) and (3)–(5), we get

$$H_d=-\frac{2\pi b^2}{a^2}I_0\left\{1+2C_2\left(\log\frac{2}{\beta}-\frac{3}{2}\right)+C_4+\frac{1}{2}C_6+\cdots\right\}. \quad (6)$$

Hence the demagnetizing field H_d is a function of the cross-sectional area, the length of the tube I_0, and the constants C_2, C_4, C_6, etc.

3. EXPERIMENTS

(a) Determination of the Magnetic Field Inside the Tube

A uniform field was produced by a solenoid of 120 cm in length and 5.3 cm in inner diameter. The iron tube used was an ordinary water pipe reduced to a uniform thickness and having a length of 60.8 cm, outside diameter of 2.48 cm, and inside diameter of 2.29 cm. It was placed coaxially with, and in the middle of, the solenoid.

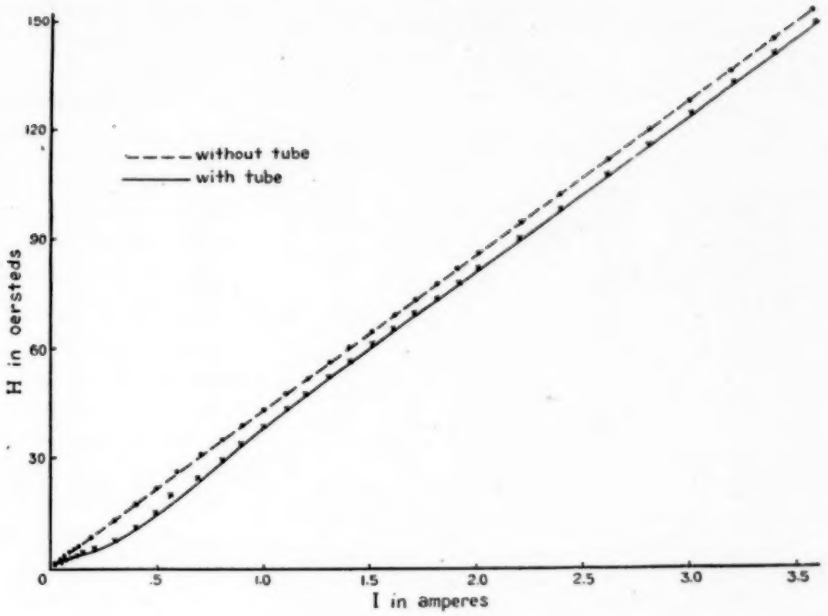

FIG. 1. The magnetic field H inside the tube as a function of the exciting current I.

A search coil was wound on a fiber frame large enough to be readily slipped into the middle of the tube. The field was measured by the ballistic method as usual.

Before taking readings the tube was demagnetized. The exciting current ranging from 0 to 3.6 amperes was applied in 33 steps. For each step the reversal throw of the galvanometer deflection was observed, and the mean of the two deflections was used in calculation.

The iron tube was then removed, but the search coil kept in the original position. These observations were repeated. The magnetic fields thus determined are plotted in Fig. 1 against the exciting current.

It is seen that the two curves are similar to those obtained by Wall. The only difference is that the two curves do not run as close together at high exciting currents as do Wall's. This is probably due to the smaller dimensional ratio

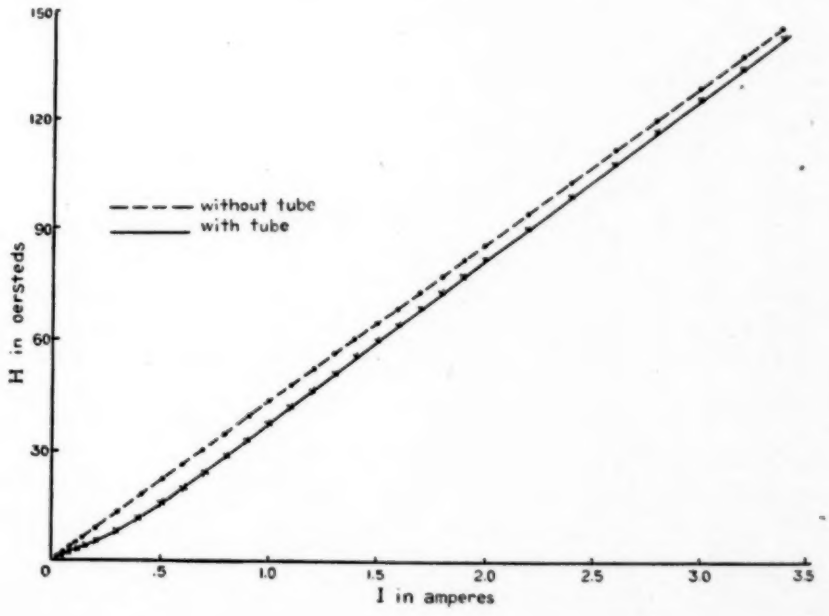

FIG. 2. The magnetic field H outside the tube as a function of the exciting current I.

TABLE Ia. Magnetic field outside the rod. Search coil at the middle of the rod.

Exciting current in amperes	Magnetic field in oersteds		Percent reduction of $\frac{H-He}{H}\times 100$
	H (without tube)	He (with tube)	
0.06	2.67	2.64	1.01
0.10	4.40	4.31	2.05
0.20	8.65	7.53	12.96
0.40	17.34	16.27	6.17
0.60	26.10	25.30	3.07
0.80	34.72	34.00	2.07
1.0	43.44	42.74	1.61
1.2	51.91	51.21	1.35
1.4	60.21	39.64	0.95
1.6	68.61	67.88	1.06
1.8	77.19	76.24	1.10
2.0	85.28	84.62	0.77
2.2	94.77	94.57	0.21
2.4	103.05	102.86	0.18

TABLE Ib. Magnetic field outside the rod. Search coil at 25 cm from one end of the rod.

Exciting current in amperes	Magnetic field in oersteds		Percent reduction of $\frac{H-He}{H}\times 100$
	H (without tube)	He (with tube)	
0.06	2.67	2.64	1.09
0.10	4.38	4.28	2.15
0.20	8.64	7.16	17.07
0.30	12.97	10.32	20.43
0.40	17.30	14.72	14.89
0.60	25.21	24.41	3.17
0.80	34.36	33.27	3.16
1.0	42.93	41.83	2.56
1.1	47.02	46.09	1.98
1.3	55.58	54.49	1.96
1.4	60.05	59.09	1.60
1.6	68.14	67.42	1.08
1.8	76.46	75.93	0.69
2.0	84.80	84.54	0.31
2.2	92.85	92.66	0.21
2.4	102.51	102.34	0.17

TABLE Ic. Magnetic field outside the rod. Search coil at 15 cm from one end of the rod.

Exciting current in amperes	Magnetic field in oersteds		Percent reduction of $\frac{H-He}{H}\times 100$
	H (without tube)	He (with tube)	
0.06	2.62	2.52	3.78
0.10	4.32	4.04	6.39
0.14	6.41	5.42	12.29
0.20	8.49	6.63	21.93
0.30	12.74	8.31	34.82
0.40	16.99	10.83	36.29
0.60	25.37	18.33	27.75
0.80	33.69	27.58	18.15
1.0	42.07	37.76	10.25
1.1	46.22	42.30	8.49
1.3	54.71	51.12	6.56
1.4	59.05	55.65	5.79
1.6	67.07	64.04	4.52
1.8	75.56	72.14	4.53
2.0	83.28	80.19	3.71
2.2	90.33	86.83	3.88
2.4	99.23	95.73	3.53

(length/diameter) of the tube investigated in the present case.

(b) Determination of the Magnetic Field Outside the Tube

In this experiment the same solenoid and the same iron tube as in (a) were used. The search coil is, however, quite different from the previous one. It consists of a differential coil with two separate windings of equal number of turns wound one upon another in opposite sense. Any change of magnetic flux inside the inner layer of the winding will induce no e.m.f. in the two windings as a whole, but any change of flux in between the inner and outer layers of the coil will induce an e.m.f. By inserting a long solenoid of a small cross section in the differential coil and by adjusting the number of turns of the coil windings, compensation can be rendered complete.

The field in the middle and on the outside of the tube was measured with this differential search coil. Measurements were repeated with the coil kept in the same position while the tube was removed. The results are shown in Fig. 2. Curves in Figs. 1 and 2 are remarkably similar.

(c) Determination of the Magnetic Field Outside an Iron Rod

Since the magnetic field outside the tube is reduced, it is to be naturally expected that the field outside an iron rod should also be reduced. A long Armco iron rod, 80 cm in length and 0.6 cm in diameter, was tested in the same way as in experiment (b). Three experiments were performed. In the first the differential coil was placed in the middle of the rod, in the second and the third, at 25 cm and 15 cm from one end of the rod, respectively. The intensities of the magnetic fields thus determined and the amounts of percent reduction calculated from them are given in Tables Ia–c and the curves plotted against exciting current and against exciting field are shown in Figs. 3 and 4.

(d) Determination of the Intensities of Magnetization Along the Tube

For this experiment the same solenoid and iron tube as used in experiments (a) and (b) were

TABLE II. Distribution of intensity of magnetization along the tube. x = distance from the middle of the tube. a = half-length of the tube. I_0 = intensity of magnetization at the middle of the tube. I = intensity of magnetization at distance x from the middle of the tube. H = magnetizing field in oersteds.

				I/I_0									I/I_0				
x/a	H=0.95	1.81	3.52	6.10	8.70	17.28	25.80	38.67	x/a	H=51.57	64.35	72.88	81.61	94.02	110.98	119.51	136.62
0	1.00	1.00	1.00	1.00	1.00	1.00	1.00	1.00	0	1.00	1.00	1.00	1.00	1.00	1.00	1.00	1.00
0.07	1.00	1.00	0.99	0.99	0.99	0.99	0.99	1.00	0.07	1.00	1.00	1.00	1.00	1.00	1.00	1.00	1.00
0.14	0.98	0.98	0.98	0.97	0.97	0.98	0.98	0.99	0.14	0.99	1.00	1.00	1.00	1.00	1.00	1.00	1.00
0.22	0.97	0.96	0.95	0.95	0.95	0.96	0.97	0.98	0.22	0.99	1.00	1.00	1.00	1.00	1.00	1.00	1.00
0.29	0.96	0.93	0.93	0.92	0.92	0.94	0.95	0.97	0.29	0.98	0.99	0.99	1.00	1.00	1.00	1.00	1.00
0.36	0.94	0.91	0.89	0.89	0.89	0.91	0.92	0.95	0.36	0.97	0.98	0.99	0.99	1.00	1.00	1.00	1.00
0.43	0.90	0.89	0.85	0.84	0.85	0.87	0.89	0.93	0.43	0.95	0.97	0.98	0.99	0.99	1.00	1.00	1.00
0.51	0.88	0.83	0.80	0.79	0.80	0.82	0.85	0.90	0.51	0.93	0.96	0.96	0.98	0.98	0.99	0.99	1.00
0.58	0.83	0.78	0.75	0.74	0.74	0.77	0.81	0.85	0.58	0.90	0.93	0.94	0.96	0.97	0.98	0.98	0.99
0.65	0.77	0.72	0.68	0.67	0.67	0.70	0.74	0.80	0.65	0.85	0.89	0.90	0.93	0.94	0.95	0.96	0.97
0.72	0.70	0.65	0.61	0.59	0.60	0.63	0.67	0.73	0.72	0.78	0.83	0.85	0.88	0.90	0.92	0.93	0.94
0.76			0.56	0.55	0.55	0.58	0.61	0.69	0.76	0.74	0.79		0.84		0.90	0.91	
0.79	0.62	0.56	0.52	0.50	0.51	0.54	0.57	0.64	0.79	0.69	0.74	0.77	0.80	0.83	0.86	0.87	0.89
0.83	0.55	0.51	0.47	0.45	0.45	0.48	0.52	0.58	0.83	0.64	0.69	0.70	0.74	0.77	0.81	0.82	0.84
0.87	0.51	0.45	0.41	0.39	0.40	0.42	0.46	0.52	0.87	0.57	0.62	0.64	0.68	0.70	0.74	0.76	0.78
0.90	0.44	0.39	0.35	0.33	0.33	0.36	0.39	0.44	0.90	0.49	0.53	0.55	0.59	0.61	0.66	0.66	0.68
0.92									0.92	0.44	0.50		0.54	0.56	0.60		0.63
0.94	0.53	0.31	0.28	0.26	0.26	0.28	0.31	0.35	0.94	0.39	0.43	0.44	0.48	0.50	0.54	0.54	0.56
0.95	0.32	0.29	0.26	0.24	0.24	0.26	0.29	0.33	0.95	0.37	0.40	0.42	0.45	0.47	0.51	0.52	

again used. A search coil of small length was prepared, which can slide freely on the tube. After demagnetizing the tube, the exciting field was increased from 0 to 138 oersteds in sixteen steps. For each step the field was kept constant and the intensities of magnetization at different positions, at 1 or 2 cm apart, were measured. Sixteen sets of data are given in Table II where the values I/I_0 are expressed in terms of galvanometer deflections when the search coil was placed in the middle and at any other position x/a. Eight out of sixteen sets of data are plotted in Fig. 5 showing the distribution of intensity of magnetization along the tube.

4. CALCULATION OF THE DEMAGNETIZING FIELD

The demagnetizing field is calculated from Eq. (6) in which the constants c's are determined by Eq. (1). As the terms involving the power of x/a greater than 8 are negligibly small, it will be sufficiently accurate to use four terms in Eq. (1) for calculating the value of I/I_0. For the sake of simplicity, replacing any three of the values of x/a in Eq. (1) by A, B, and D and the corresponding values of $1-I/I_0$ by E, F, and G, respectively, we obtain the following three simultaneous linear equations:

$$E=A^2C_2+A^4C_4+A^6C_6,$$

$$F=B^2C_2+B^4C_4+B^6C_6,$$

and

$$G=D^2C_2+D^4C_4+D^6C_6.$$

Solving for C's in terms of A, B, D, E, F, and G and substituting the actual values of x/a and the corresponding values of I/I_0 given in Table II, we obtain the numerical values of C's, which are given in Table III. The value of I_0 in Eq. (6) is computed on the assumption that the effective field within the material is the same as that in the free space inside the tube.

The demagnetizing fields both inside and outside the tube and the corresponding percent reduction for different exciting fields are calculated and given in Table III. For comparison the percent reduction of the exciting field obtained through experiments and that by calculation are plotted in Figs. 6 and 7. It is evident that in

TABLE III. Demagnetizing field inside and outside the tube. H_i = exciting field inside the tube in oersteds. H_0 = exciting field outside the tube in oersteds. C_2, C_4, C_6 = constants. H_{di} = demagnetizing field inside the tube in oersteds. H_{d0} = demagnetizing field outside the tube in oersteds. $H_{di}/H_i\times100$ = percent reduction of the exciting field inside the tube. $H_{d0}/H_0\times100$ = percent reduction of the exciting field outside the tube.

H_i	H_0	C_2	C_4	C_6	H_{di}	H_{d0}	$(H_{di}/H_i)\times100$	$(H_{d0}/H_0)\times100$
0.95	0.95	0.58	−0.50	0.81	0.10	0.10	10.40	10.17
1.81	1.81	0.82	−0.79	0.89	0.33	0.32	18.12	17.65
3.53	3.52	1.08	−1.40	1.35	1.13	1.10	32.09	31.19
6.11	6.10	1.09	−1.30	1.23	2.59	2.51	42.43	41.15
8.70	8.70	1.09	−1.37	1.32	3.98	3.85	45.67	44.27
17.37	17.21	0.88	−0.86	0.97	6.51	6.18	37.46	35.91
25.92	25.70	0.69	−0.52	0.76	7.03	6.84	27.14	26.64
38.79	38.55	0.37	0.09	0.38	6.02	5.91	15.52	15.32
51.62	51.36	0.23	0.09	0.50	5.20	5.12	10.08	9.98
64.50	64.20	0.08	0.27	0.41	4.11	4.08	6.37	6.36
73.03	72.76	0.06	0.16	0.54	4.10	3.87	5.61	5.32
81.78	81.44	−0.004	0.24	0.46	3.34	3.34	4.08	4.10
93.51	94.53	0.004	0.10	0.57	3.25	3.26	3.48	3.44
110.24	111.71	0.020	−0.08	0.69	3.20	3.19	2.90	2.86
118.69	120.32	0.001	0.06	0.66	3.28	3.28	2.82	2.72
135.49	137.75	0.004	−0.11	0.68	2.96	2.96	2.19	2.15

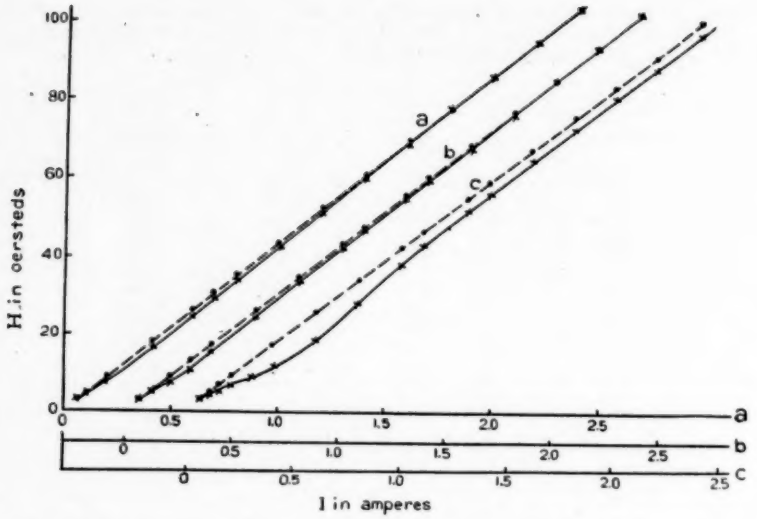

FIG. 3. The magnetic field H outside the rod as a function of the exciting current I. a, the search coil is in the middle of the rod; b and c, the search coils are at 25 cm and 15 cm from one end of the rod, respectively. The upper I axis is for curve a, the middle for curve b, and the lower for curve c. The dotted line represents the field without the rod; the solid line represents the field with the rod.

each case the theoretical and experimental curves nearly coincide, except in the central part where the former is a little higher than the latter.

5. DISCUSSION

The reduction of the magnetic field outside the tube or rod as shown in Fig. 2 or Fig. 3 can hardly be explained by Wall's theory of magnetization. It is merely a necessary consequence of the theory of demagnetization; for the free poles should produce their demagnetizing effect in the whole space. The striking similarity of the two pairs of curves, shown in Figs. 1 and 2, strongly support this argument. Furthermore, it

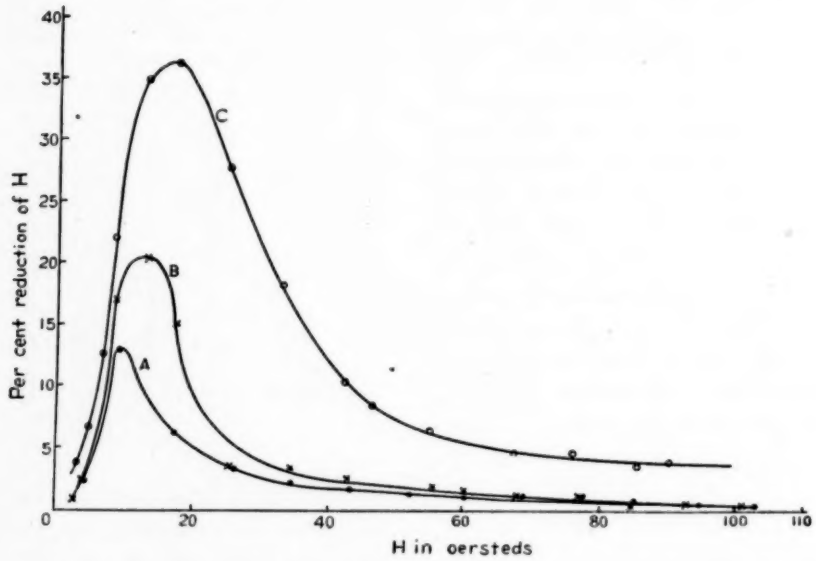

FIG. 4. The percent reduction of the exciting field H outside the rod as a function of the exciting field H. A, the search coil is in the middle of the rod; B and C, the search coils are at 25 cm and 15 cm from one end of the rod, respectively.

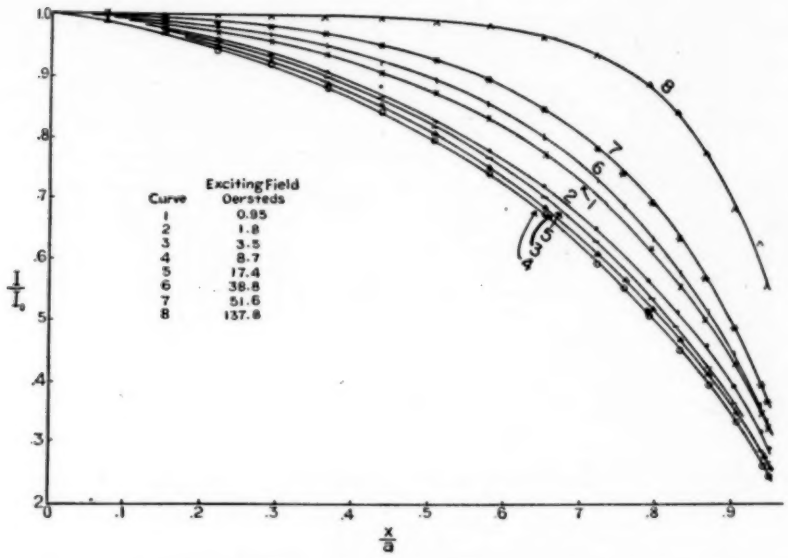

FIG. 5. The distribution of intensity of magnetization along the tube. I is the intensity of magnetization at x cm from the middle of the tube; I_0, the intensity of magnetization in the middle of the tube; a, the half-length of the tube.

is of interest to compare the behavior of the curves shown in Fig. 3. It will be noticed that those curves in solid lines coincide in the case of a and b with those in broken lines at the ends of the curves. This means: (1) the demagnetizing effect of the end surfaces on the central region about 20 cm long, is entirely negligible; (2) the demagnetizing effect due to the free poles distributed along the rod is also negligibly small in the central region at high exciting currents. We are thus enabled to understand that the magnetic field within the tube is practically unaffected by

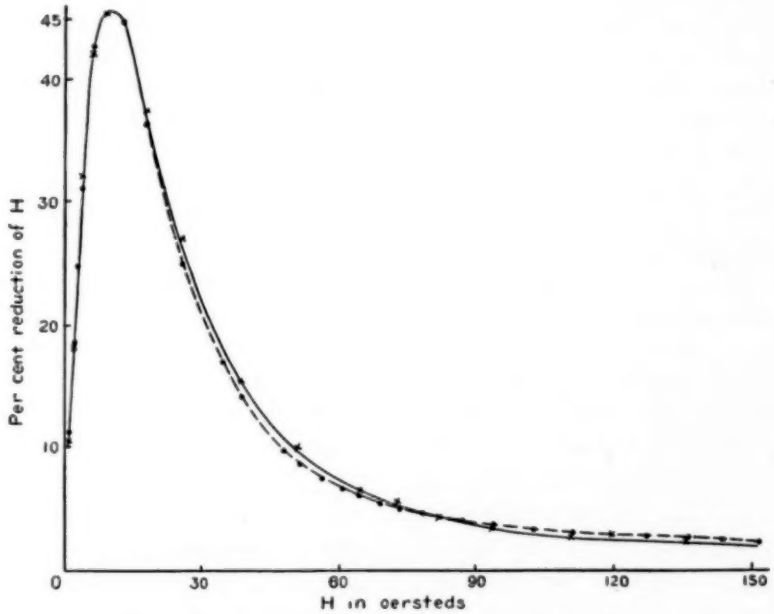

FIG. 6. The percent reduction of the exciting field H inside the tube as a function of the exciting field H. The broken line gives the experimental curve and the solid line gives the theoretical curve.

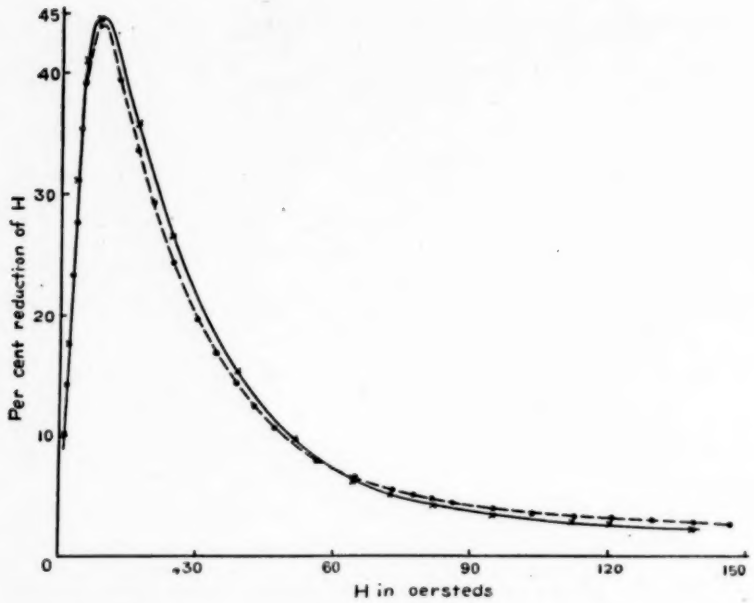

FIG. 7. The percent reduction of the exciting field H outside the tube as a function of the exciting field H. The broken line gives the experimental curve and the solid line gives the theoretical curve.

the material of the tube when magnetized to saturation as claimed by Wall. If the exciting current does not exceed 2.2 amperes, the demagnetizing effect on the central region produced by the free poles cannot be overlooked. The effect reaches a maximum when the exciting current is within the range of 0.2 to 0.5 ampere. On Wall's theory it seems difficult to explain why the percent reduction of the magnetic field represented by curve C should be higher than that by curve B, and that by curve B should be higher than that by curve A (Fig. 4), but these can be easily understood from the demagnetizing effect due to the free poles distributed along the whole length of the tube, which falls to a minimum in the middle of the rod and increases towards its two ends.

An inspection of the general features of the family of curves shown in Fig. 5 will render the above statement clear. Two points are worthy of note: (1) The slope of each curve increases, in general, with the value of x/a, indicating that the density of free poles and hence the demagnetizing fields produced by them also increases from the middle towards the end of the tube. Although the free poles may be few in number in the central portion of the tube, they may have notable demagnetizing effect in their immediate neighborhood. Unless the tube is sufficiently long, this effect cannot be neglected. (2) When the exciting field increases from zero onward, the slope of the curves for the same value x/a, but not too close to $x/a=1$, also increases and reaches a maximum value, corresponding to the exciting field of 8.7 oersteds; any further increase of the exciting field makes the slope of the curves gradually decrease. There is reason to infer that if the tube is long enough and the exciting field high enough, the slope of the greater part of the curve will decrease to zero as its limit, i.e., the magnetization of the greater part of the tube is uniform. Since the slope of the curve at a given point denotes the density of the free poles in the corresponding position of the tube, and the density of the free poles is proportional to the demagnetizing force, we may say that the demagnetizing force of the free poles increases from zero to a maximum value corresponding to the exciting field of 8.7 oersteds and then decreases when the exciting field increases from zero up to a considerably high value. The above statement qualitatively explains, on the theory of demagnetization, the nature of the curves shown in Figs. 1–3.

6. CONCLUSION

From the above discussion and from the close agreement between the calculated percent reduction of the magnetic field and the experimental values shown in Figs. 6 and 7, it may be concluded that the reduction of the magnetic field inside and outside the tube is due to the demagnetizing effect of the free poles distributed along the whole length of the tube, or in other words, the reduction of the magnetic field in the neighborhood of the tube can be accounted for by the theory of demagnetization without introducing any other hypothesis.

ACKNOWLEDGMENT

The author wishes to thank Dr. J. W. Shih for many helpful discussions in the course of this investigation.

PHYSICAL REVIEW VOLUME 66, NUMBERS 3 AND 4 AUGUST 1 AND 15, 1944

On the Existence of Atomic Nitrogen in the Upper Atmosphere of the Earth

TA-YOU WU
Department of Physics, National University of Peking, and Institute of Astronomy, Academia Sinica, Kunming, China

(Received June 10, 1944)

Evidence for the existence of atomic nitrogen in the upper atmosphere is presented. It is shown that the absence of certain lines of NI and the absence of continuous absorption which leads to the dissociation of N_2 cannot be considered conclusive evidence against the existence of atomic nitrogen. Relative densities of the *E* and *F* layers are discussed, and it is shown that observations of high density in the *F* layer may be compatible with the existence of atomic nitrogen. Possible transitions which produce the night sky spectrum are discussed.

PARTLY on the basis of the observed spectra of the night sky and of the aurora and partly on the basis of the absence in the laboratory of continuous absorption by the nitrogen molecule leading to dissociation $N_2+h\nu\rightarrow N+N$, the view is held by many investigators that in the upper atmosphere oxygen exists in the atomic and nitrogen in the molecular state. On this view many attempts have been made by various investigators to deal with such problems as the existence of various ionized layers, the density at different heights in the atmosphere, the excitation mechanism of the radiations of the aurora and the night sky, etc. The purpose of the present note is to present some arguments for the view that there may exist atomic nitrogen in the upper atmosphere, and to indicate the changes that this picture entails in our present view of the above-mentioned problems.

I

One of the reasons for supposing nitrogen to exist in the molecular state in the atmosphere is that while the forbidden lines $^1D-^1S$, $^3P-^1D$ of oxygen OI are the most prominent radiations in night sky and the aurora, the forbidden lines $^4S-^2P$, $^4S-^2D$ of NI are absent in these spectra. Kaplan has pointed out the possible presence of the $^4S-^2P$ line in the spectrum of the night sky.[1] While this identification, if confirmed by more observational data, would establish the existence of atomic nitrogen, it must be emphasized that the absence of this and the $^4S-^2D$ line constitutes no proof against the presence of atomic nitrogen. The transition probability of $^4S-^2P$ is of the order of 1 per second and the lifetime of the ^2P state is thus comparatively short. Any $N(^2P)$ atoms produced by dissociation by solar radiation (see Section II below) will rapidly settle down into the states ^2D and ^4S on the emission of the lines $^2D-^2P$ and $^4S-^2P$. The lifetime of the ^2D state is of the order 10^5 seconds so that the failure to observe the line $^4S-^2D$ may only mean an insufficiently large number of $N(^2D)$ atoms. Unless $N(^2P)$ are excited by proper and

[1] J. Kaplan, Phys. Rev. **56**, 858 (1939); **57**, 249 (1940).

frequent processes in the night sky and in the aurora, there may be considerable N(^4S) and N(^2D) atoms without revealing themselves in the spectrum.

II

Perhaps the main reason for believing in the absence of atomic nitrogen in the upper atmosphere is the absence of continuous absorption by N_2 down to 600A in the ultraviolet that leads to the dissociation of the molecule. Now, according to the configuration theory, of the many theoretically possible molecular states resulting from two N atoms, the following can combine by dipole transitions with the normal state $X\,{}^1\Sigma_g^+$ of N_2: two ${}^1\Pi_u$ states from N(^2D)+N(^2D); one ${}^1\Sigma_u^+$ and three ${}^1\Pi_u$ states from N(^2D)+N(^2P); and two ${}^1\Sigma_u^+$ and three ${}^1\Pi_u$ states from N(^2P)+N(^2P). Some, if not all, of these are repulsive states so that continuous absorption by N_2 in the normal state $X\,{}^1\Sigma_g^+$ will lead to dissociation. Thus

$$N_2(X\,{}^1\Sigma_g^+)+h\nu\rightarrow N(^2P)+N(^2P)({}^1\Sigma_u^+;\,{}^1\Pi_u), \quad (1)$$

$$N_2(X\,{}^1\Sigma_g^+)+h\nu\rightarrow N(^2P)+N(^2D)({}^1\Sigma_u^+;\,{}^1\Pi_u), \quad (2)$$

$$N_2(X\,{}^1\Sigma_g^+)+h\nu\rightarrow N(^2D)+N(^2D)({}^1\Pi_u). \quad (3)$$

That such continuous absorptions have not been observed in the laboratory may be due to the circumstance that the potential energy curves of these repulsive states rise very steeply with the decrease in internuclear distance so that, by the Franck-Condon principle, absorption will not be appreciable until the radiation frequency is very much greater than ν_0 given by $h\nu_0=D+E$, where D is the dissociation energy of the normal state $X\,{}^1\Sigma_g^+$ and is 7.35 volts, and E is the sum of the excitation energies of the two resulting N atoms from the ^4S state. Thus appreciable absorptions by the processes (1), (2), (3) may lie in the region beyond 500A not yet explored in the laboratory, and in the region $\lambda>600$A the absorption may be so weak that they are masked by the very strong absorptions of the Hopfield and the Worley-Jenkins bands that lead to the ionization of N_2.

Despite the situation that dissociative absorption will take place only for radiations of very short wave-length, an appreciable number of N_2 may still be dissociated since there is now strong evidence that there is a great abundance of high frequency radiations emitted by the sun.[2] They are probably due to the radiative recombinations of electrons and ionized atoms carried through the photosphere by convective transfer, and their energy density may be very much greater than that of a blackbody at ~6000°K, possibly by some high powers of 10. As shown later, a calculation of the degree of dissociation of N_2 is yet not possible on account of the lack of pertinent informations. The point, however, is that the processes (1), (2), (3) are theoretically possible provided there are radiations of sufficiently high frequency, for the existence of which there seems now to be strong astrophysical evidence.

III

Consider now briefly some of the consequences of the existence of atomic nitrogen in the upper atmosphere. On account of the smaller mass of the N atom, the dissociation of N_2 will lead to a greater density, at a given height, than that obtained on the assumption of a N_2 and O mixture. Thus estimates based on the assumption that N_2 and O are in diffusive equilibrium above ~150 km show that the air density in the F layer (~250 km) is about 1/5000 of that in the E layer.[3] However, from the observed collision frequencies by radio wave experiments, it is known that the air density in the F layer is about 1/30 of that in the E layer. This abnormally high density in the F layer may be partly due to the dissociation of N_2 into N atoms.

The dissociation of N_2 will also give rise to an ionized layer due to the ionization of the N atoms. When the variation of the degree of dissociation with height is known, it will be possible to calculate the height of this ionized layer.[4] This may contribute to a better understanding of the nature of the various ionized layers now known. Unfortunately a calculation of the variation of the degree of dissociation with height is not yet possible for reasons given later.

IV

Another observed fact connected with the problem of the ionized layers may perhaps be

[2] Cf. A. Eddington, M. N. R. A. S. **101**, 177 (1941); **102**, 154 (1942).

[3] S. K. Mitra and H. Rakshit, Ind. J. Phys. **12**, 47 (1938); S. K. Mitra and A. K. Banerjee, *ibid.* **13**, 117 (1939).

[4] Bates, Buckingham, Massey, and Unwin, Proc. Roy. Soc. **A170**, 322 (1938).

understood on the introduction of atomic nitrogen in the upper atmosphere. The effective recombination coefficients of electrons are observed to be $\simeq 1.2\times10^{-8}$ and 0.8×10^{-10} cm³/sec. in the E and F layers, respectively. In the prevalent theory,[5] the electrons are removed by direct radiative recombinations with positive ions

$$n^+ + e \rightarrow n + h\nu, \quad \text{recombination coeff.} = \alpha_e,$$

and through attachment by a neutral particle forming a negative ion, and subsequent nonradiative recombinations between the positive and the negative ions, yielding two excited atoms

$$n + e \rightarrow n^- + h\nu, \quad \text{attachment coeff.} = a,$$
$$n^- + n^+ \rightarrow n' + n'', \quad \text{transfer coeff.} = \alpha_i.$$

On denoting the concentrations by simply e, n^-, n^+, and letting

$$\lambda = n^-/e,$$

then, since $e + n^- = n^+$, one has

$$(1+\lambda)(de/dt) = dn^+/dt,$$

$$dn^+/dt = -\alpha_e e n^+ - \alpha_i n^- n^+,$$

and

$$de/dt = -(\alpha_e + \lambda\alpha_i)e^2.$$

Theoretical calculations of Bates *et al.* show that for oxygen, $\alpha_e \simeq 10^{-12}$ cm³/sec. and $\alpha_i \simeq 10^{-11}$ cm³/sec.[5] Thus to obtain an effective recombination coefficient in agreement with the observed values above, the ratio λ must be of the order 100–1000 in the E layer and 10 in the F layer. The high concentration of negative ions in the E layer is supported by the observed variations of terrestrial magnetism and is understandable if one assumes that there oxygen atoms are abundant and, having an electron affinity of 2.2 volts, readily form O^- ions. The equilibrium ratio λ of negative ion − electron is determined by the rates of attachment above and of detachment

$$O^- + X \rightarrow OX + e, \quad \text{detachment coeff.} = d,$$

where X is a neutral particle, namely,

$$\lambda = \frac{O^-}{e} = \frac{aO}{\Sigma d_i X_i}.$$

The summation is taken over all the probable detachment processes, for example, $X = O, O_2, N_2$, etc. Now on the prevalent view of a N_2, O atmosphere, the concentration of O would increase relative to that of N_2 in passing from the E to the F layer so that a decrease of λ in passing from the E to the F layer is difficult to understand. On the other hand, on assuming N_2 to be dissociated, the ratio O/N of the concentrations of oxygen and nitrogen atoms will decrease with height. Since the N atoms are probably just as active in the detachment process but form no negative ions on account of their very small electron affinity, the value λ will accordingly decrease in passing from the E to the F layer.

Bates *et al.* have pointed out the possibility of thermal detachment in the F layer as a cause of the comparatively low concentration of negative ions. As the electron affinity of O atom is 2.2 volts, the temperature must be quite high for thermal detachment to be important. As the N_2 are mostly dissociated by radiations of frequency very much greater than ν_0 given by $h\nu_0 = D + E$ (see Section II above), the resulting atoms will possess high kinetic energies. This would result in a high temperature in the upper atmosphere, on which there seems to be general agreement among different authors but which has been ascribed to the energy of electrons in the ionization of the atoms rather than of the atoms in the dissociation of the molecules.

V

A difficulty of the prevalent view that nitrogen exists as N_2 and is hence confined to the lower strata (below ~250 km) of the atmosphere is that, according to it, the observed nitrogen bands from high aurora become difficult to understand. There does not seem to be a plausible theory that can account for the excitation of the various radiations of nitrogen, especially for the sunlit aurora that have been observed at heights as great as ~800 km and of which the negative bands of N_2^+ are particularly enhanced. The theory of Maris and Hulburt attempts to ascribe the aurora to particles sent up with great velocities to very great heights on collisions of the second kind with excited atoms or molecules in the uppermost region of the atmosphere, ionized by solar radiations, and spiraling down along the earth's magnetic lines of force toward the polar regions. It has been shown, however,

[5] Bates, M. N. R. A. S. **100**, 25 (1939), has calculated the theoretical absorption coefficient of N atom.

recently by the writer that the mechanism suggested by these authors is entirely inadequate for explaining the aurora.[6] On our present view here, the extension of atomic nitrogen to great heights may at least provide for the presence of nitrogen molecules in the upper atmosphere by such recombination processes as

$$N+N\rightarrow N_2+h\nu$$

(Vegard-Kaplan and other bands of N_2),

$$N+N^+\rightarrow N_2^++h\nu$$

(first negative bands of N_2^+).

VI

Finally, on the assumption that there exist in the upper atmosphere atomic oxygen and nitrogen produced by the processes (1), (2), (3) and

$$O_2(X\,^3\Sigma_g^-)+h\nu\rightarrow O(^3P)+O(^1D), \qquad (4)$$

the writer has recently proposed a theory of the excitation mechanism of the night sky spectrum.[7] The key processes are the radiative recombinations between the atoms, forming metastable molecules of N_2 and O_2:

$$N(^4S)+N(^2D)(^3\Sigma_g^+;\,^3\Pi_g)\rightarrow N_2(A\,^3\Sigma_u^+)+h\nu, \qquad (5)$$

$$N(^2D)+N(^2D)(^3\Pi_g)\rightarrow N(A\,^3\Sigma_u^+)+h\nu, \qquad (6)$$

$$O(^3P)+O(^3P)(^3\Pi_g)\rightarrow O(C\,^3\Sigma_u^+)+h\nu. \qquad (7)$$

The strong Vegard-Kaplan bands are excited by (5) and (6). Collisions among the various metastable atoms and molecules provide for the excitation of the various radiations. For example, the green and red lines of OI are excited by the processes

$$2O_2(C\,^3\Sigma)\rightarrow O_2(X\,^3\Sigma)+O(^3P)+O(^1S)+0.12\text{ volt}, \qquad (8)$$

$$O(^3P)+N(^2D)\rightarrow O(^1D)+N(^4S)+0.47\text{ volt}. \qquad (9)$$

A high metastability of $O_2(C\,^3\Sigma)$ will enable its concentration to build up and the process (8) will explain the small rise in intensity of the green line $^1D-{}^1S$ in the first part of the night. On the other hand, with an initially large number of $O(^3P)$ and $N(^2D)$ atoms produced by (1), (2), (3), (4), and their gradual depletion by recombination and other processes, the process (9) may explain the decrease of intensity of the red line $^3P-{}^1D$ immediately after sunset. Without assuming the presence of N atoms, the excitation of the Vegard-Kaplan bands and the other bands of N_2 seem very difficult to explain.[7]

VII

From the foregoing discussions, it seems very desirable to settle the question whether N_2 is dissociated in the upper atmosphere by calculating theoretically the degree of dissociation as a function of the pressure in the atmosphere. This would necessitate a knowledge of the radiation energy density ρ_ν of the proper wavelength, the absorption coefficient τ_ν as a function of frequency, the temperature T of the atmosphere where dissociation is being calculated, and the effect of "cycles" of such processes for the formation of the normal $N_2(X\,^1\Sigma_g^+)$ and the removal of $N(^4S)$ as

$$N(^4S)+N(^2D)\rightarrow N_2(A\,^3\Sigma_u^+)+h\nu,$$

$$N_2(A\,^3\Sigma_u^+)\rightarrow N_2(X\,^1\Sigma_g^+)+\text{Vegard-Kaplan bands}.$$

On ignoring the effect of such processes and considering the process (3) alone, one readily obtains the following dissociation formula

$$\frac{[N]^2}{[N_2]}=\frac{2g_N^2}{g_{N_2}hr_0^2}\left(\frac{MkT}{8\pi}\right)^{\frac{1}{2}}e^{-D/kT}(1-e^{-h\omega/kT})W\frac{c^3}{8\pi h}\cdot\int_{\nu_0}^{\infty}\frac{1}{\nu}\tau_\nu\rho_\nu e^{-\tau_\nu p/2Mg}d\nu\Big/\int_{\nu_0}^{\infty}\tau_\nu e^{-h\nu/kT}\nu^2d\nu,$$

where $[N]$, $[N_2]$, and the g's are the concentrations and the statistical weights of the atoms and the molecule; ω is the vibrational frequency, r_0 the nuclear separation, $2M$ the mass of the molecule $N_2(X\,^1\Sigma)$; W is the dilution factor and is $\sim 4\times10^{-6}$; and p is the partial pressure of N_2 at the height where the degree of dissociation is being calculated. As $[N]^2/[N_2]$ is exceedingly sensitive to the values of ρ_ν, T, and τ_ν, and as these quantities are not known with any certainty, any estimate of the degree of dissociation with the use of questionable values for these quantities will be premature.

[6] T. Y. Wu, Proc. Ind. Acad. Sci. **A18**, 345 (1943).
[7] T. Y. Wu, Proc. Ind. Acad. Sci. **A18**, 40 (1943).

On the Interaction of Radiation and Two Electrons* †

PETER HAVAS
Pupin Physics Laboratories, Columbia University, New York, New York

(Received June 8, 1944)

The quantum theory of radiation describes the effect of retardation in the interaction of two electrons by the mutual emission and absorption of light quanta. A study has been made of a process involving the interaction of two electrons and any number of quanta. It was noted that the number of terms involving virtual quanta needed to describe the retardation in the usual first-order approximation of perturbation theory depends on the number of real quanta involved in the process under consideration. It was shown that, nevertheless, the resulting expression obtained by summing over all the intermediate states involving virtual quanta is of the same form for any process. Møller's formulas for the retarded interaction of two electrons with no light quanta and with one light quantum emitted are special cases of our equation.

I. INTRODUCTION

IT is well known that the quantum mechanical Hamiltonian of a system of charged particles obeying Dirac's equation and the radiation field can be written[1]

$$H=H_p+H_r+H_s+H', \tag{1a}$$

where H_p represents the Hamiltonian of the particles, H_r that of the light quanta, H_s the electrostatic energy of the particles, and H' the interaction of the particles and the field. We have

$$H_s=(1/2)\sum e_i e_k/r_{ik} \tag{1b}$$

and

$$H'=-\sum e_k(\boldsymbol{\alpha}_k\cdot\mathbf{A}(k)), \tag{1c}$$

where e_k is the charge and $\boldsymbol{\alpha}_k$ the Dirac matrix for the kth particle, $\mathbf{A}(k)$ the vector potential evaluated at the position of e_k and r_{ik} the distance between the ith and kth particle.

Equation (1a) contains an explicit expression for the instantaneous Coulomb interaction only, as given by (1b). The effect of retardation is included in H' and is described by a mutual emission and absorption of light quanta. In the simplest possible case of retarded interaction of two particles in the absence of radiation, it consists of the emission of just one quantum by one particle and reabsorption by the other and vice versa.[2] The purpose of this paper is to show that while in the more general case of the interaction of any number of light quanta with two particles the retardation corresponds to emissions and absorptions described by a large number of terms involving virtual quanta, we can sum all these terms and obtain an expression for the retarded interaction which is of the same form for any process.

II. THE MATRIX ELEMENT

As it is not possible with the present methods to solve the Schrödinger equation $H\psi=-i\hbar(\partial\psi/\partial t)$ with the Hamiltonian (1a) directly, a perturbation theory is required. The method often used treats the terms (1b) and (1c) for the interaction as small perturbations causing transitions from a state E_0 with a certain energy and momentum of the particles and a certain number of quanta to another state E_F. The transition probability is zero unless the total energy is conserved, and then it is given by the well-known equation[3]

$$w_{E_0E_F}=(2\pi/\hbar)\rho_{E_0}|H'_{E_0E_F}|^2, \tag{2a}$$

where ρ_{E_0} is the density of the final or initial states with energy E_0, and

$$H'_{E_0E_F}=\int\psi_0^*(H_s+H')\psi_F d\tau \tag{2b}$$

is the matrix element for the transition. The

* A thesis submitted in partial fulfillment of the requirements for the degree of Doctor of Philosophy in the Faculty of Pure Science, Columbia University.

† Publication assisted by the Ernest Kempton Adams Fund for Physical Research of Columbia University.

[1] For the general theory and the notation used see W. Heitler, *The Quantum Theory of Radiation* (Oxford University Press, 1936), Chapter III.

[2] This case was first calculated with a correspondence method by C. Møller, Zeits. f. Physik **70**, 686 (1931) and Ann. d. Physik **14**, 531 (1932). The present method was first used for this problem by H. Bethe and E. Fermi, Zeits. f. Physik **77**, 296 (1932).

[3] W. Heitler, reference 1, p. 90.

matrix element has a value different from zero for the Coulomb interaction of two particles, in which case it is equal to

$$(4\pi\hbar^2c^2e_1e_2/|\Delta\mathbf{p}|^2)(u_{01}^*u_1)(u_{02}^*u_2), \quad (3a)$$

for two *free* particles, and for transitions involving emission or absorption of just one light quantum, where it is given by

$$-e(2\pi\hbar^2c^2/k_\lambda)^{\frac{1}{2}}(u_a^*\alpha_e u_b). \quad (3b)$$

Here the u's are the Dirac amplitudes of the electrons and α_e is the component of α in the direction of polarization of the light quantum k_λ. The momentum is conserved for these transitions.

If the matrix element for the direct transition is zero, we have to use a succession of simple transitions leading from the initial to the final state through a number of intermediate states, for which we still have conservation of momentum, but no longer conservation of energy. We have to replace (2b) by

$$H'=\sum \frac{H'_{0,1}H'_{1,2}\cdots H'_{F-2,F-1}H'_{F-1,F}}{(E_0-E_1)(E_0-E_2)\cdots \times(E_0-E_{F-2})(E_0-E_{F-1})}, \quad (4)$$

where the denominator contains the product of the differences of the energies of the initial and intermediate states, and the numerator the products of the matrix elements for the successive simple transitions. These transitions have to be chosen in such a way that the total expression (4) is of the lowest possible order in the electronic charge e for which it does not vanish,[4] but otherwise we have to sum over all possible successions of intermediate states. We can see from (3a) and (3b) that the matrix element for interaction with a light quantum is proportional to e and the Coulomb interaction is proportional to e^2 and therefore equivalent to two interactions with light.

After these general considerations let us now consider a process involving $z+Z$ light quanta and two particles. Then our energy balance for the initial and final states is

$$E_0=E_1^0+E_2^0+a+b+\cdots+z+A+B+\cdots+Z =E_1^F+E_2^F=E_F, \quad (5)$$

where E_1^0, E_1^F and E_2^0, E_2^F are the energies of the first and second particle in the initial and final state, respectively, and $a\cdots z$ and $A\cdots Z$ are the energies of the light quanta. We have written the equation in a form corresponding to absorptions only, but our calculations include emissions as well, as the only difference would be a change in sign throughout for the energy and momentum of the particular light quantum. Furthermore, we can include positrons as well as electrons by changing the sign of the energy and momentum of the particle.

The conservation of momentum requires

$$\mathbf{p}_1^0+\mathbf{p}_2^0+\mathbf{a}+\mathbf{b}+\cdots +\mathbf{z}+\mathbf{A}+\mathbf{B}+\cdots+\mathbf{Z}=\mathbf{p}_1^F+\mathbf{p}_2^F. \quad (6)$$

The first non-vanishing matrix element for such a process is of the order $z+Z+2$ in e. It involves $z+Z$ transitions due to the interaction of the particles with all the light quanta and one transition due to the instantaneous Coulomb interaction of the two particles. We obtain a matrix element of the same order if we have instead of the instantaneous Coulomb interaction a retardation described by one transition corresponding to the emission of a light quantum K' by one particle and a second transition due to the absorption of this quantum by the second particle. Any succession of transitions involving the same light quantum more than once or more than one Coulomb interaction would either be of a higher order than those just considered or would not fulfill the conditions (5) and (6).

We note that we cannot expect (4) to give finite results for any values of the energies and momenta of the particles and quanta involved subject to the conditions (5) and (6) only. We assume for the moment that we have to deal with non-vanishing denominators of (4) only and shall discuss the limitations of the first-order approximation later.

Let us now consider the possible successions of interactions in detail. We can have one particle interacting with any n quanta, and the other one with the remaining $z+Z-n$ quanta. Furthermore, the interactions of the n quanta with the first particle can take place in any order (and likewise for the $z+Z-n$ quanta and the second particle). In addition the Coulomb inter-

[4] It is a well-known difficulty of the quantum theory of radiation that any calculation of a process in a higher than the lowest possible order leads to divergencies.

action can take place after the interaction with any $n+M$ quanta. Then one has to sum over both signs of spin and energy of the electron in the intermediate states. Finally the exclusion principle has to be taken into account by making the total matrix element antisymmetric in the coordinates of the two particles.[5]

We do not attempt to sum over all these possibilities since we want only to study the form of the retardation for a given Coulomb interaction. From now on we limit our calculations to that part of the sum, which has the same numerator in (4), namely,

$$(-e)^{z+Z+2}[(2\pi\hbar^2c^2)^{z+Z+2}/(a\cdots zA\cdots Z)]^{\frac{1}{2}} \times \prod_{1,1}^{n,M} \prod_{n+2,M+2}^{z,Z} (u_1^{*n-1}\alpha_n u_1^{n})(u_2^{*M-1}\alpha_M u_2^{M}) \times \begin{cases} 2(u_1^{*n}u_1^{n+1})(u_2^{*M}u_2^{M+1})/|\Delta\mathbf{p}|^2 \text{ for the instantaneous Coulomb interaction} \\ \sum_{\text{directions of polarization}} [(u_1^{*n}\alpha_{K'}u_1^{n+1}) \times (u_2^{*M}\alpha_{K'}u_2^{M+1})/K'] \text{ for the retardation,} \end{cases} \tag{7}$$

with $K'=|\Delta\mathbf{p}|$, the absolute value of the change in momentum of either particle due to the Coulomb interaction.

For the moment we consider the two parts for instantaneous and retarded interaction separately. The part containing the instantaneous Coulomb interaction corresponds to the following process:

$$\left.\begin{array}{l}\text{Electron } e_1 \text{ emits (or absorbs)} \\ \quad a;\, b;\, \cdots\, n \\ \text{Electron } e_2 \text{ emits (or absorbs)} \\ \quad A;\, B;\, \cdots\, M\end{array}\right\}\text{Instantaneous}$$

$$\text{Coulomb interaction}\begin{cases} e_1 \text{ emits (or absorbs)} \\ \quad n+1;\, \cdots\, z \\ e_2 \text{ emits (or absorbs)} \\ \quad M+1;\, \cdots\, Z. \end{cases}$$

We denote the light quanta (and their energies) by small letters if they interact with the first electron and by capital letters for the second electron.

We have already arbitrarily ordered the quanta which interact with particle 1, and separately the quanta which interact with particle 2. We still have to sum over all possible orders of interaction subject to these limitations. For example, we can have one process where e_1 interacts with $a, b, \cdots n$ and then e_2 with $A, B, \cdots M$ but also another one where e_1 interacts with a, then e_2 with A, then again e_1 with $b, c, \cdots$ and similar possibilities. The only restriction (beyond the arbitrary partial ordering of quanta mentioned above) is that the order of interaction for each particle has to be the same and that the Coulomb interaction can take place only after e_1 has interacted with the light quantum n and e_2 with M, but before their interactions with $n+1$ and $M+1$, respectively.

We note that the part of our sum which contains the instantaneous Coulomb interaction can be factored into a product of the Coulomb term and of two series, the one containing all the successions of transitions taking place before the Coulomb interaction and the other containing the successions of transitions taking place thereafter.

Now we have to consider the case where the Coulomb interaction is replaced by the emission and subsequent absorption of a virtual quantum K', which transfers the same amount of momentum. It is essential to keep in mind that *this need not take place in two consecutive steps.*[6] *The only limitation is that* e_1 *can only emit* K' *after its interaction with* n *and before its interaction with* $n+1$, *and that* e_2 *can only absorb* K' *after its interaction with* M *and before its interaction with* $M+1$ *and vice versa.* The extreme case would be the succession of interactions where one particle has emitted K' and interacted with all z quanta and is therefore in its final state, while the second particle is still in its initial state.

We note that we can no longer factor the sum describing the retardation as in the case of the instantaneous Coulomb interaction. Furthermore, we see that because of the fact that the emission and absorption of K' need not take

[5] For this last point compare, e.g., N. F. Mott and H. S. W. Massey, *The Theory of Atomic Collisions* (Oxford University Press, 1933), Chapter XV.

[6] This point has not been emphasized before. The expression given by W. Heitler, reference 1, p. 101, Eq. (31), takes account of consecutive steps only. It is therefore *not* the general matrix element for the retarded interaction of two particles. The same criticism applies to the paper by W. Heitler and L. Nordheim, J. de phys. et rad. 5, 449 (1934), which gives the same expression. The actual calculations of this paper neglect the retardation, however, so that no error is introduced.

place in two consecutive steps, the sum describing the retardation will contain more terms than the sum containing the instantaneous interaction. The number of terms needed to describe the retardation depends on the number of quanta involved in the entire process. This appears strange, at least formally, as there seems to be no reason why the expression for the interaction of one particle with radiation and for the instantaneous interaction of two particles should be of the same form independent of the process, but not the one for the retarded interaction. But we have to keep in mind that we are still describing the retarded interaction by virtual quanta, and we shall see that the expression obtained after eliminating them is again independent of the process under consideration as it should be.

We first simplify the notation for the energy differences appearing in the denominator of (4). If the first transition were due to the absorption of light quantum a by e_1, then this particle would have the energy $E_1^a=(|\mathbf{p}_1^0+\mathbf{a}|^2+\mu^2)^{\frac{1}{2}}$ and the difference between the energy of the initial and the first intermediate state would be

$$a+E_1^0-E_1^a$$

as the second particle is unchanged. We denote this difference by $\langle E_1^a\rangle$. Similarly we put

$$a+b+\cdots+m+E_1^0-E_1^m=\langle E_1^m\rangle \quad (8a)$$

with $E_1^m=(|\mathbf{p}_1^0+\mathbf{a}+\mathbf{b}+\cdots+\mathbf{m}|^2+\mu^2)^{\frac{1}{2}}$,

$$A+B+\cdots+L+E_2^0-E_2^L=\langle E_2^L\rangle \quad (8b)$$

with $E_2^L=(|\mathbf{p}_2^0+\mathbf{A}+\mathbf{B}+\cdots+\mathbf{L}|^2+\mu^2)^{\frac{1}{2}}$.

If now we have an intermediate state reached by the interaction of e_1 with m quanta and of e_2 with L quanta, then the energy difference is

$$a+b+\cdots+m+A+B+\cdots$$
$$+L+E_1^0+E_2^0-E_1^m-E_2^L=\langle E_1^m\rangle+\langle E_2^L\rangle. \quad (8c)$$

III. A THEOREM

Let

$$A_0=0, A_1, A_2, \cdots A_n$$
$$B_0=0, B_1, B_2, \cdots B_m$$

be two sets of numbers, subject only to the restriction $A_i\neq -B_k$ for any i, $k\neq 0$.

Let (A, B) stand for any product of $n+m$ factors of the form A_i+B_k, where we obtain each factor from the preceding one by replacing *either* A or B by the following number of its set.

Theorem: The sum of the reciprocals of all possible (A, B) obtained by starting with either A_0+B_1 or B_0+A_1 is

$$S_{n,m}=\sum 1/(A, B)=1/A_1A_2\cdots A_nB_1B_2\cdots B_m.$$

We shall prove the theorem by induction. It is certainly true for $n=1$ and $m=1$ since

$$\frac{1}{A_1(A_1+B_1)}+\frac{1}{B_1(A_1+B_1)}=\frac{1}{A_1B_1}.$$

As the sum does not depend on the initial order of the numbers in the two sets, it is sufficient to show that if we add another number A_{n+1} at any place to the set $A_1\cdots A_n$ and construct $S_{n+1,m}$, it will be equal to $S_{n,m}/A_{n+1}$. The proof can be demonstrated most easily if we insert A_{n+1} between A_0 and A_1. We shall use the symbol $(A_i+B_k)\rightarrow(A_{i+1}+B_k)$ to indicate a step which changes an A to the value indicated, and likewise for a change of the B.

We now proceed to construct $S_{n+1,m}$. We start with the factor (B_0+A_{n+1}). Summing all the $1/(A, B)$ which can be obtained by $(B_0+A_{n+1})\rightarrow(B_0+A_1)$ and then proceeding according to our rule, we simply obtain $S_{n,m}^{A_1}/A_{n+1}$ where $S_{n,m}^{A_1}$ indicates those terms of $S_{n,m}$ which start with (B_0+A_1). For $(B_1+A_0)\rightarrow(B_1+A_{n+1})\rightarrow(B_1+A_1)$ we obtain $S_{n,m}^{B_1}/(B_1+A_{n+1})$ and for $(B_0+A_{n+1})\rightarrow(B_1+A_{n+1})\rightarrow(B_1+A_1)$ we obtain $B_1S_{n,m}^{B_1}/[A_{n+1}(B_1+A_{n+1})]$ where $S_{n,m}^{B_x}$ indicates the sum of those terms of $S_{n,m}$ which start at (B_1+A_0) and continue with A unchanged up to (A_0+B_x) and then change to (A_1+B_x).

Proceeding in this fashion and adding the terms with the same $S_{n,m}^{B_x}$ as factor, we obtain

$$S_{n,m}^{A_1}/A_{n+1}$$

$$\left(\frac{1}{B_1+A_{n+1}}+\frac{B_1}{A_{n+1}(B_1+A_{n+1})}\right)S_{n,m}^{B_1}= S_{n,m}^{B_1}/A_{n+1}$$

$$\left(\frac{1}{B_2+A_{n+1}}+\frac{B_2}{(B_1+A_{n+1})(B_2+A_{n+1})}+\frac{B_1B_2}{A_{n+1}(B_1+A_{n+1})(B_2+A_{n+1})}\right)S_{n,m}^{B_2}=S_{n,m}^{B_2}/A_{n+1},$$

and the general term is from the method of construction

$$B_1B_2B_3B_4\cdots B_xS_{1,x}S_{n,m}^{B_x}=\frac{B_1B_2\cdots B_x}{A_{n+1}B_1B_2\cdots B_x}S_{n,m}^{B_x}= \qquad S_{n,m}^{B_x}/A_{n+1},$$

where $S_{1,x}$ indicates the sum of all the (A, B) formed from $A_0=0, A_{n+1}$ and $B_0=0, B_1, B_2\cdots B_x$ and for which the theorem holds true by assumption since $x\leq m$ and $1\leq n$.

Adding the right-hand side we obtain

$$S_{n+1,m}=(S_{n,m}^{A_1}+S_{n,m}^{B_1}+S_{n,m}^{B_2}+\cdots+S_{n,m}^{B_x}+\cdots+S_{n,m}^{B_m})/A_{n+1}=S_{n,m}/A_{n+1}$$

which is what was to be proved.

IV. SUMMATION OF THE SERIES

We first sum the series defined in Part II containing the instantaneous Coulomb interaction. We remember that we could factor this series and we have already defined our $\langle E_1^m\rangle$ and $\langle E_2^L\rangle$ by the relations (8) in such a manner that we can immediately apply our theorem to the first factor containing the successions of interactions taking place before the instantaneous Coulomb interaction, i.e., up to $\langle E_1^n\rangle$ and $\langle E_2^M\rangle$.

Before we can sum the part containing the interactions taking place after the instantaneous Coulomb interaction, we have to simplify the notation for this part also. But we cannot use the same definitions as before since now the momentum of the particles has been changed not only by the interaction with the light quanta, but by their Coulomb interaction as well. The change in momentum of the first particle is equal and opposite to the change in momentum of the second one, and is given from (6) by

$$\Delta\mathbf{p}=\mathbf{p}_1^{n+1}-\mathbf{p}_1^n=\mathbf{p}_1^F-[\mathbf{p}_1^0+\mathbf{a}+\mathbf{b}+\cdots+\mathbf{z}]=-\mathbf{p}_2^F+[\mathbf{p}_2^0+\mathbf{A}+\mathbf{B}+\cdots+\mathbf{Z}]. \quad (9)$$

We define now

$$\langle E_1^p\rangle=-p-(p+1)-\cdots-z+E_1^F-E_1^p \quad (10a)$$

with

$$E_1^p=(|\mathbf{p}_1^F-\mathbf{p}-\cdots-\mathbf{z}|^2+\mu^2)^{\frac{1}{2}},$$

$$\langle E_2^Q\rangle=-Q-(Q+1)-\cdots-Z+E_2^F-E_2^Q \quad (10b)$$

with

$$E_2^Q=(|\mathbf{p}_2^F-\mathbf{Q}-\cdots-\mathbf{Z}|^2+\mu^2)^{\frac{1}{2}},$$

where now $\langle E_1^p\rangle$ is the energy difference for an intermediate state in which the first particle has interacted with the first $p-1$ quanta and the second particle has interacted with all Z quanta and similarly for $\langle E_2^Q\rangle$. The energy difference for an intermediate state in which e_1 has interacted with $p-1$ quanta and e_2 with $Q-1$ quanta, is given by

$$a+b\cdots+(p-1)+A+B\cdots+(Q-1)+E_1^0+E_2^0-E_1^p-E_2^Q$$

which from (5) is equal to

$$-p-\cdots-z-Q-\cdots-Z+E_1^F+E_2^F-E_1^p-E_2^Q=\langle E_1^p\rangle+\langle E_2^Q\rangle. \quad (10c)$$

Now we can apply our theorem again if we let $\langle E_1^s\rangle, \langle E_1^{s+1}\rangle\cdots\langle E_1^{n+1}\rangle$ correspond to $A_1\cdots A_n$ and $\langle E_2^Z\rangle, \langle E_2^{Z-1}\rangle\cdots\langle E_2^{M+1}\rangle$ to $B_1\cdots B_m$.

Hence we obtain finally for the sum of the terms containing the instantaneous Coulomb interaction, omitting for the moment the factors common to the entire series given in (7),

$$\frac{2(u_1^{*n}u_1^{n+1})(u_2^{*M}u_2^{M+1})}{|\Delta\mathbf{p}|^2}\times\frac{1}{\langle E_1^a\rangle\cdots\langle E_1^s\rangle\langle E_2^A\rangle\cdots\langle E_2^Z\rangle}. \quad (11)$$

We now proceed to the summation of the part of the series containing the retardation. We noted before that whereas the terms containing the instantaneous Coulomb interaction could be separated into the product of a series containing terms up to n and M only and another series containing the terms from $n+1$ and $M+1$ up, no such separation is possible for the terms containing the retardation. Our former definitions for the $\langle E\rangle$'s were consistent as we always had to deal with $\langle E\rangle$'s from the same part of the series. Now, however, we may have an intermediate state where the first particle has already emitted the $(n+1)$th light quantum while the other particle has not yet absorbed the K' quantum (describing the retardation), i.e., we have terms of the form

$$a+\cdots+n+\cdots+(p-1)+A+\cdots+L+E_1^0+E_2^0-E_1^p-E_2^L-K'$$

and if we define now

$$\Delta E=+E_1^{\,p}-[E_1^{\,0}+a+b+\cdots+z]$$
$$=-E_2^{\,p}+[E_2^{\,0}+A+B+\cdots+Z], \quad (12)$$

we can write this term

$$\langle E_1^{\,p}\rangle+\langle E_2^{\,L}\rangle+\Delta E-K'. \quad (13a)$$

For the case where K' had been emitted by the second particle, we obtain a general term of the form

$$A+\cdots+(Q-1)+a+\cdots$$
$$+g+E_1^{\,0}+E_2^{\,0}-E_1^{\,q}-E_2^{\,Q}-K'$$

which can be written

$$\langle E_1^{\,q}\rangle+\langle E_2^{\,Q}\rangle-\Delta E-K'. \quad (13b)$$

Let us sum first the part corresponding to the emission of K' by the first particle. Calling $\Delta E-K'=X$, we have then a series where each term is the product of expressions defined as before, except that at the step $\langle E_1^{\,n}\rangle\rightarrow\langle E_1^{\,n+1}\rangle$ we do not take $\langle E_1^{\,n+1}\rangle$, but $\langle E_1^{\,n+1}\rangle+X$, then $\langle E_1^{\,n+2}\rangle+X$ and so on. However, the step $\langle E_2^{\,M}\rangle\rightarrow\langle E_2^{\,M+1}\rangle$ subtracts the X again. The sum can therefore only include those terms where $\langle E_1^{\,n+1}\rangle$ is reached before $\langle E_2^{\,M+1}\rangle$.

We split the sum into partial sums according to the point at which the K' is absorbed, i.e., into sums with the same r occurring in the transition $(\langle E_1^{\,r}\rangle+\langle E_2^{\,M}\rangle+X)\rightarrow(\langle E_1^{\,r}\rangle+\langle E_2^{\,M+1}\rangle)$ where r can have any value between $n+1$ and $z+1$ (with $\langle E_1^{\,z+1}\rangle=0$). Then each sum can be factored into two sums containing the terms before and after this transition, respectively. Then we can apply our theorem without difficulty up to this transition, with $\langle E_1^{\,a}\rangle$, $\cdots\langle E_1^{\,n}\rangle$, $\langle E_1^{\,n+1}\rangle+X$, $\langle E_1^{\,n+2}\rangle+X$, $\cdots\langle E_1^{\,r}\rangle+X$ corresponding to A_1, $\cdots A_n$ and $\langle E_2^{\,A}\rangle$, $\cdots\langle E_2^{\,M}\rangle$ corresponding to B_1, $\cdots B_m$. We can furthermore apply it to the terms after this transition, with $\langle E_1^{\,s}\rangle$, $\cdots\langle E_1^{\,r}\rangle$ corresponding to A_1, $\cdots A_n$ and $\langle E_2^{\,Z}\rangle$, $\cdots\langle E_2^{\,M+1}\rangle$ to B_1, $\cdots B_m$. (For the single term obtained for $p=z+1$ we have simply $\langle E_2^{\,Z}\rangle$, $\cdots\langle E_2^{\,M+1}\rangle$.)

Adding the partial sums again we obtain

$$\frac{1}{\langle E_1^{\,a}\rangle\cdots\langle E_1^{\,n}\rangle\langle E_2^{\,A}\rangle\cdots\langle E_2^{\,Z}\rangle}$$
$$\times\Big\{\frac{1}{(\langle E_1^{\,n+1}\rangle+X)\langle E_1^{\,n+1}\rangle\langle E_1^{\,n+2}\rangle\cdots\langle E_1^{\,s}\rangle}$$
$$+\frac{1}{(\langle E_1^{\,n+1}\rangle+X)(\langle E_1^{\,n+2}\rangle+X)\langle E_1^{\,n+2}\rangle\cdots\langle E_1^{\,s}\rangle}+\cdots$$
$$+\frac{1}{(\langle E_1^{\,n+1}\rangle+X)(\langle E_1^{\,n+2}\rangle+X)\cdots(\langle E_1^{\,s}\rangle+X)X}\Big\}.$$

But the expression in brackets is just equal to the sum $\sum 1/(A,B)$ formed from the sets $0, X$ and $0, \langle E_1^{\,s}\rangle\cdots\langle E_1^{\,n+1}\rangle$, and therefore the entire sum is equal to

$$1/(\langle E_1^{\,a}\rangle\cdots\langle E_1^{\,s}\rangle\langle E_2^{\,A}\rangle\cdots\langle E_2^{\,Z}\rangle X).$$

We can sum the second part, corresponding to emission of K' by the second particle, in exactly the same way, only having $-\Delta E-K'$ instead of $\Delta E-K'$. Adding these two sums we obtain

$$\frac{(u_1^{*n}\alpha_{K'}u_1^{n+1})(u_2^{*M}\alpha_{K'}u_2^{M+1})}{K'}$$
$$\times\frac{2K'}{\langle E_1^{\,a}\rangle\cdots\langle E_1^{\,s}\rangle\langle E_2^{\,A}\rangle\cdots\langle E_2^{\,Z}\rangle(\Delta E^2-K'^2)}. \quad (14)$$

Now we have to sum over the directions of polarization of K' and add the expressions (11) and (14). As the independent directions of polarization are mutually perpendicular and perpendicular to the direction of propagation of K', we have

$$\sum(u_1^{*n}\alpha_{K'}u_1^{n+1})(u_2^{*M}\alpha_{K'}u_2^{M+1})$$
$$=(u_1^{*n}\alpha u_1^{n+1})\cdot(u_2^{*M}\alpha u_2^{M+1})$$
$$-(u_1^{*n}\alpha\mathbf{K}'u_1^{n+1})(u_2^{*M}\alpha\mathbf{K}'u_2^{M+1})/K'^2.$$

Remembering that $\mathbf{K}'=\Delta\mathbf{p}$, we obtain finally for that part of the matrix element (4) which corresponds to the interaction of z quanta with e_1 and Z quanta with e_2 with fixed order of interaction for each particle and which corresponds to Coulomb interaction after n and M as discussed before

$$(-e)^{z+Z+2}[(2\pi\hbar^2c^2)^{z+Z+2}/(a\cdots zA\cdots Z)]^{\frac{1}{2}}\frac{\prod_{1,1}^{n,M}\prod_{n+2,M+2}^{z,Z}(u_1^{*n-1}\alpha_n u_1^{n})(u_2^{*M-1}\alpha_M u_2^{M})}{\langle E_1^{\,a}\rangle\cdots\langle E_1^{\,s}\rangle\langle E_2^{\,A}\rangle\cdots\langle E_2^{\,Z}\rangle}$$
$$\times\frac{1}{|\Delta\mathbf{p}|^2-(\Delta E)^2}2\{(u_1^{*n}u_1^{n+1})(u_2^{*M}u_2^{M+1})-(u_1^{*n}\alpha u_1^{n+1})\cdot(u_2^{*M}\alpha u_2^{M+1})$$
$$+[-(\Delta E)^2(u_1^{*n}u_1^{n+1})(u_2^{*M}u_2^{M+1})+(u_1^{*n}\alpha\Delta p u_1^{n+1})(u_2^{*M}\alpha\Delta p u_2^{M+1})]/|\Delta\mathbf{p}|^2\}, \quad (15)$$

where $\Delta\mathbf{p}$ and ΔE are given by (9) and (12), $\langle E_1^a\rangle\cdots\langle E_1^n\rangle$ and $\langle E_2^A\rangle\cdots\langle E_2^M\rangle$ by (8) and $\langle E_1^{n+1}\rangle\cdots\langle E_1^s\rangle$ and $\langle E_2^{M+1}\rangle\cdots\langle E_2^Z\rangle$ by (10).

Equation (15) includes the summation over all the terms of (4) having the same numerator (7), but the summation over all the different possible numerators has still to be done for any particular process as discussed before.

V. DISCUSSION

Comparison of the expression containing the retarded interaction (15) with the expression containing only the instantaneous Coulomb interaction (11) shows that the sole difference is that the factor

$$\frac{4\pi\hbar^2c^2e_1e_2}{|\Delta\mathbf{p}|^2}(u_1^{*n}u_1^{n+1})(u_2^{*M}u_2^{M+1}) \tag{16}$$

is replaced by

$$\frac{4\pi\hbar^2c^2e_1e_2}{|\Delta\mathbf{p}|^2-(\Delta E)^2}\cdot\Big\{(u_1^{*n}\cdot u_1^{n+1})(u_2^{*M}\cdot u_2^{M+1})-(u_1^{*n}\boldsymbol{\alpha}u_1^{n+1})\cdot(u_2^{*M}\boldsymbol{\alpha}u_2^{M+1}) + \frac{-(\Delta E)^2(u_1^{*n}\cdot u_1^{n+1})(u_2^{*M}\cdot u_2^{M+1})+(u_1^{*n}\boldsymbol{\alpha}\Delta\mathbf{p}u_1^{n+1})\cdot(u_2^{*M}\boldsymbol{\alpha}\Delta\mathbf{p}u_2^{M+1})}{|\Delta\mathbf{p}|^2}\Big\}, \tag{17}$$

independent of the process under consideration. This is in spite of the fact that in (4) the number of terms needed to describe the retardation did depend on the process. Equation (16) is simply the usual matrix element (3a) for the instantaneous Coulomb interaction applied to the particular transition $n\to n+1$, $M\to M+1$ of our calculations. We see that by eliminating the virtual quanta, we have obtained an expression (17) analogous to the matrix element (3a) which can be used as a matrix element for the retarded interaction for any process involving the interaction of radiation and two electrons.[7] Using (17) the retarded interaction can then be treated as a single transition in the succession of intermediate states appearing in the total matrix element (4). Therefore the above noted difficulty of a dependence of the form of the retarded interaction on the particular process under consideration was only apparent.

While we have obtained this correspondence of the expressions (16) and (17) for the instantaneous and retarded interactions from the *summed* expressions (11) and (15), we can nevertheless, if desirable, use our "matrix element of retarded interaction" even before summing without introducing an error. The formalism of perturbation theory assigns a meaning to the summed expression only, and we are therefore justified in using any expansion whatsoever, as long as the summed expressions agree. But we could not have obtained the correspondence without *first* summing our series. If we fix our attention on just one term of the series involving the instantaneous interaction, i.e., a fixed order of interactions of the light quanta with the first and second particle, it is impossible to assign a correspondence to a definite part of the series involving the retardation. This is due to the fact that, as pointed out before, the emission and absorption of the virtual quanta need not take place in two consecutive steps.

In the case that no radiation is present (15) reduces to (17) alone. Equation (17) can then be further simplified. $\Delta\mathbf{p}$ is just equal to $\mathbf{p}_1^F-\mathbf{p}_1^0$, and we obtain from Dirac's equation $\boldsymbol{\alpha}(\mathbf{p}_1^F-\mathbf{p}_1^0)u=(E_1^F-E_1^0)u=\Delta E\cdot u$ and therefore our expression reduces to

$$\frac{4\pi\hbar^2c^2e_1e_2}{|\Delta\mathbf{p}|^2-(\Delta E)^2}\times[(u_1^{*0}u_1^F)(u_2^{*0}u_2^F)-(u_1^{*0}\boldsymbol{\alpha}u_1^F)\cdot(u_2^{*0}\boldsymbol{\alpha}u_2^F)]$$

which is just the expression obtained by Møller.[8]

It can be seen similarly that (15) reduces to the expression obtained by Møller for the interaction of two particles and one light quantum,[8] the only other case for which the matrix element has been calculated directly. In this case we have still to include a summation of the expressions (15) over the four possibilities that the retarded interaction can take place before or after the interaction with the light quantum and that the light quantum can interact with either one of the

[7] It should be remembered that our result has been derived for a process involving two particles. Its validity for processes involving more than two particles remains to be proved. See also footnote 6.

[8] C. Møller, Proc. Roy. Soc. 152, 481 (1935).

two particles. In addition to these cases (15) can be used to calculate the emission of several quanta at the collision of two particles. It can also be applied to the problem of creation of an electron-positron pair due to simple or multiple scattering of a γ-ray, as in the Dirac theory the presence of a positron in the final state can be described by the presence of an electron with negative energy in the initial state.

It should be noted that while we started from an expression which involved both particles in intermediate states simultaneously, each factor in the denominator of expression (15) involves one particle in an intermediate state at a time only. Therefore the method of Casimir[9] for summing over both signs of the energy of the particles in the intermediate states can now be applied directly.

Furthermore we can easily see that our expression (15) reduces to the known formula for the case where one particle can be considered as infinitely heavy. Then the energy is conserved for the interaction of the electron and the quanta, but not the momentum, because of the presence of the nucleus. The heavy particle cannot interact with the light quanta, but only with the electron. Therefore it does not pass through any intermediate states, and we have to put $(u_2^{*0}u_2^{F})=1$ and $(u_2^{*0}\alpha u_2^{F})=0$. With these changes, (15) together with the definitions (8a) and (10a) correctly describes the interaction of one electron with radiation or the creation of a pair of particles by the scattering of γ-rays in the field of a nucleus.

In the course of our calculations we have arbitrarily assumed that none of the energy differences in the denominator of (4) vanishes, and we have now to study the limits of applicability of (15). This expression diverges in two cases. The first case occurs when any of the $\langle E_1^{z}\rangle$'s or $\langle E_2^{\nu}\rangle$'s vanish (found by putting the expressions (8a, b) and (10a, b) equal to zero). As each of these $\langle E\rangle$'s refers to one particle only, the limitation introduced hereby is the same as for a process involving the interaction of radiation and a single particle. In the familiar cases this excludes processes which involve light quanta with the same energy and momentum in both the initial and final states and which could therefore be described by an approximation of lower order in e than the one applied.

The second case occurs when $|\Delta\mathbf{p}|^2-(\Delta E)^2=0$. This is the case for vanishing interaction of the two particles. Then our process splits up into two independent processes each involving a single particle and a certain number of quanta. Again these could have been calculated in a lower order approximation. This case is similar to the situation for the calculation of the scattering of two charged particles in a non-relativistic first order approximation, where we obtain the Rutherford formula, which diverges for zero deviation, i.e., vanishing interaction of the two particles. There, however, the exact solution is known, and it again reduces to the Rutherford formula for all but vanishing deviation angles, for which it also remains finite.[10] Unfortunately the exact solution of the relativistic two-body problem is not known.

Inspecting formulas (8c), (10c), and (13a, b), we might expect still other cases of divergencies if these expressions vanish, while these cases cannot be seen directly from our final Eq. (15). But these expressions can be indefinitely small without any indication of a maximum in the summed expression, due to cancellations. This can be seen directly from the proof of our theorem. If a number A_i of one set is almost equal to the negative of a number B_k of the other set, we can still apply the theorem. If we call $B_k=-A_i+\epsilon$, the sum depends upon ϵ as $1/(-A_i^2+A_i\epsilon)$, with $\epsilon\gtrless 0$, which is a monotonically varying function of ϵ. Therefore (15) does not show any resonance-like behavior in the neighborhood of the values obtained by putting the expressions mentioned above equal to zero.

The author wishes to thank Dr. Joseph M. Keller for his interest and helpful discussions.

[9] H. Casimir, Helv. Phys. Acta **6**, 287 (1933).

[10] W. Gordon, Zeits. f. Physik **48**, 180 (1928), in particular Eq. (7′), p. 190, and the following discussion.

Lifetimes of Resonance Lines of Cadmium*

HAROLD W. WEBB AND HELEN A. MESSENGER**
Pupin Physics Laboratories, Columbia University, New York, New York
(Received May 20, 1944)

The mean lifetime of the triplet resonance line $5^1S_0-5^3P_1$, 3261A, of cadmium was measured by the alternating voltage method. The value found was 2.14×10^{-8} second, with an estimated precision of three percent. Similar measurements made to determine the mean lifetime of the singlet resonance line, $5^1S_0-5^1P_1$, 2288A, showed that the excitation which resulted in the emission of this line was mainly due to cascading from a higher level (or levels) by infra-red transitions, the excitation to the 5^1P_1 level by electron impact being relatively much less probable than that to the higher level. The lifetime of the infra-red transition was found to be 9.0×10^{-9} second. From the form of the curve showing the dependence of the persistence of the radiation emitted by the excitation tube upon the vapor concentration, the mean lifetime of the 2288A transition was estimated as approximately 2.1×10^{-9} second. The lifetime of the subordinate series lines 5086–4800–4678A was found to be 10^{-7} second, but since the measurements were affected by absorption and re-emission of the radiation, this value can be taken only as the maximum possible value of this lifetime. For the diffuse subordinate series lines, 5^3P-5^3D, similar measurements showed that their lifetime was not greater than 10^{-7} second.

THE lifetimes of each of the two resonance states of cadmium, 5^1P_1 and 5^3P_1, has been measured by several methods. Koenig and Ellett,[1] by measuring directly the decay of the resonance radiation in a stream of cadmium vapor, found for the lifetime of 3261A ($5^1S_0-5^3P_1$), 2.5×10^{-6} sec. Kuhn[2] obtained the value 2.3×10^{-6} sec. by the magneto-rotation method, and Ellett[3] and Soleillet,[4] from studies of the depolarization in a magnetic field, obtained the values 2.3×10^{-6} and 2×10^{-6} sec., respectively. The lifetime of 2288A ($5^1S_0-5^1P_1$) as measured by Kuhn,[5] again using the magneto-rotation method, was 1.98×10^{-9} sec. Zemansky[6] found the value 1.99×10^{-9} sec., using the line absorption method of Ladenburg and Reiche. Soleillet[4] computed the value of this lifetime as 10^{-9} sec. from the magnetic depolarization data; however, to account fully for his results, he resorted to the assumption that there existed a second hyperfine energy level of the 5^1P_1 state with the lifetime of 10^{-6} sec., which is not in accord with the generally accepted theory.

Measurements of the lifetimes of these two resonance lines of cadmium made by use of the alternating voltage method, previously employed to measure the lifetimes of lines of hydrogen, mercury, and potassium,[7] are described in this paper, together with some results obtained in studying the lifetimes of several subordinate series lines in the cadmium spectrum for which no earlier measurements are on record.

METHOD

The method used in determining the mean lifetimes of lines has been described in the several earlier papers[7] and will be but briefly discussed here. The radiation studied was produced in an excitation tube which contained cadmium vapor at low pressure and which was provided with a grid for controlling the excitation. This radiation, isolated by suitable filters, passed to a photoelectric tube so designed that saturation occurred at very low values of its control-grid voltage. An alternating sinusoidal voltage was applied to the control-grids of the respective tubes in phase. The bias voltage on the excitation tube grid insured that excitation occurred only during a known fraction of the positive half-cycle, and a

* Publication assisted by the Ernest Kempton Adams Fund for Physical Research of Columbia University.
** Hunter College, New York, New York.
[1] H. D. Koenig and A. Ellett, Phys. Rev. **39**, 576 (1932).
[2] W. Kuhn, Naturwiss. **13**, 725 (1925).
[3] A. Ellett, Phys. Rev. **33**, 124 (1929).
[4] P. Soleillet, Comptes rendus **187**, 212 (1928).
[5] W. Kuhn, Naturwiss. **14**, 48 (1926).
[6] M. Zemansky, Zeits. f. Physik **72**, 587 (1931).
[7] F. G. Slack, Phys. Rev. **28**, 1 (1926); H. W. Webb and H. A. Messenger, Phys. Rev. **33**, 319 (1929); R. H. Randall, Phys. Rev. **35**, 1161 (1930); P. H. Garrett, Phys. Rev. **40**, 779 (1932); D. Sinclair and H. W. Webb, Phys. Rev. **50**, 440 (1936).

suitable bias voltage on the photoelectric tube caused the current to the collecting electrode to reverse with the voltage on the control-grid. At low frequencies radiation reached the photoelectric tube only in the positive half-cycle, and hence there was no reverse photoelectric current. At higher frequencies, the radiation, because of its persistence, reached the tube in both half-cycles; the positive current was reduced, and reverse current appeared. The net photoelectric current to the collecting electrode therefore diminished with increasing frequency and approached asymptotically a "final level" when the persistence resulted in a uniform emission from the excitation tube.

The first step in the measurement of τ, the lifetime of a line, by this method, was the determination for this radiation of the "static characteristics" of the excitation tube (radiation as a function of grid voltage) and of the photoelectric tube (photoelectric current as a function of grid voltage, for constant radiation). The alternating voltages were then applied to the control-grids of the two tubes in phase and the photoelectric current measured for a suitable range of values of the frequency f. The voltages applied to the grids were made the same for all frequencies to maintain constant the total radiation excited. The results are expressed as the ratio R of the photoelectric current at the frequency f to the photoelectric current at a frequency so low that the persistence of the radiation was practically negligible. This will be called the "reference frequency" hereafter. Data from the curve obtained when R was plotted as a function of f were used to compute τ, the mean lifetime of the line.

In measuring the lifetimes of resonance lines the absorption of the radiation presents a serious complication. Each photon absorbed produces an excited atom which persists in its excited state with the same mean lifetime as an atom originally excited by electron impact. The observed radiation consists, then, of photons which come directly from atoms excited by impact and photons which leave the excitation tube after one or more absorption-re-emission processes. This increases the persistence in the mass of vapor in the excitation tube, and hence the "apparent" lifetime T is greater than τ, the difference increasing with the vapor pressure. To determine τ it is therefore necessary to correct for the effect of absorption and re-emission, which it is difficult to compute precisely, or else to make measurements at pressures so low that absorption is negligible. This occurs at such low pressures that the radiation is usually insufficient for precise measurements. For example, in measuring the lifetime of 2288A, it was necessary to work at a vapor pressure below 1.5×10^{-6} mm. At this pressure the kinetic mean free path of the electrons in the vapor was of the order of 10^4 cm, so that the efficiency of the excitation tube was exceedingly low. This difficulty, usually encountered only in measurements with resonance lines, proved troublesome also in measurements on subordinate series lines when intense excitation was used.

APPARATUS

Figure 1 shows schematically the essential elements of the apparatus used, for the measurements with 3261A and 2288A. In the main it was similar to that used in earlier experiments and fully described by Garrett.* The excitation tube is shown in cross section. The envelope was of fused quartz; S was an indirectly heated, oxide coated cathode; G, the control-grid, was of nickel mesh and covered only the front half of the cathode; W, the wall grid, was of nickel mesh on the front, or window, side and of solid sheet in the rear. Since it was essential that absorption of radiation be reduced to a minimum, the tube was

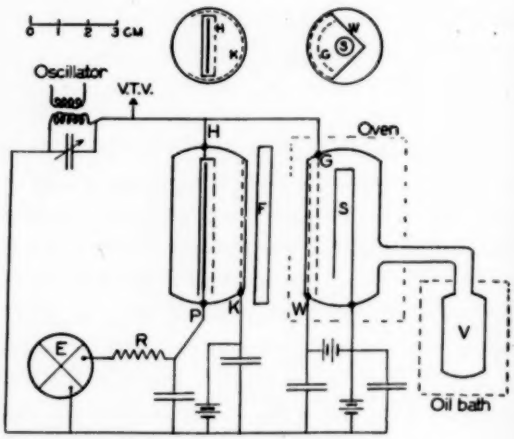

FIG. 1. Diagram of apparatus.

* P. H. Garrett, reference 7, p. 781.

so designed that by the application of suitable voltages to the grids excitation would occur mainly between G and W and radiation reach the window by traversing only a thin layer of vapor. The tubes were sealed off after evacuation in the usual manner, with especial care to eliminate traces of mercury.

Adjoining the excitation tube was a reservoir V, on the walls of which a thin layer of carefully purified cadmium metal had been evaporated before the tube was sealed off from the pumps. This reservoir was immersed in an oil bath, electrically heated, and maintained by a thermostat within 0.5°C of the temperature corresponding to the vapor pressure desired in the tube. The body of the tube was in an oven consisting of a copper cylinder with very heavy walls heated by gas jets. A fused quartz window opposite the cathode transmitted the radiation. The temperature of the oven was held only slightly higher than that of the oil bath to permit the concentration of cadmium atoms N in the tube to be taken as that corresponding to the temperature of the bath without correction. This concentration was computed from the vapor pressure given by the formula in the *International Critical Tables* for the appropriate range.

The photoelectric tube used in studying the resonance radiations is shown in cross section in the figure. The envelope was of quartz. The sensitive surface was magnesium, selected for the measurements with 3261A and 2288A because its long wave-length limit is in the neighborhood of 4000A and its maximum sensitivity is near 2500A.[8] This was deposited on the plate P, a nickel sheet 1 cm×4 cm. The control grid H was rectangular in cross section and was of nickel mesh in the front and of sheet nickel on the sides and back with a clearance of 2 mm between it and P. The shape and clearance were designed to give current-voltage ($H-P$) characteristics which would reverse sharply with the voltage and to cut down the time lag of the tube produced by the time of passage of the photoelectrons between P and H. The auxiliary electrode K was also of nickel mesh and served to prevent the return to P of electrons which had passed through the grid H into the region between H and K. The plate P was coated with magnesium by the method described by Rentschler.[9] An auxiliary electrode (not shown in the figure) was used, consisting of a magnesium wire, 1 mm in diameter, placed between H and K, parallel to the axis of the tube. After baking the tube and outgassing the electrodes, the tube was filled with argon at a suitable pressure and with the magnesium wire as cathode and the electrodes P and H as anode, a coating of magnesium was deposited on P by sputtering. The argon was then removed by absorption by cocoanut charcoal contained in a side tube immersed in liquid air. After the argon had been absorbed, this tube was sealed off.

Provision was made for interposing between the excitation and photoelectric tubes various filters including a quartz cell containing pure cadmium vapor. A water cell, with windows of quartz or of glass with high ultraviolet transmission, was interposed between the tubes when it was necessary to protect the photoelectric tube from the heat of the oven.

Photoelectric current was measured by a sensitive quadrant electrometer. To avoid disturbances on opening the electrometer key and to simplify the high frequency circuit, the lead from P was connected to ground through a condenser C of approximately double the capacity between P and H. The electrometer was connected in parallel with this condenser through a resistance R of 13×10^9 ohms, which isolated it from the high frequency circuit.

A vacuum-tube oscillator with loosely coupled tuned secondary circuit was the source of the alternating voltage. A calibrated peak voltmeter was employed to measure and monitor the voltage. By the use of switches, not shown in the figure, either grid could be connected independently to sources of direct potential or to the source of alternating voltage. When alternating voltage was used on both grids, their terminals were connected as directly as was possible to minimize any differences between the magnitudes and phases of the voltages on these two electrodes.

The cadmium absorption cell employed as a filter in some of the measurements was especially useful in determining the purity of the resonance

[8] A. L. Hughes and L. A. DuBridge, *Photoelectric Phenomena* (McGraw-Hill Book Company, Inc., New York and London, 1932), p. 162.

[9] H. C. Rentschler and D. E. Henry, J. Frank. Inst. **223**, 135 (1937).

radiations. It was a cylindrical cell of fused quartz, 2 cm in diameter with plane faces 1 cm apart. Solid cadmium in a side tube, the temperature of which was controlled by an electric heater, furnished cadmium vapor at the desired concentration. The body of this cell was enclosed in an oven to keep the vapor at a temperature slightly higher than that of the side tube. Quartz windows permitted the transmission of the radiation to and from the cell.

EXPERIMENTAL PROCEDURE AND RESULTS

3261A

The measurements of the mean lifetime of the resonance triplet resonance line 3261A were made with vapor concentrations in the excitation tube ranging from 8.7×10^{12} atoms cm^{-3} (204°C) to 3.3×10^{14} atoms cm^{-3} (280°C). The radiation 2288A, which was very intense at these concentrations, was filtered out with a Corex D filter (Corning Glass Company), which absorbed all wave-lengths shorter than 2500A. When testing for the presence of wave-lengths other than 3261A in this filtered radiation, the cadmium absorption cell was interposed between the excitation tube and the Corex D filter. With $G-S$ equal to 11.0 volts, and the excitation tube at 214°C, approximately the temperature at which precise measurements were desired, no measurable amount of radiation was transmitted by the absorption cell when the vapor pressure therein was 0.05 mm (300°C), showing that of wave-lengths above 2500A the excitation tube was emitting substantially only 3261A. The absorption coefficient for this line computed from the absorption measurements taken at lower pressures in the absorption cell, was $1.3\times10^{-14}N$.

Measurements to determine the lifetime were made with the bias voltage $W-S=4.5$ volts, and bias voltage $K-P=4.5$ volts. In each determination of the lifetime it was first necessary to determine the "static characteristics" of the excitation and photoelectric tubes for the radiation in question at the selected vapor pressure. When the intensity of 3261A radiation in the excitation tube was studied as a function of the $G-S$ voltage, taken with $H-P$ constant at three volts, the curve first showed the excitation of 3261A at $G-S=4.5$ volts, with no correction for contact potential or drop in the leads. The accepted excitation potential for this line is 3.8 volts. At higher voltages there were several breaks in the curve, which departed sufficiently from a linear relation between radiation and voltage to necessitate a graphical calculation when determining an accurate value of the lifetime. The static characteristics of the photoelectric tube were of exceptionally simple form. Saturation was reached when $H-P$ was little more than 0.4 volt. The reversal point was at $H-P=-0.1$ volt, making it unnecessary to use a bias voltage on $H-P$ during the alternating voltage measurements. The reverse current was approximately 30 percent of the positive saturation current and varied only 5 percent as $H-P$ was varied from -2 to -9 volts. In such measurements special care is necessary to eliminate the effects of charges which accumulate on the walls of the tube and give erroneous results.

When the alternating voltages were applied to the control-grids, the peak value used was 6.6 volts, with a fixed bias of 4.5 volts applied to $G-S$, so that radiation was excited only in the positive half-cycle. The crest voltage attained by $G-S$, 11.1 volts, was sufficiently low to insure that the radiation excited and transmitted through the filter was substantially 3261A and that the ionization was negligible. A test made with alternating voltage applied to $G-S$ only, $H-P$ being held at constant voltage, showed the electrometer current to be independent of the frequency, indicating that the voltage applied at the external terminals of G and S was the same as that between the electrodes G and S and that the behavior of the excitation tube could be predicted from the static characteristics. With the alternating voltage applied directly to $G-S$ and $H-P$, a series of measurements was made to determine the $R-f$ curve for each of several concentrations of cadmium vapor in the range specified above. In this case R was the ratio of the photoelectric current at the frequency f to that at the reference frequency, 1300 cycles. It was found that the final level R_∞, the value of R approached asymptotically by the curve at high frequencies, agreed well with that calculated from the static characteristics. This is an important check, signifying that the behavior of the photoelectric tube could be correctly predicted from these characteristics.

The lowest concentration at which the energy was sufficient to make precise measurements possible was that corresponding to 218.5°C. At this concentration the secondary radiation resulting from absorption and re-emission which reached the photoelectric tube was less than 10 percent of that resulting from direct excitation. At this concentration the $R-f$ curve was taken with special care, and a precise value of R for $f=80{,}500$ cycles, 0.647, was determined by repeated observations. Then from the $R-f$ curves taken at oil bath temperatures of 244°, 232°, 215°, and 203°C, respectively, the values of the frequency f_0, for which R had this same value, 0.647, were also determined. Graphical calculations made from the respective static characteristics of

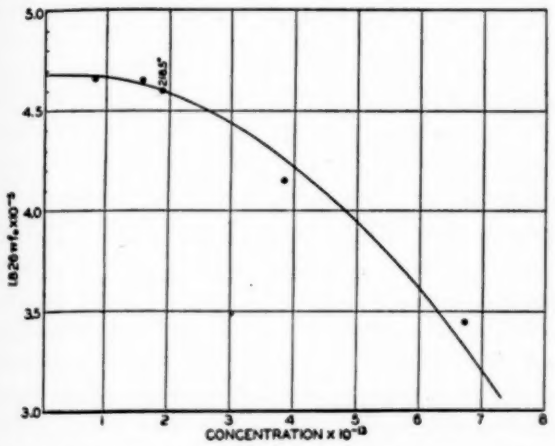

FIG. 2. Curve to determine lifetime of 3261A. $\tau=1.826\pi f_0 \times 10^{-6}$ sec. for zero concentration of cadmium atoms.

the excitation and photoelectric tubes show that if the radiation had been emitted from the excitation tube according to a simple exponential relation (i.e., all radiation direct and no absorption and re-emission), τ, the lifetime of the line, would have been given by $\tau=(1.826\pi f_0)^{-1}$ sec. In Fig. 2 the values of $1.826\pi f_0$, determined from the five curves, are plotted as a function of the vapor concentration. Extrapolation of this curve to zero concentration gives the correct value of $1/\tau$ since the effect of absorption is thus eliminated. This extrapolation would ordinarily be difficult to carry out with precision because the form of the curve for low concentrations is not easily calculated from the tube geometry. However, for the tube used, the form of the curve is approximately known from the very careful measurements of the lifetime of the 2537A line of mercury made by Garrett,* who used an excitation tube approaching closely in size, shape, and positions of electrodes the tube used in these measurements. The curve drawn in Fig. 2 is the curve of Fig. 3b of his paper, with the scales so adjusted that the curve passes through the precisely determined point for 218.5°C and best approximates the experimental curve for higher values of the concentration. The departure of the experimental points from this curve is in every case within the experimental error of the measurements. The ratio of the scales of abscissas is approximately the reciprocal of the ratio of the atomic absorption coefficients of the two lines. For zero concentration the curve gives $1.826\pi f_0=1/\tau=0.467\times10^5$ sec.$^{-1}$. The mean lifetime of the line 3261A is therefore determined as 2.14×10^{-6} sec., the precision of the measurements being estimated as better than three percent.

This result is about seven percent lower than values given by the magneto-rotation and magnetic depolarization methods.[2-4] The value 2.5×10^{-6} sec., found in the measurements of Koenig and Ellett,[1] was probably subject to larger error than the other methods because of the difficulties inherent in the method.

In the measurements here reported, the excitation of the 5^3P_1 level by cascading from higher levels was considered as a possible source of error. However, a series of studies made with varied peak voltages indicated this excitation to be negligible.

Some additional measurements made with 3261A are of interest because of the light they throw upon the effect of the absorption-re-emission process. These were made with a second excitation tube which was practically identical in construction with the tube used in the measurements just described except that the envelope was of glass of high ultraviolet transmission, instead of quartz. The average value of τ calculated from measurements with this tube was double that determined with the first tube for the same vapor density and electrode voltages. The measurements were inconsistent and not reproducible. With a peak alternating voltage of 4.5 volts on $G-S$ and $H-P$, and temperatures between 200°

* P. H. Garrett, reference 7, p. 784.

and 214°C, the calculated lifetime varied between 6.4 and 3.8×10^{-6} sec. On the other hand, when the peak voltage was decreased to 1.5 volts, the calculated lifetime was 2.3×10^{-6} sec. Absorption measurements showed that the radiation measured was still substantially 3261A. These spurious results were later found to be due to a defective coating on the hot cathode. The greater part of the electron emission was from the lower tip of the cathode, which was not opposite the window of the oven. The bulk of the radiation which reached the photoelectric tube was excited in this region and could reach the photoelectric tube only by being absorbed by the vapor in the region opposite the window and reradiated. As a result the calculated lifetime was approximately twice the true lifetime. The variability in the results and their dependence upon voltage was due to the variation of the distribution of the emission over the surface of the cathode with time and applied voltage. When the window was lowered to expose the active part of the cathode, the measurements gave results in close agreement with those found with the quartz tube.

2288A

A series of measurements was made to study the behavior of the principal series resonance line 2288A, with the same quartz excitation and photoelectric tubes as were used with 3261A.

The concentration of cadmium vapor in the excitation tube was varied between 1.6×10^{10} (113°C) and 2.7×10^{12} (184°C), atoms cm^{-3}. The more precise and significant measurements were made at temperatures of the reservoir V below 140°C and with crest values of the voltage $G-S$ less than 10.5 volts. Under these conditions the only radiation emitted by the excitation tube, to which the photoelectric tube responded, was 2288A. To test the radiation for the presence of 3261A, a Corex D filter which absorbs all wavelengths shorter than 2500A was interposed between the tubes. When the temperature of the reservoir was below 170°C and the crest value of $G-S$ was less than 12 volts, no radiation was transmitted which could be detected by the photoelectric tube; i.e., no radiation between 2500A and 4000A was present in a measureable amount. To test for radiation shorter than 2500A, other than 2288A, absorption measurements were made with the cadmium vapor absorption cell between the excitation and photoelectric tubes. The radiation tested was from the excitation tube when the reservoir was at 145°C. The tubes were separated so that the distance between excitation tube and absorption cell was 72 mm and that between absorption cell and photoelectric tube was 90 mm. With high pressures in the absorption cell, absorption was practically complete, indicating that the radiation affecting the photoelectric tube was essentially 2288A.

With lower pressures in the absorption cell, the absorption coefficient of cadmium vapor for this radiation was computed to be $1.75\times10^{-11}N$, which agrees, within the precision of the observations, with the value, $1.64\times10^{-11}N$, given by Zemansky.[6] In these calculations allowance was made for that part of the radiation scattered from the absorption cell which reached the photoelectric tube.

Throughout this series of measurements the voltages $W-S$ and $K-P$ were held at 4.5 volts. The static characteristics were determined in the manner described above. That of the excitation tube (radiation as a function of $G-S$) was very nearly a straight line with an intercept on the voltage axis at 6.0 volts. The accepted excitation potential for 2288A is 5.4 volts. The characteristic of the photoelectric tube was of the usual form with saturation for $H-P$ less than 1 volt. The current reversal occurred at -0.7 volt.

The $R-f$ curves were made with fixed bias voltages; $G-S$ equal to 4.5 and $H-P$ to -0.7 volt. The alternating voltage impressed upon the directly connected external terminals of G and H was maintained for all frequencies at 5.0 volts, peak value. The reference frequency was 14,000 cycles. It was found, however, that the radiation from the excitation tube decreased with increase in frequency as determined by applying alternating voltages to $G-S$ only, $H-P$ being held constant. To correct for this, the ratio of the radiation for each frequency to that for the reference frequency was determined. The observed value of R was then corrected to correspond to equal radiation excited at all frequencies, by dividing by this ratio. The cause of this variation was presumed to be voltage drop in the leads within the excitation tube at high frequencies, resulting in a voltage difference between the

electrodes less than that between their external terminals. A decrease in the electrode voltage $G-S$ of 3 percent would have accounted for the maximum observed variation of the radiation emitted, which was about 10 percent. A corresponding decrease in the voltage on the electrodes of the photoelectric tube would have had negligible effect on the measurements.

The results of the measurements are shown in Fig. 3, which gives, as a function of the concentration of cadmium atoms, the values of the "apparent lifetime" of the radiation emitted by the excitation tube. In an earlier paper the authors have shown[7] that in the case of radiation excited by electron impact, provided (a) that absorption is negligible, (b) that the excitation of radiation in the excitation tube is proportional to the instantaneous value of the alternating voltage during the positive half-cycle, and zero during the negative half-cycle, and (c) that the current in the photoelectric tube passes abruptly from a positive saturation value to a negative saturation value upon reversal of the alternating voltage, the relation between R and f is given by

$$R=1-\tfrac{1}{2}(1+s)(4\pi^2f^2\tau^2)(1+4\pi^2f^2\tau^2)^{-1}; \quad (1)$$

Here s is the ratio of the negative to the positive photoelectric saturation current, and τ is the mean lifetime of the radiation from the excited atom. Except for the effect of absorption and reradiation at the higher concentrations, these conditions were well satisfied in the measurements with 2288A as seen from the static characteristics and the bias voltages selected for the electrodes. When no complications due to absorption are involved, τ can easily be found from the curves. From (1) we find:

$$\text{for} \quad f=\infty, \quad R=R_\infty=1-\tfrac{1}{2}(1+s); \quad (2)$$

$$\text{for} \quad f=f_1=1/(2\pi\tau),$$

$$R=R_1=1-\tfrac{1}{4}(1+s)=\tfrac{1}{2}(1+R_\infty). \quad (3)$$

$$\text{Hence} \quad \tau=(2\pi f_1)^{-1}, \quad (4)$$

where f_1 is the frequency for which R is the mean of unity and the final asymptotic level R_∞, approached by the curve at high frequencies. In Fig. 3, the values of $(2\pi f_1)^{-1}$ were found from the experimental curves, and from the value of s calculated from the photoelectric characteristic. The use of this value instead of the experimentally determined value was necessary because of the difficulty of making measurements at sufficiently high frequencies and because the curves departed markedly from the curve as given by the equation. The experimental curves dropped more sharply than the theoretical curve, and R fell to a value considerably lower than R_∞ as calculated from the static characteristic. Although it was not possible to verify this by measurements at sufficiently high frequency, there were indications that this low value of R was a minimum and that the curves would have approached the theoretical value of R_∞ had higher frequencies been used.

The extrapolation of the curve in Fig. 3 to zero concentration, to eliminate the effect of absorption and reradiation, gave 11.0×10^{-9} sec. for the limiting value of $(2\pi f_1)^{-1}$. This would give a lifetime of 2288A about five and one-half times as great as the value 1.99×10^{-9} sec. found by earlier investigators.[5,6] Because of this large difference in the results and because of the unusual form of the experimental curves, it seemed probable that the process under investigation was more complex than the simple excitation of 2288A postulated in the computations. This was confirmed by a study of the form of the curve in Fig. 3. For brevity, let $(2\pi f_1)^{-1}$ be represented by T. The increase in T with the vapor concentration N is a complex function involving the geometry of the tube and cannot be readily computed. The earlier work of the authors and that of Garrett[7] with the

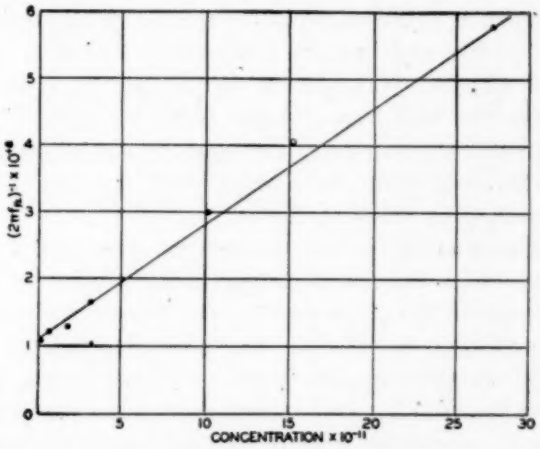

FIG. 3. Curve showing persistence of 2288A as a function of the concentration of cadmium atoms. The value of $(2\pi f_1)^{-1}$ at zero concentration equals $\tau+\tau_1$.

2537A line of mercury showed that the relation between T and N is given approximately by the equation

$$T=T_0+ANb\tau, \tag{5}$$

where A is the atomic absorption coefficient and b the "effective thickness" of the vapor traversed by the radiation. In the case of the mercury radiation, the constant T_0 is identical with τ, the lifetime of the resonance radiation. From (5) we have

$$\tau=(1/Ab)(dT/dN). \tag{6}$$

The value of b can in general be only roughly estimated from the geometry of the tube. However, the tube used in this work was nearly identical in design and dimensions with that used by Garrett, whose results are well described by (5) if b is taken as equal to 0.5 cm. Using this value of b and Zemansky's value of A, 1.64×10^{-11}, and dT/dN, 1.73×10^{-20}, determined from the curve, we find from (6) the value $\tau=2.1\times10^{-9}$ sec., which, considering the approximations used, agrees well with the value 1.99×10^{-9} sec. determined by other methods.[6]

The possibility that the peculiar shape of the curve was due to a phase shift, causing the voltage on the excitation tube grid to lag behind the voltage applied to the photoelectric tube grid, was investigated. Such a phase shift would have resulted in a curve having a final level below the R_∞ calculated from the static characteristics. A comparison of the curves at high and low concentrations of cadmium vapor showed equal differences between the minimum values of R and R_∞ although the frequencies used in the two cases differed by a factor of ten. Since the phase shift should have decreased with the frequency, it was concluded that it was not sufficient to cause significant error.

The most consistent explanation of these results is that under the conditions of the experiment, the excitation of the atoms by electron impact was mainly to a level (possibly several levels) a few tenths of a volt above the 5^1P_1 level, and that excitation of the 5^1P_1 level was by an infra-red transition to it from the higher level. The persistence of 2288A observed by the method used in these measurements would depend, therefore, upon both the lifetime of the 5^1P_1 state and on τ_1 the lifetime of the infra-red transition. Since the photoelectric surface was sensitive only to the 2288A radiation, under the conditions used in these measurements the $R-f$ curves for such a cascade process are described by the equation

$$R=1-\frac{1+s}{2}\frac{\tau_1/\tau}{\tau_1/\tau^{-1}} \times\left[\frac{4\pi^2f^2\tau_1^2}{1+4\pi^2f^2\tau_1^2}-\frac{\tau}{\tau_1}\frac{4\pi^2f^2\tau^2}{1+4\pi^2f^2\tau^2}\right]. \tag{7}$$

From this equation it can be shown that with an error of less than two percent, T_0, the value of T at zero concentration, determined as described above is equal to $\tau+\tau_1$. Using the earlier determined value of τ, 1.99×10^{-9} sec., we find for the lifetime of the infra-red transition, or average lifetime of the several transitions if there were more than one, 9.0×10^{-9} sec. The curve representing Eq. (7) has the peculiarities observed in the experimental curves. It drops more sharply than the curve described by (1), falls to a minimum well below R_∞ and at high frequencies approaches it as a limiting value. Substituting in it the values of τ and τ_1, found above, we find, for zero concentration a minimum value of R at $f=5f_1$, 0.06 below R, which agrees approximately with the observed values. This result is similar to that found for the corresponding line in the mercury spectrum 1849A by the authors.* It was shown that when excitation was produced by electron impact, practically all of the 1849A radiation emitted by the tube was due to cascading from a level about 0.4 volt above the 6^1P_1 level, this infra-red transition having a lifetime of 2.1×10^{-6} sec. This result agreed with that of Eldridge[10] who had found by other methods that for excitation by electron impact, the bulk of 1849A was excited indirectly through transitions from higher levels.

Subordinate Series Lines

Studies made to determine the mean lifetimes of several of the subordinate series lines of cadmium gave results which were not conclusive, but are briefly described because of certain interesting facts brought out by the measurements. These measurements were made with the potas-

* H. W. Webb and H. A. Messenger, reference 7, p. 326.
[10] J. A. Eldridge, Phys. Rev. **23**, 685 (1924).

sium photoelectric tube previously used and described by Randall.[7] Filters were employed to isolate the lines being studied. To obtain sufficient energy in these lines it was found necessary to use voltages on the grid of the excitation tube which resulted in considerable ionization. There is consequently some uncertainty as to how closely the excitation followed in time the voltage impressed upon the grid. Numerous checks indicated, however, that this was not a serious source of error in the frequency range employed. A more serious one was the very considerable absorption of the radiation by atoms in the 5^3P states which in most of the measurements tended to obscure the effect of the persistence in the higher energy states. Figure 4 shows a typical $R-f$ curve taken

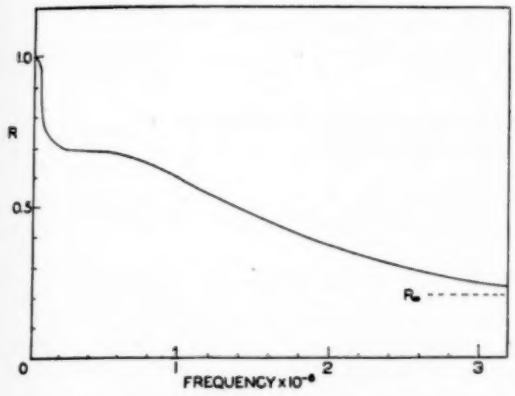

FIG. 4. $R-f$ curve for the group of subordinate series lines 5086–4800–4678A. Values of f_1 occur at 45,000 and 1.6×10^6 cycles, for the two sections of the curve, respectively.

under these conditions. Initially the curve falls off sharply to a value of R well above the final level, R_∞. The frequencies at which this drop occurs corresponded to a persistence one to two times as great as that which would be due to the lifetime of 3261A. Since the filters between the tubes did not transmit 3261A but only the subordinate series lines under measurement, it was concluded that this initial drop was due to absorption of the subordinate series lines by atoms in the 5^3P states and their subsequent re-emission. The decrease of R at very much higher frequencies will be discussed below.

Measurements of the mean lifetime of the 6^3S_1 level, from which emission of the lines 5086, 4800, and 4678A takes place, were made with a special excitation tube. This had an envelope of Pyrex glass and a cathode similar to that used in the other tubes. It was constructed with two coaxial electrodes of nickel mesh, G_1 and G_2, with radii 4.5 mm and 8.0 mm, respectively, and a coaxial wall electrode of sheet nickel W with radius 18 mm. The radiation was observed parallel to the axis through a window at the end of the tube, and baffles in the tube were so placed that only radiation from the region between G_2 and W reached the photoelectric tube. Corning filters 368 and 429 cut off all radiation of wave-length less than 4100A and isolated the subordinate series lines 5086, 4800, and 4678A as a group. The bias voltages used on the electrodes were: $W-S=45$ volts; $G_2-S=15$ volts. The alternating voltage, of 15 volts peak value, was applied between G_1 and S. The $R-f$ curve shown in Fig. 4 is typical of a group taken with a vapor pressure of 8.4×10^{-4} mm (216°C).

The initial drop of R was from 1.00 to 0.69, and the frequency for which R had the half-value (0.85) for this drop was 45,000 cycles, corresponding to a lifetime of 3.5×10^{-6}, which is approximately double the lifetime of 3261A. The value of R remained nearly constant until the frequency 500,000 cycles was reached, after which it dropped gradually to the final level 0.21. The f_1 for this portion of the curve was taken as the frequency, 1.6×10^6 cycles, for which R was the mean of the values 0.69 and 0.21. Assuming that this second drop in the curve was determined by the lifetime of the 6^3S_1 state and that no absorption and re-emission of these subordinate series lines was present, we find the lifetime of this state is approximately 10^{-7} sec. $(2\pi f_1)^{-1}$. If absorption-re-emission processes were involved, this would be simply an upper limit which these experiments set for this lifetime. Some measurements made on these same lines with the tube of glass of high transmission in the ultraviolet, described earlier, gave values of f_1 in the neighborhood of 8×10^6 cycles, which can be interpreted as the result of sufficient absorption and re-emission of the radiation to increase the average persistence of the 6^3S_1 state to double that of the true mean life.

With a set of filters isolating the group of diffuse subordinate series lines 5^3P-5^3D, similar measurements were carried out. The curves are in most respects similar to those just described,

and show that the value for the lifetime is not greater than 10^{-7} sec.

A detailed explanation of these curves is difficult. The initial drop seems best explained as dependent on the subordinate series radiation which was excited more or less continuously in the region screened from the photoelectric tube by the baffles and which was absorbed and reradiated by the excited atoms in the 5^3P states found in the unscreened part of the tube. The corresponding persistence would then be the same as the persistence of the 5^3P states in that part of the tube. The second drop in the curve, which occurred at high frequencies, would be explained in the case of the sharp series as due to the direct excitation to the 6^3S level (or 5^3D level for the diffuse series) of atoms in the unscreened region during the positive half-cycle of the alternating voltage and their radiation to the photoelectric tube either directly or with not more than one or two absorption-re-emission steps. For this radiation the persistence would be of the order of the mean lifetime of the level in question. Because of the uncertainties as to the exact processes involved in the measurements, the above results can probably be relied upon only as to the order of magnitude of the lifetimes.

The authors take this opportunity to thank Dr. Herbert N. Otis for his assistance in this investigation.

PHYSICAL REVIEW VOLUME 66, NUMBERS 3 AND 4 AUGUST 1 AND 15, 1944

Production of Single Mesotrons by Non-Ionizing Radiation at Altitudes of 10,600 ft. and 14,200 ft.

JULIUS TABIN
University of Chicago, Chicago, Illinois
(Received May 31, 1944)

The production of single mesotrons in various materials was studied by means of an apparatus consisting of 46 Geiger-Mueller counters arranged in 10 different three-, four-, and fivefold coincidence sets. The producing layers consisted of different thicknesses of paraffin, iron, and lead. The results indicate that photons are the most probable agent for the production of the single mesotrons. The cross section for the mesotron production has been calculated for the various producing materials.

INTRODUCTION

IN 1938 Schein and Wilson[1] published a paper concerning the production of penetrating cosmic-ray secondaries in the atmosphere above 20,000 feet. They found considerable production at 25,000 feet and indicated that the secondary particles observed were produced by photons. Since then, many attempts have been made to identify the nature of the producing radiation. Shonka[2] found the production to be as high as 6.1 percent in a producing layer of 20 cm of lead at an altitude of 14,200 feet. Only 1.5 percent was attributed to penetrating radiation arising from photons. The other 4.6 percent was ascribed to neutral particles of greater penetration (neutrons). Schein, Jesse, and Wollan[3] undertook the investigation of the production of penetrating particles by non-ionizing radiation as a function of altitude. Their results indicated that an appreciable production takes place above 23,000 feet with increasing altitude. Because the intensity of the produced mesotrons followed the intensity of the soft component, photons were considered as the most probable producing agent. Rossi and Regener[4] studied the production of mesotrons at 14,200 feet. They found a definite production which was attributed to either neutrettos or high energy neutrons. They arrived at this conclusion because it appeared that the producing radiation had a large probability of

[1] M. Schein and Wilson, Phys. Rev. **54**, 304 (1938).
[2] F. Shonka, Phys. Rev. **55**, 24 (1939).
[3] Schein, Jesse, and Wollan, Phys. Rev. **56**, 613 (1939).
[4] B. Rossi and V. Regener, Phys. Rev. **58**, 837 (1940).

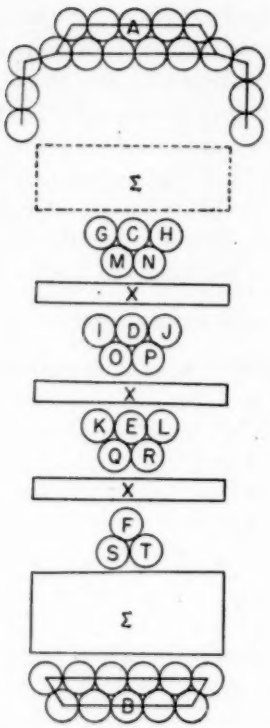

FIG. 1. Counter arrangement.

traversing several centimeters of lead without generating secondary ionizing particles. Regener,[5] in 1943, reported that the production of non-shower-producing particles by photons at altitudes up to 11,500 feet was as high as 10 percent of the total penetrating component. All these different investigations definitely showed that there exists a production of mesotrons by non-ionizing radiation. However, no definite evidence was available to indicate the nature of the mesotron-producing radiation.

The following experiment was carried out at Mt. Evans, Colorado (14,200 feet), in order to determine whether photons are able to produce single mesotrons. This seemed possible by investigating the absorption of the mesotron producing radiation as a function of thickness in materials of different atomic numbers.

APPARATUS

The counter arrangement used in the following experiment is schematically represented in Fig. 1. The forty-six counters were arranged into ten different three-, four-, and fivefold coincidence circuits. The seventeen counters A and also the eleven counters B were each connected in parallel. Counter batteries A and B completely covered and extended in both directions beyond the solid angle subtended by counters $CDEF$. The coincidence circuits were of a conventional type similar to those used by Schein, Jesse, and Wollan in their balloon flights. The resolving power of the circuits was tested and found to be approximately 10^{-5} sec. Hence, for the three-, four-, and fivefold coincidences chance coincidences were negligible. Each coincidence circuit operated an individual neon light which was photographed by a Simplex movie camera whenever a pulse occurred simultaneously in the so-called master coincidence set. Counters $CDEF$ constituted this master set. A coincidence pulse in the master set corresponded to the passage of a penetrating particle[6] through the lead layers X. Thus, by observing the neon lights which were photographed during each exposure on the same film, one could determine which of the various possible coincidence sets were tripped simultaneously with the master set.

All counters were 1 in. in diameter, but of two different lengths. The counter batteries A and B consisted of counters 13.5 in. long. All other counters were 6 in. long. The tubes were filled with a mixture of 90 percent argon and 10 percent alcohol. Each counter tube had a voltage plateau of at least 200 volts, and all were matched so that they had very nearly the same starting potential. They all were then connected to the same high voltage supply and were operated at 1240 volts. The counters were mounted in a wooden stand which contained various lead layers X and Σ' and provided space for the insertion of a producing layer. In Fig. 1 the producing layer is designated by Σ. This layer could be varied up to a thickness of 11.5 cm. Σ consisted of paraffin, iron, and lead. The three lead layers X were used to discriminate between penetrating particles and electrons, and each had a thickness of either 0.64 cm or 1.59 cm of lead. Since a thickness of 0.6 cm is very nearly equal to a radiation unit in lead, an electron passing through all three lead absorbers should have an extremely high probability of emerging

[5] V. Regener, Phys. Rev. **64**, 252 (1943).

[6] Since most of these particles are later shown to be mesotrons, they will be referred to as such in the rest of this paper.

as a cascade shower below each of the lead layers X. To determine whether the particle which tripped the master set was an electron or a mesotron, several groups of counters were arranged in seven separate coincidence sets so as to indicate the presence of showers below the various lead layers. Counters *GCHF* formed a fourfold and *MNF* a threefold coincidence set. Pulses in these sets showed the presence of a shower directly below the producing layer Σ. Counters *IDJF*, *KELF*, and *CFST* constituted three fourfold (coincidence sets), and counters *OPF* and *QRF* two threefold coincidence sets. Coincidence pulses from any of these counter arrangements indicated that showers were present below the lead layers X. It is to be noted, however, that a small percentage of the threefolds occurring below only one single layer X could be due to the presence of knock-on electrons kicked out of one of the lead layers by a mesotron.[7] The lead layer Σ', 6.98 cm thick, was used to absorb low energy mesotrons.

ACDEF formed a fivefold coincidence set. If this set was tripped, the presence of an ionizing particle traversing the producing layer Σ and the layers X was indicated. A coincidence in *CDEF* which was not accompanied by a coincidence in *ACDEF* generally meant the production of an ionizing particle in layer Σ by non-ionizing radiation. These produced particles were attributed to single mesotrons when such an event was unaccompanied by a pulse in any of the seven shower sets. The lower set of counters B was also connected with the master set *CDEF* in a fivefold coincidence. A coincidence in this set showed whether or not a particle tripping the master set had enough energy to traverse the 6.98 cm of the lead absorber Σ'.

With the six side-counters in bank A removed, some cases were found where ionizing particles entered from the side and were scattered in the producing layer in such a way that they tripped the master set. Such events appeared similar to the production of an ionizing particle in Σ. After adding the six "police" counters in A, however, the presence of side particles was detected as a coincidence *ACDEF* and hence did not represent a production process by non-ionizing radiation. Air showers had no effect on the production of single mesotrons because they were eliminated by tripping at least one of the shower sets in the neighborhood of counters *CDEF*. The efficiency of the banks of counters A and B was very nearly 100 percent. This high efficiency could be obtained only by using tubes of relatively small diameter, thereby reducing the single counting rate in each of the tubes in banks A and B.

EXPERIMENT

In order to determine if single mesotrons could be produced by non-ionizing rays, over 20,000 pictures of mesotrons tripping the master set were taken at Mt. Evans. From preliminary tests conducted at Echo Lake, Colorado (10,600 feet), it was determined that the frequency of the above process, if it existed at all, was a very small percentage of the frequency of the penetrating component. It was necessary to keep all the counters in a fixed position during the entire course of the experiment. Therefore, in the final arrangement, the only variables were the thickness of the lead layers X and the thickness and material of the producing layer Σ. The inefficiency of the upper bank of counters was tested by removing the producing layer Σ. When this was done, all the cases where only the coincidence set *CDEF* was tripped and which were unaccompanied by a simultaneous discharge in set *ACDEF* could then be attributed to inefficiency of A. Likewise, the inefficiency of the counter bank B was tested by removing lead layer Σ'. These inefficiency tests were repeated several times during the course of the experiment and were found to average 0.24 percent of the frequency of the penetrating component.[8] Since the position of the counters was not changed during the entire course of the experiment, the actual production of single mesotrons could be obtained by correcting the measured frequency of production processes for the inefficiency in A and B.

RESULTS AND INTERPRETATION

The results on production of single penetrating particles on Mt. Evans and Echo Lake are given in Table I. A slow particle refers to a mesotron or any other penetrating particle of lower energy

[7] This effect proved to be negligibly small for the infrequent number of produced mesotrons.

[8] The inefficiency did not exceed 0.4 percent during the entire course of the experiment.

TABLE I. Data obtained at Mount Evans and at Echo Lake.

	At Mount Evans													At Echo Lake	
Material used for the producing layer	Paraffin					Lead						Iron		Lead	Para.
Column	1	2	3	4*	5	6	7	8	9	10	11	12	13	14	15
Thickness of producing layer Σ in cm	1.27	3.81	11.40	11.40	11.40	1.27	3.81	11.40	0.64	1.27	11.40	1.27	11.40	10.10	11.40
Lead layer X in cm	1.59	1.59	1.59	1.59	0.64	1.59	1.59	1.59	0.64	0.64	0.64	1.59	1.59	1.59	1.59
Number of mesotrons incident on Σ per hour	0107	99.0	95.2	88.6	110	66.3	79.2	66.0	53.3	87.1	68.4	113	90.3	71.3	78.5
Produced penetrating mesotrons per hour**	0.61	0.41	0.66	0.74	1.09	0.05	0.39	0.11	0.09	0.25	0.12	0.00	0.30	0.11	0.26
Produced slow mesotrons per hour**	.06	0.32	0.42	0.19	1.30	0.41	0.22	0.23	0.63	1.64	0.37	0.02	1.04	0.22	0.16

* An additional 57.2 cm of paraffin was placed above counter bank A.
** Inefficiency has been subtracted from the apparent values of the production.

which trips set $CDEF$ but is unable to traverse the absorbing layer Σ'.[9] The experiment also gave interesting information about multiple production in different materials and cascade showers in lead. The results of these investigations will be reported at a later date.

The single particles which are produced and which traverse the master set $CDEF$ are penetrating particles, providing none of the shower sets is simultaneously tripped. Most of these penetrating particles must be mesotrons since protons would require an average energy of 4×10^8 ev to traverse the lead layers interposed between the counters, and there is no evidence for the existence of protons of such high energies at altitudes of Mt. Evans. Many cloud-chamber photographs have been taken by various observers, but only protons of lower energy ($E<10^8$ ev) were found.[10]

There are different lines of evidence which tend to throw light on the nature of the producing radiation. (1) Cosmic-ray photons are mainly absorbed by pair-production processes with a cross section which is proportional to the square of the atomic number Z. One should expect that if the mesotron-producing radiation consists of photons, it would be absorbed according to this law. Since the absorption of photons in lead ($Z=82$) is very great, one would expect the production by photons to reach saturation in a lead thickness of 2–3 cm. In paraffin, where Z is very much smaller, one would not expect saturation until a producing layer of about a meter is reached. One can see from Table I that in lead, and particularly in that part dealing with the production of slower mesotrons passing through the 0.64-cm lead layers X (columns 9, 10, 11), this effect is very well pronounced. The apparent decrease in production with 11.4 cm of lead is due to the self-absorption of the produced mesotrons in the 11.4 cm of lead. In 11.4 cm of paraffin this effect does not occur, and one sees that saturation is not reached in this thickness. In order to find out whether the production is saturated in a still larger thickness, an additional paraffin layer of 57.2 cm was placed above the upper counter bank A. This paraffin completely covered the solid angle of the four counters $CDEF$ of the master set. If saturation were reached, most of the produced mesotrons would originate in the 57.2-cm paraffin block, trip the counter bank A, and thereby enter the producing layer of 11.4 cm as an ionizing particle. One would, therefore, expect a very abrupt drop in the registered production of mesotrons by non-ionizing radiation. Referring again to Table I, one sees very distinctly,

TABLE II. Number and energy of mesotrons produced in lead.

Single mesotrons produced per hr.	Av. energy of produced mesotrons
1.64	1.6×10^8 ev
0.41	2.1×10^8 ev
0.22	2.5×10^8 ev
0.37	3.1×10^8 ev
0.23	3.5×10^8 ev

after comparing the total production of mesotrons in column 3 and 4, that this does not occur, showing that in paraffin there is no saturation effect with a thickness of 57.2 cm.

(2) The energy range of the mesotrons pro-

[9] In the table a production of particles always refers to a production process by non-ionizing radiation.
[10] C. D. Anderson and S. Neddermeyer, Phys. Rev. **50**, 263 (1936). W. M. Bostick, Phys. Rev. **61**, 557 (1942). W. M. Powell, Phys. Rev. **61**, 670 (1942). W. E. Hazen, Phys. Rev. **65**, 67 (1944).

duced in lead which are stopped in Σ' are computed from the ionization loss in lead and are given in Table II. (The results were calculated from the number of produced mesotrons which were stopped in the lead layer Σ'). In this computation it was assumed that all the produced mesotrons originated from a layer one cm below the top of the producing lead block Σ. Table II shows that there is a considerable drop in the number of produced mesotrons at energies lower than 1.6×10^8 ev. It should be noted that in the photon spectrum at 10,000 and 14,000 feet altitudes a similar change occurs around energies of about 2×10^8 ev.[11] Assuming a mesotron rest mass of 200 electron masses, it takes at least 10^8 ev to create a single mesotron. If the probability of production does not change appreciably with photon energy in the neighborhood of 10^8 ev, there should then be a drop in the energy spectrum of the produced mesotrons at an energy of about 10^8 ev such as observed, provided the produced mesotrons are created by photons.

(3) The increase in production of single mesotrons between the altitudes of Echo Lake and Mt. Evans can be seen by comparing the data at Echo Lake (given in columns 14 and 15 of Table I), with the corresponding production at Mt. Evans (given in columns 3 and 8). This increase in the case of paraffin[12] amounts to a ratio of 2.6. The increase in production is roughly of the same order of magnitude as the increase in the intensity of the soft component (photons) between the two altitudes. This ratio is about 2 according to Greisen.[13]

Comparing the number of produced single mesotrons in lead found in this experiment with that obtained under very similar conditions in a stratosphere balloon flight carried out in collaboration with Dr. Schein in 1942, we find at 5 cm Hg pressure that the number of mesotrons produced in 2 cm of Pb is about 100 times the value (Table I, columns 6 and 7) obtained at Mt. Evans. In the same balloon experiment the increase in the photon intensity[14] for energies higher than 10^8 ev was measured and found to be 600 between sea level and altitudes corresponding to 5 cm Hg pressure. Since the photon intensity increases by a factor of eight between sea level and Mt. Evans,[13] one should, therefore, expect an increase in the production of mesotrons by non-ionizing radiation between Mt. Evans and an atmospheric height equivalent to 5 cm Hg to be $600/8=75$, which is in as good agreement as can be expected under the conditions imposed.[15] This comparison is very rough and represents only an order of magnitude consideration.

The arguments presented under 2 and 3, while not conclusive, definitely favor photons as possible producing agents of slower mesotrons. Argument 1 substantiates this conclusion strongly since photons are the only non-ionizing rays which are able to explain the observed differences in absorption between paraffin and lead.

Assuming photons as the producing agent, one can calculate the cross sections for the mesotron production for the various producing materials. From the data obtained in paraffin, it is considered probable that the mesotrons are created by collisions with the atomic nucleus of the producing material. Under these assumptions the cross section in smaller thicknesses of paraffin can be calculated from the formula,

$$N=N_0e^{-n\sigma t},$$

where σ represents the cross section for mesotron production by photons; N, the number of photons passing through the thickness t without being absorbed by mesotron production; N_0, the number of incident photons; and n, the number of nuclei per cc. Changing to logarithms and expanding, we get,

$$n\sigma t=\log\left(\frac{N_0}{N}\right)=\frac{N_0-N}{N_0}+\frac{1}{2}\left(\frac{N_0-N}{N_0}\right)^2+\frac{1}{3}\left(\frac{N_0-N}{N_0}\right)^3+\cdots.$$

Since the number of produced mesotrons (N_0-N) is very small in comparison with the number of photons N_0 striking the producing layer, the

[11] W. E. Hazen, Phys. Rev. **65**, 67 (1944).

[12] A similar comparison in lead cannot be made because the self-absorption in the producing lead layer overshadows the major production of slow mesotrons.

[13] K. Greisen, Phys. Rev. **61**, 212 (1942).

[14] The photon intensity was put proportional to the measured number of cascade showers produced in 2 cm of Pb by non-ionizing rays.

[15] The thickness of the producing layer and the counter geometry were not identical in the two cases.

higher order terms can be neglected and,

$$n\sigma t \simeq (N_0 - N)/N_0$$

and, therefore,

$$\sigma \simeq [(N_0 - N)/N_0](1/nt).$$

For paraffin this formula gives the correct value for the cross section for thicknesses in which the absorption of photons by pair production is negligible. This is very nearly the case for thicknesses of 1.27 cm and 3.81 cm. It was estimated that if we take the absorption of photons by pair production into account, the cross section would change by about 5 percent. In lead and iron the absorption of photons by pair production is appreciable even in the smallest thicknesses used. In this case the formula gives a value which may be considered a lower limit for the cross section for mesotron production by photons.

For monatomic substances $n = (6.02 \times 10^{23} \times \text{density})/\text{atomic weight}$. This gives for lead $n = 3.2 \times 10^{23}$ and for iron $n = 6.2 \times 10^{23}$ nuclei per cc. In order to get n for paraffin we use the formula C_nH_{2n+2}. This leads to a value for n of 1.0×10^{23} nuclei per cc.

From Hazen's experiments[11] the number of photons with energies higher than 10^8 ev is about 10 percent of the total number of mesotrons passing through 4.8 cm of lead. The value of N_0 was obtained from the measured number of mesotrons incident on the producing layer Σ and passing through 4.8 cm of lead.

Using the experimental values for N_0 and N, we get for the cross sections per atomic nucleus for this process:

$$\sigma_{\text{par.}} = 5 \times 10^{-25} \text{ cm}^2; \quad \sigma_{\text{lead}} = 1 \times 10^{-24} \text{ cm}^2;$$

$$\sigma_{\text{iron}} = 4 \times 10^{-25} \text{ cm}^2.$$

These values are about equal to the areas of the corresponding nuclei calculated by using the approximate formula for the radius of a nucleus $r = r_0 Z^{\frac{1}{3}}$,[16] where r_0 is the range of the nuclear forces $= 1.4 \times 10^{-13}$. The areas calculated in this way are,

$$A_{\text{par.}} = 2 \times 10^{-25} \text{ cm}^2; \quad A_{\text{lead}} = 2 \times 10^{-24} \text{ cm}^2;$$

$$A_{\text{iron}} = 1 \times 10^{-25} \text{ cm}^2.$$

This result favors the hypothesis that the mesotron production by photons has to be considered as a direct interaction between the photon and the atomic nucleus.

In conclusion the author wishes to express his appreciation to Dr. Marcel Schein for suggesting the problem and for his numerous suggestions and consultations throughout this work. He also wishes to express his thanks to General L. A. Lawson and Captain Innes-Taylor for their generous hospitality at Echo Lake, to Mr. George E. Cramner and Dr. William Hyslop for making possible the stay at Mt. Evans, and to Dr. A. H. Compton for his continuous support in these investigations.

[16] This formula can be considered only as a fair approximation for elements of higher atomic numbers, like Pb.

Letters to the Editor

PROMPT publication of brief reports of important discoveries in physics may be secured by addressing them to this department. The closing date for this department is the third of the month. Because of the late closing date for the section no proof can be shown to authors. The Board of Editors does not hold itself responsible for the opinions expressed by the correspondents. Communications should not in general exceed 600 words in length.

Gases Evolved by Magnetized Iron in Sulfuric Acid

R. L. HOFF, J. J. NAUGHTON, R. SMOLUCHOWSKI, AND H. H. UHLIG
Research Laboratory, General Electric Company, Schenectady, New York
May 29, 1944

SEVERAL months ago we were asked to report whether oxygen was one of the products resulting from the reaction of magnetized iron with dilute sulfuric acid. The first experiment was set up as shown in Fig. 1. A piece of Swedish iron 4.7 cm×1.2 cm diameter was placed in 5 percent sulfuric acid within the field of a solenoid whose strength at the center measured 286 oersteds. The acid was prepared from distilled water boiled vigorously for more than one hour and cooled in nitrogen to remove appreciable dissolved oxygen. Gas evolved by the iron specimen was collected in a glass-stoppered tube and sealed to a microgas-analysis equipment designed for the analysis of gases in metals. Oxygen was determined by change in pressure of the dried gas, after reacting with hydrogen over hot platinum and condensing out water in a solid CO_2 trap. The complete analysis was as follows.

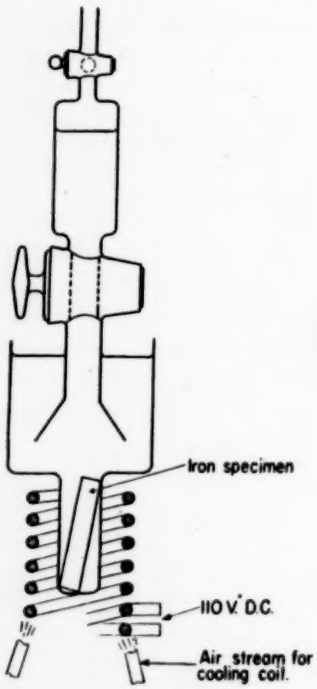

FIG. 1. Experimental arrangement to collect gases from magnetized iron in dilute sulfuric acid.

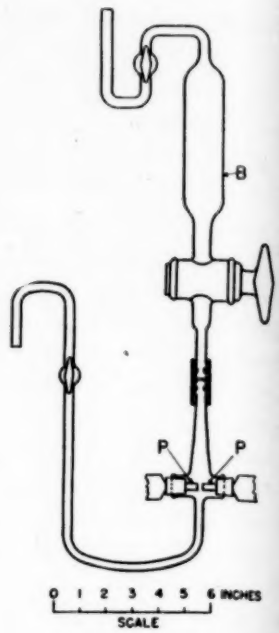

FIG. 2. Arrangement for the collection of gases from pole pieces *P*.

Oxygen	0.0±0.2 vol. percent
Hydrogen	94.7 vol. percent
Hydrocarbon as methane	4.5 vol. percent
Residue as nitrogen	0.5 vol. percent

The method was sensitive to better than 0.2 vol. percent oxygen, but within this limit, none was found.

Another experiment was performed in the apparatus shown in Fig. 2. The field strength used was now much higher, namely, 13,000 oersteds (measured in air) between two 0.64-cm ($\frac{1}{4}$ in.) diameter pole pieces *P* of Swedish iron separated by a 0.16-cm ($\frac{1}{16}$ in.) gap. Water likewise was boiled and cooled in nitrogen, and at no time was it in contact with air. Gases were collected in tube *B* in which there was always some water above the stopcocks in order to prevent gas leakage. Analyses were performed by two methods: One was the same as that described above and gave the same negative result; the second method using 150-ml samples was that of oxygen absorption in pyrogallol. The result of the latter analysis was 0.02 to 0.05 vol. percent oxygen. The difference between gas collected with and without magnetic field was within the limit of error and random in sign.

On the Quantization of Probability

HENRY F. DUNLAP
University of New Mexico, Albuquerque, New Mexico
March 2, 1944

THE recently proposed quantization of probability[1] leads to an apparent contradiction when applied to a particular problem.

Consider an enclosure of volume *V*, containing a grain of sand of volume *G*. The enclosure is assumed field free

except for the gravitational field of the grain of sand. If v is any subvolume of V large enough to contain G, then the *a priori* chance of finding the grain of sand at any instant in v is

$$P = v/V.$$

Now suppose that V is made so large that P is less than one chance quantum. According to the postulate of quantized probability, the grain of sand cannot exist in v. But v was *any* subvolume of V, hence the grain of sand cannot exist anywhere in V. An attempt to remove the contradiction by assuming that geometrical space is quantized in such a way that the smallest allowable volume is greater than v fails, since v was initially taken to be larger than G, the volume of the grain of sand.

[1] Alfred N. Goldsmith, Phys. Rev. **64**, 377 (1943).

Comments on "On the Quantization of Probability" by Henry F. Dunlap

ALFRED N. GOLDSMITH
580 Fifth Avenue, New York, New York
March 12, 1944

WHILE the writer would prefer to leave the analysis of such thoughtful comments relative to the consequences of the probability-quantization theory as are given in the foregoing commentary to active specialists in the field of probability theory, he desires nevertheless to offer the following brief suggestions.

In the commentary a conclusion is reached that, under the stated conditions and in accord with probability quantization, the hypothetical "grain of sand cannot exist" any longer. At first sight, this seems a common-sense conclusion derivable from the premises.

But if probability is indeed quantized, "common sense" in its everyday meaning will not serve in such an analysis, any more than "common sense" particularly and reliably assists us in the realm of quantum physics. It is possible to examine the problem from a different viewpoint and to draw a different conclusion. Let us for example first substitute for "grain of sand" the probably more appropriate term "smallest elementary particle." Such a particle might be of electronic dimensions or even less. Let us also substitute for "cannot exist" the phrase "cannot be located" or "cannot be discerned." This substitute language seems more in accord with the necessary treatment of the problem. We can then paraphrase the above commentary by stating that quantized probability appears to require that a sufficiently small particle enclosed in an adequately large volume becomes unlocatable by any physical means. This conclusion is not found troublesome or self-contradictory by this writer.

It may seem a radical or strange conclusion to state that when an extremely small particle is enclosed in a sufficiently large space it is, in a physical sense, altogether lost according to our chance-quantum theory. This would be tantamount to saying that it has become literally unfindable by any means available to the would-be observer. Yet this conclusion seems no more radical than others freely accepted by modern physicists. Our "lost particle" would be no more unfindable than is an amount of energy less than one quantum or an amount of matter less than the smallest elementary particle, both according to present-day theory. Our "lost particle" has no presence in our physical world in any meaningful sense, and no experiment, no matter how intellectually ingenious, will serve to locate it. The physical quest for such a particle thus becomes as meaningless as the search for an absolute frame of reference for motion. Such at least might be the inevitable consequence of probability quantization as the writer sees it, and he finds nothing intellectually repugnant in such a conclusion.

It should, however, be stressed, as it was in the original letter describing probability quantization, that no assertion is made as to the correctness and validity of the theory of quantized chance. It was there urged that this theory continue to be thoroughly explored, keeping in mind, however, that the final conclusion will doubtless be reached by experimentation.

The above commentary is appreciated by the writer and is believed by him to be a stimulus to further study of the subject. It is hoped that such study will deal with methods for the experimental proof or disproof of probability quantization as well as with attempted applications of such a theory to certain small-scale or infrequent electrical phenomena. In these last-mentioned realms the new theory might display special utility or significance.

Magnetic Ions

V. D. HOPPER
Department of Physics, University of Melbourne, Melbourne, Australia
March 27, 1944

EHRENHAFT[1] has described experiments which he claims establish the existence of "magnetic ions." His method involves a measurement of the velocity of small particles (radii approximately 10^{-5} cm) of various elements (Ni, Fe, Mn, Cr, Sb) which are acted on by the earth's gravitational field and a uniform vertical magnetic field produced by an electromagnet. The particles are illuminated at right angles to the direction of the field and are observed in a direction normal to both the field and the direction of illumination.

An attempt has been made to verify his conclusions by slightly modifying the apparatus used by T. H. Laby and the author[2] in the determination of the electronic charge, a horizontal magnetic field being substituted for the electric field used in that determination. The magnetic field was produced by a small *permanent* Alnico magnet which has a strong field strength of about 1000 oersteds at the midpoint between the poles. Fine particles of nickel (radii of the order of 10^{-5} cm) were drawn by an air current between the poles of the magnet and then allowed to settle under the action of the vertical gravitational and the horizontal magnetic fields, and their path was observed by means of a microscope. Thousands of particles have been observed, many being in the field of view at the one time, but no particle has been detected moving in such a manner as to verify the "magnetic ion" hypothesis. In the center of the magnetic field all particles fell vertically,

and on either side of the central line particles either remained undeflected or deflected towards the nearer pole. No particles crossed the center of the field. This result agrees with existing theories of magnetic induction for the non-uniform but symmetrical field between the poles of the magnet. The experiment has been repeated with iron and rouge particles with the same results. Increase in illumination also made no difference except that vertical convection currents were produced when excessive heat entered the chamber.

A possible explanation of Ehrenhaft's results is that the particles he observed were electrically charged and were acted on by some stray electric field such as that produced between the coils of the electromagnet. A typical particle observed by Ehrenhaft has a radius of approximately 10^{-5} cm and maximum velocity due to the electromagnet of 10^{-2} cm/sec. Assuming that this velocity is due to an electric field and that the particle possesses a charge of ne where n is the number of electrons each of charge $e(\approx 4.8\times10^{-10}$ e.s.u.) and applying the corrected form of Stokes's law, one finds that the field required to produce this velocity is of the order of $0.3/n$ e.s.u. or $90/n$ volt/cm.

Thus for sufficiently highly charged particles a velocity of the above magnitude would be observed for very small electric fields (of say <1 volt/cm) and these small fields may be produced by the potential differences between the two halves of the electromagnet or electrostatic leakage effects from the generator.

[1] Felix Ehrenhaft, Phys. Rev. **57**, 659 (1940); Ann. d. Physik **11e**, Sec. 13, 151 (1939–40); Science **96**, 228 (1942); J. Frank. Inst. **253**, 225 (1942).
[2] V. D. Hopper and T. H. Laby, Proc. Roy. Soc. **A178**, 242 (1941).

Test for Change of Pole Strength of Permanent Magnet

J. E. GOLDMAN
Westinghouse Research Laboratories, East Pittsburgh, Pennsylvania
May 22, 1944

AT the Pittsburgh meeting of the American Physical Society, F. Ehrenhaft[1] reported an approximately 10 percent loss of strength of a permanent magnet in an experiment in which acidulated water is placed between the poles of the magnet in contact with the pole faces and allowed to remain so for a period of time. The energy loss of the magnet is claimed by Ehrenhaft to have gone into the "magnetolysis" of the water. In view of the unusual character of these results, it was decided to repeat Ehrenhaft's experiment as described in the *Bulletin of the American Physical Society*.

In our experiment, a stabilized Alnico permanent magnet was used, the strength of which was measured on five successive days before the commencement of the experiment in the same laboratory where the entire experiment was conducted. Measurements were made by means of a ballistic galvanometer and search coil, the ballistic galvanometer having been calibrated by a standard of mutual inductance prior to each measurement. The accuracy of the apparatus is better than 1 percent. A special attachment was constructed to assure that in each measurement the search coil would start and come to rest at precisely

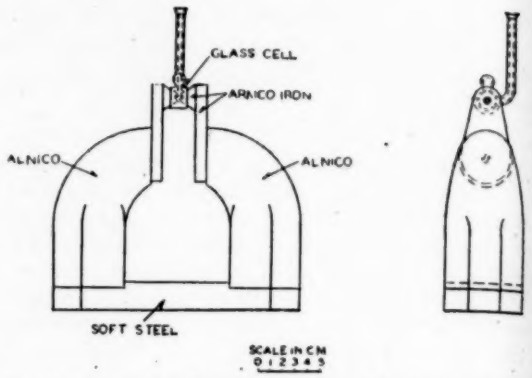

FIG. 1. Arrangement of permanent magnet pole pieces and glass cell containing acidulated water.

the identical position. Pole pieces for the Alnico magnet were made of Armco iron, the end of each terminating in a truncated cone the face of which was 6 mm in diameter. The geometrical arrangement is shown in Fig. 1. Measurements of the field before and after the experiment were carried out both with and without the pole pieces. The height of each pole piece was carefully measured under a microscope by comparison with a standard height gauge. The accuracy of this measurement was ±0.004 mm. The purpose of this last phase of the investigation was to follow any possible change in gap length that might accompany the action of the acid on the soft iron pole faces.

Two experiments were carried out to test directly Ehrenhaft's results. In one, 4 percent H_2SO_4 was placed in the glass cell, and the iron pole faces were exposed to the acid. As expected, there was a violent display of bubbles due to the liberation of hydrogen by the iron. At the end of 18 hours, the field of the magnet was measured and found to be identical with the value obtained at the beginning of the experiment within the measure of experimental error.

In the second experiment, the conditions were the same except that a 12 percent sulfuric acid solution was used in place of the weaker one used previously. This concentration was estimated to be of approximately maximum electrolytic activity. The entire pole structure with all but the pole face covered with paraffin was immersed in the solution and allowed to remain so for a similar period of time. No measurable decrease in field was observed as a result of this experiment. It is estimated that from the commencement of the investigation until its completion, the magnet poles were exposed to the "magnetolytic" action of the acid for approximately 60 hours during all of which time the magnet was not removed from its original surroundings, i.e., from the same laboratory where the measurements were made. The total magnetic flux at the pole face of the original Alnico magnet was $11{,}700\pm50$ maxwells. This value was the same at the end of the experiment as at the beginning. It may be added parenthetically that when the experiment was carried out with the pole faces covered with paraffin and the acid previously boiled to drive off dissolved gases, no bubbles at all were observed when the acid was placed in the cell whereas they are observable if the acid is not previously boiled.

[1] F. Ehrenhaft, Phys. Rev. **65**, 349 (1944).